===== **REVIEW** =====

Pentacarboxycyclopentadienes in Organic Synthesis

I. E. Mikhailov[a],*, G. A. Dushenko[a], and V. I. Minkin[a]

[a] Research Institute of Physical and Organic Chemistry SFU, Rostov-on-Don, 344090 Russia
*e-mail: mie@sfedu.ru

Abstract—The review summarizes the literature data on the synthesis, structure, reactivity, and rearrangements of pentacarboxycyclopentadienes and their derivatives. Their potential for creating new chiral organic catalysts for enantioselective Diels–Alder reactions, cationic polymerization of vinyl ethers, enantioselective protonation of silylenol ethers, aminomethylation, and other processes is described, and aspects of their use as effective carriers of functional groups, new ligand systems for the synthesis of metal complexes and donor-π-acceptor chromophores for organic photovoltaics are considered.

INTRODUCTION

1. SYNTHESIS AND STRUCTURE OF PCCP

2. CHIRAL ACID PCCP CATALYSTS OF ENANTIOSELECTIVE REACTIONS

3. PCCP-CATALYZED CONTROLLED CATIONIC POLYMERIZATION OF VINYL ETHERS

4. REARRANGEMENT OF ORGANIC AND ORGANOELEMENT GROUPS AND HALOGENS IN THE PCCP SYSTEM

5. EFFECTIVE CARRIERS OF FUNCTIONAL GROUPS BASED ON FLUCTUATING PCCP

6. TETRACARBOMETOXYCYCLOPENTADENYL LIGAND SYSTEMS AND THEIR METAL COMPLEXES

7. PUSH–PULL CHROMOPHORES WITH HYDRAZONE PCCP FRAGMENTS FOR ORGANIC PHOTOVOLTAICS

CONCLUSIONS

INTRODUCTION

Pentasubstituted cyclopentadienes (Cp) with alkyl, aryl, benzyl, halogen-, cyano-, and other substituents in the five-membered ring are popular organic ligands which form various metal complexes widely used as catalysts for C–H bond functionalization [1–3], cycloaddition reactions [4, 5], olefin polymerization [6, 7], and other processes [8] and are also used to create materials for chemosensorics [9], molecular electronics [10–12], and spintronics [13, 14]. Such compounds are more stable than unsubstituted Cp derivatives and have a wide range of useful properties [15–25].

Pentakis(methoxycarbonyl)cyclopentadiene (**1**) has been attracting close attention since 1942, when it was first synthesized, and already in the 1960s, its main derivatives were obtained [26]. Due to the fact that 5 CO_2Me substituents strongly stabilize the Cp anion, compound **1** is a strong organic acid, nearly as strong

as HCl, and its stable anion forms salts that are stable in air and soluble in water. Such characteristics make compound **1** attractive for medicine and green chemistry. Its metal complexes with *s*-, *p*-, *d*-, and *f*-metals coordinated mainly to the carbonyl oxygen, as well as with soft metals (Re, Ru, Rh, and Au) coordinated to the carbon centers of the Cp ring were synthesized. However, in the literature on the synthesis and structure of cyclopentadiene **1** and its metal complexes, we found only one review [27]. Publications on Cp ligands and their metal complexes, including chiral ones, contain no information on cyclopentadiene **1** derivatives [28, 29].

At present, the interest in pentacarboxycyclopentadiene derivatives (PCCP) has increased significantly, which is associated with the discovery of their new properties and possibile use as enantioselective acidic Brønsted organocatalysts [30]. In addition, a wide range of circumambulating PCCP **1** derivatives were obtained and arylazo and thio derivatives of PCCP **1** were shown to act as efficient carriers of functional groups [31]. Chiral amidinyl-Cp ligand systems and their metal complexes were synthesized [32–34], and a great number of push–pull chromophores with an acceptor hydrazone Cp fragment were obtained, which can be used in organic photovoltaics [35]. The use of the PCCP anion in the synthesis of charge-transfer complexes with organic cations and radical cations for the needs of molecular electronics and for the creation of polymer ionic liquids with high ionic conductivity was demonstrated [36–38]. The potential of ruthenium complexes of PCCP **1** in anticarcinogenic drug design was revealed [39].

An attractive feature of PCCP **1** is that its CO_2Me substituents are easily functionalized to form a wide variety of analogs. This direction is being actively developed, which has led to the preparation of new PCCP derivatives and the creation of effective organic catalysts for enantioselective Diels–Alder reactions, stereoselective aminomethylation, cationic polymerization, enantioselective synthesis of cyclic amines, and many other processes [40, 41].

1. SYNTHESIS AND STRUCTURE OF PCCP

The condensation of malonic ester **2** with 3 equiv of dimethyl acetylenedixarboxylate (**3**) in the presence of acetic acid and pyridine forms 2 isomeric cycloheptadienes **4** and **5**, which transform into salt **6** under the action of potassium acetate (Scheme 1) [26].

Acidification of an aqueous solution of salt **6** with HCl gives rise to PCCP **1**.

Recently Radtke et al. [42] reported a one-stage version of this synthesis at room temperature in the presence of benzyltrimethylammonium chloride (BTMAC) as a catalyst; the yield of the target product was 48% (Scheme 2).

According to the X-ray diffraction analysis (XRD), PCCP **1** exists in the crystalline state as 6-hydroxy-6-methoxy-1,2,3,4-tetrakis(methoxycarbonyl)fulvene [27], as well as other polycarbomethoxycyclopentadienes [43]. In a $Cl_2CDCDCl_2$ solution, according to ^{1}H NMR data, PCCP **1** is also present in the fulvic form, which undergoes intramolecular prototropic tautomerism with an activation barrier of ~ 18–19 kcal/mol in

Scheme 1.
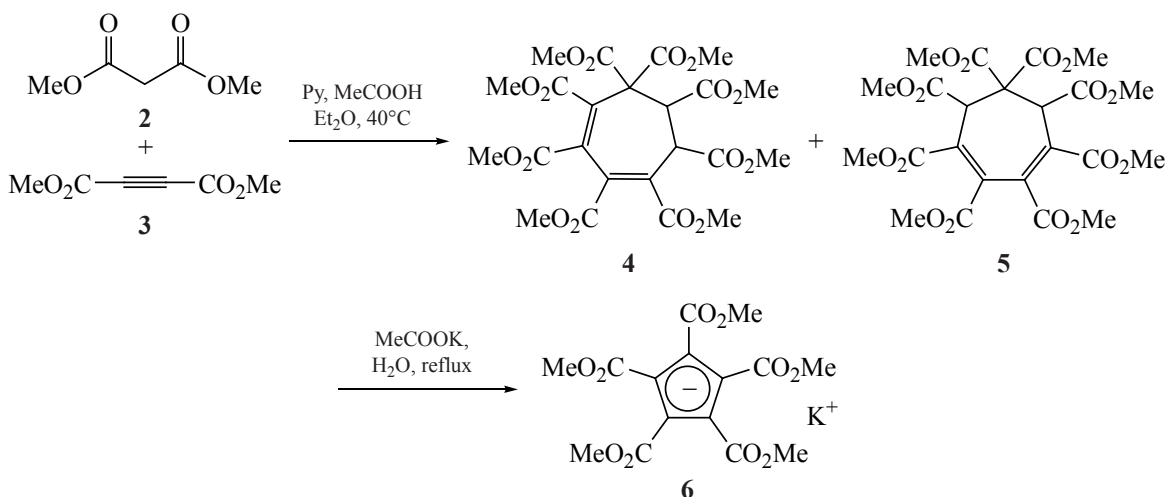
Scheme 2.
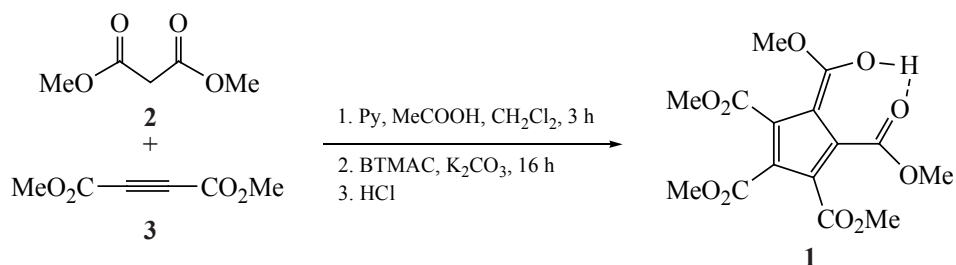
the temperature range 60–90°C. At a concentration of PCCP **1** solutions of 0.51 M and higher, the dynamics of its ^{1}H NMR spectra are concentration-dependent, on account of the intermolecular proton transfer with $\Delta G^{\neq}_{298}$ 14.5 kcal/mol (in CD$_2$Cl$_2$), and in the highly polar DMSO it completely dissociates to form an anion [44].

Quantum-chemical calculations (DFT B3LYP/6-311++G**) showed that the fulvene form of PCCP **1** in the gas phase is energetically more favorable than Cp form **1A** by ΔE_{ZPE} 7.8 kcal/mol [45]. The calculated energy barrier for thermally forbidden 1,7-O,C shifts **1** → TS (transition state) **7** → **1A** (Scheme 3) is fairly high ($\Delta E^{\neq}_{ZPE}$ 42.1 kcal/mol), while degenerate 1,5-H shifts over the periphery of the Cp ring **1A** ⇆ TS **8** ⇆ **1A'** ⇆ … should have the $\Delta E^{\neq}_{ZPE}$ barrier of 26.3 kcal/mol, a typical barrier for substituted cyclopentadienes [46].

By contrast, the 1,9-O,O'-H shifts in fulvene **1** ⇆ TS **9** ⇆ **1'** are extremely fast ($\Delta G^{\neq}_{298}$ 1.2 kcal/mol), and the subsequent rotation about the C^7=C^8 bond

1' ⇆ TS **10** ⇆ **1''**, leading to isomeric fulvene **1''**, should have the $\Delta E^{\neq}_{ZPE}$ barriers of 23.5 kcal/mol (gas) and 20.9 (CH$_2$Cl$_2$) kcal/mol (Scheme 4).

Thus, the route involving hydrogen circular migration in fulvene **1** according to Scheme 4 (**1** ⇆ TS **9** ⇆ **1'** ⇆ TS **10** ⇆ **1''**...) is energetically more favorable by 18.6 kcal/mol than the route according to scheme 3, and the calculated barrier for the former route is in good agreement with the experimental value [45].

Recently, the syntheses of pentacarboxycyclopentadienes, starting from compound **1**, have been developed [30, 40]. By transesterification in one step, the CO$_2$Me groups were functionalized to obtain a variety of aliphatic ester derivatives, and the treatment of PCCP **1** with amines gave the corresponding amides or diamides.

For example, heating L-menthol **11** with PCCP **1** under reflux in the presence of *N*-methylimidazole (NMI) yielded pentamenthyl derivative **12** in 96% yield (Scheme 5).

Scheme 3.
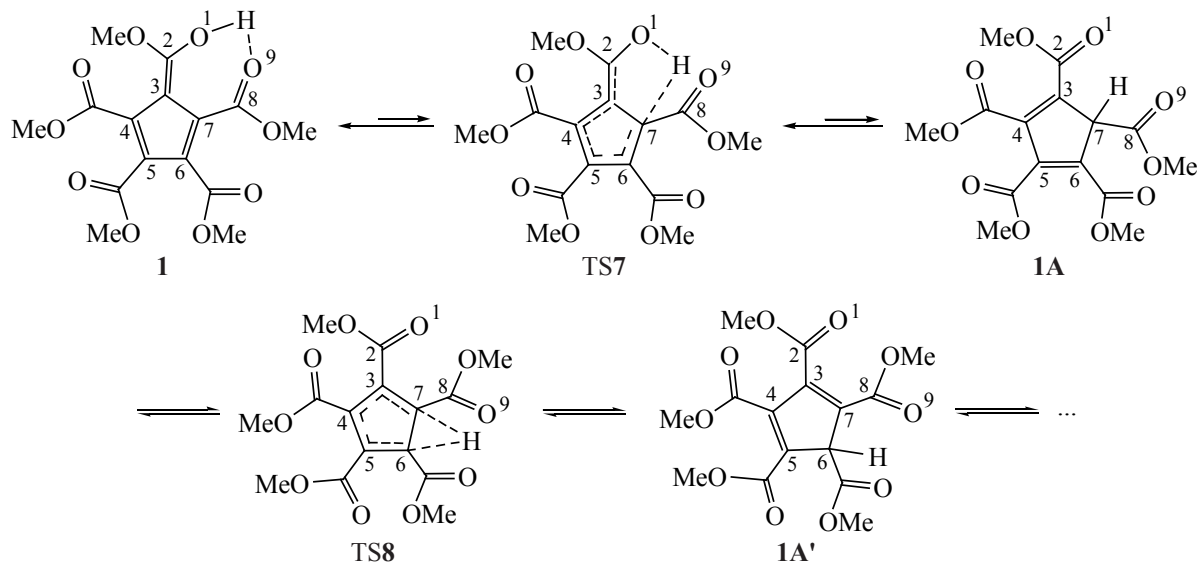
Scheme 4.
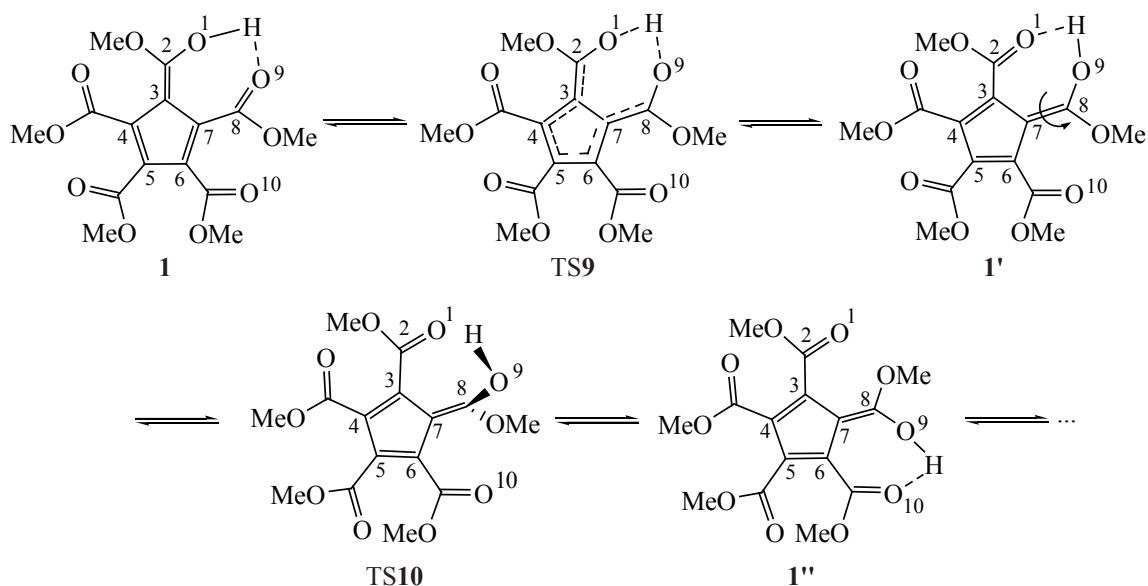
The same procedure was used to prepare in high yields PCCPs on the basis of linear alkyl **13**, alkenyl **14**, and alkynyl **15** alcohols (Scheme 6).
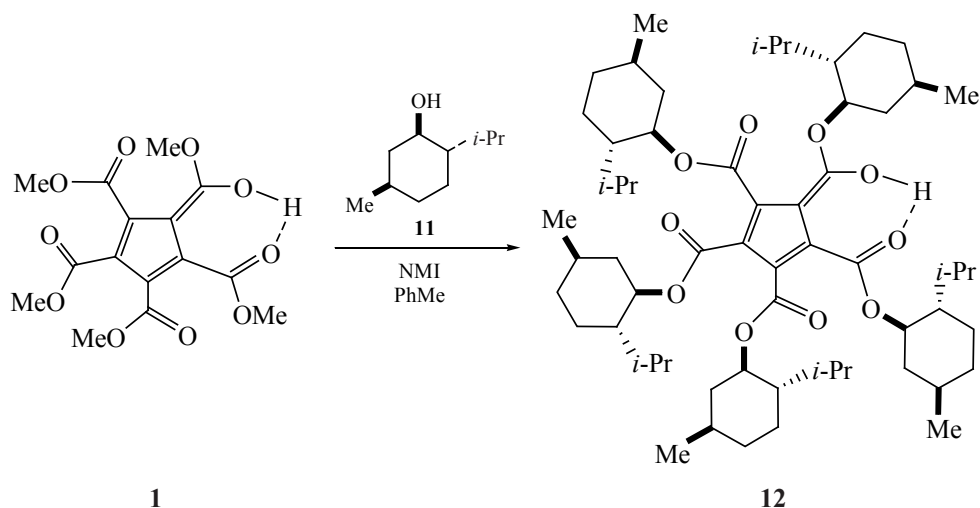
For example, a chiral derivative of terpineol (1*S*,2*S*,5*S*)-(–)-myrtanol **16** was synthesized in 97% yield, and the following derivatives of cyclic alcohols were prepared in good yields: **17** from CyOH, **18** from dicyclohexylmethanol, and **19** and **20** from chiral secondary alcohols. Even though such a large alcohol as cholesterol **21** were found possible to introduce in PCCP in 47% yield.

It was found that PCCP **1** converts into intermediate pentachloroanhydride **22** under the action of SOCl$_2$ and a catalytic amount of DMF (Scheme 7).
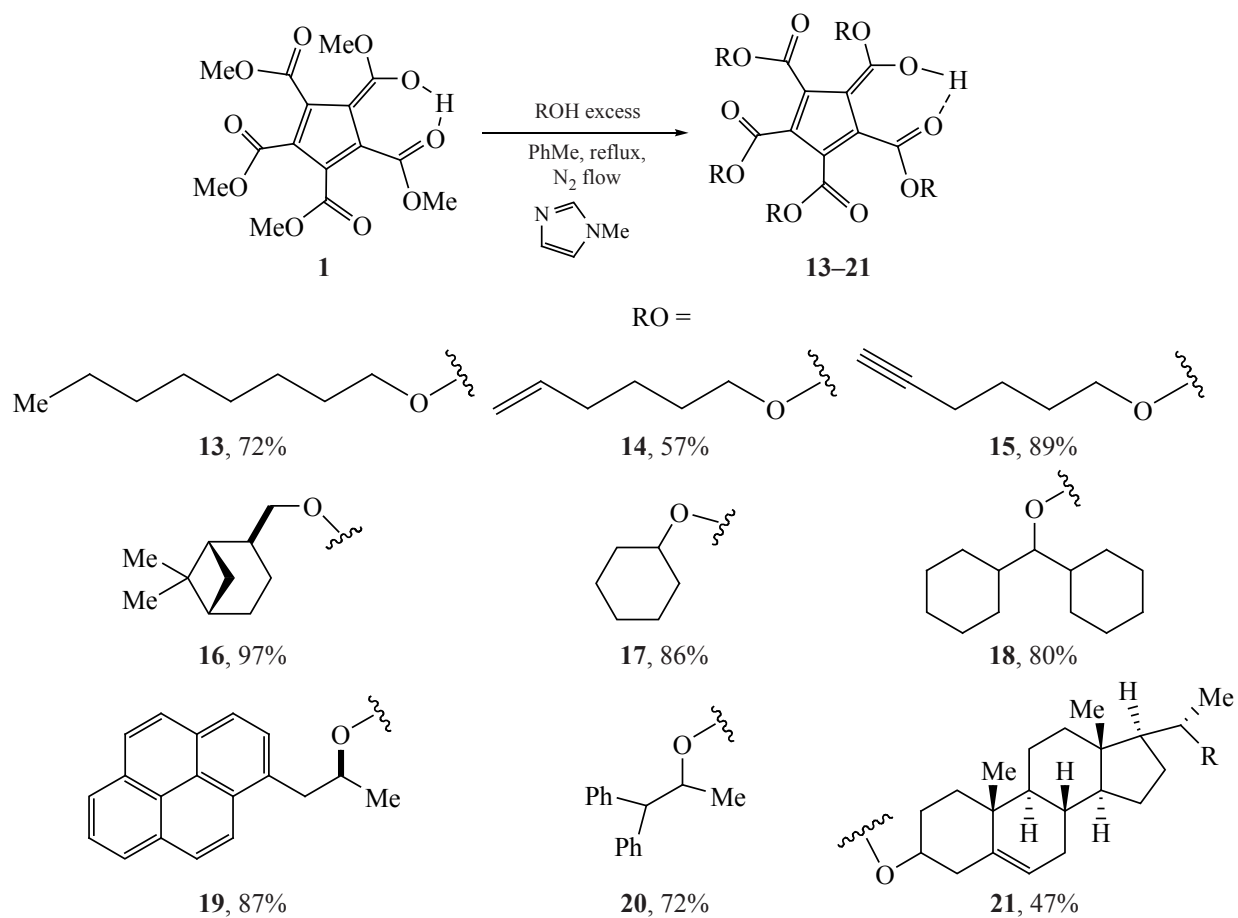
The addition of an excess of alcohol to chloroanhydride **22** led to the corresponding PCCP in moderate yield. This procedure was used to success to synthesize other PCCPs with alcohols inactive in transesterification reactions. The reactions with BnOH, (*R*)-1-phenylethanol, and (*S*)-benzylmandelate gave PCCPs **23–25**. Phenol and ethyl L-lactate were introduced in this reaction to obtain compounds **27** and **28**. PCCPs **29–31** were prepared in low yields in the presence of Na$_2$CO$_3$ to prevent decomposition of acid-sensitive esters, using *t*-BuOH, trifluoroethanol, hexafluoroisopropanol, and pentafluorophenol.

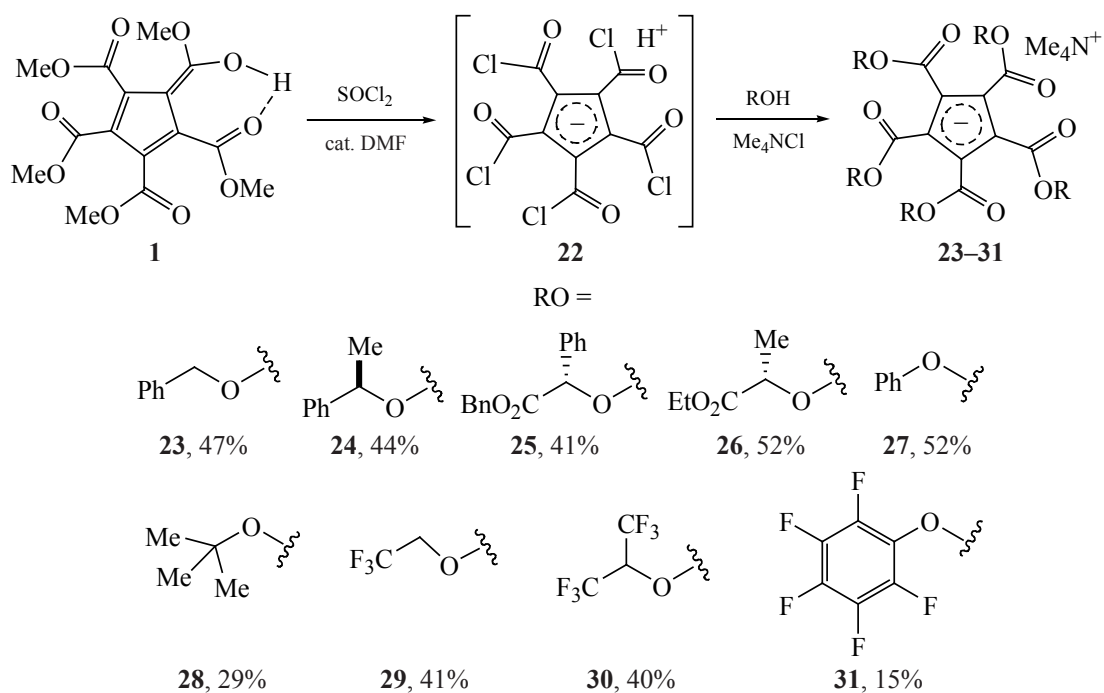The wide accessibility of amines, especially in the enantio-enriched form, stimulated the synthesis of

Scheme 5.

Scheme 6.

1 → **13–21**

ROH excess
PhMe, reflux,
N_2 flow

RO =

13, 72%   **14**, 57%   **15**, 89%

16, 97%   **17**, 86%   **18**, 80%

19, 87%   **20**, 72%   **21**, 47%

Scheme 7.

1 → **22** → **23–31**

SOCl₂
cat. DMF

ROH
Me₄NCl

RO =

23, 47%   **24**, 44%   **25**, 41%   **26**, 52%   **27**, 52%

28, 29%   **29**, 41%   **30**, 40%   **31**, 15%

Scheme 8.

32, 80%   **33**, 90%   **34**, 84%   **35**, 76%

36, 76%   **37**, 60%   **38**, 70%   **39**, 60%   **40**, 18%
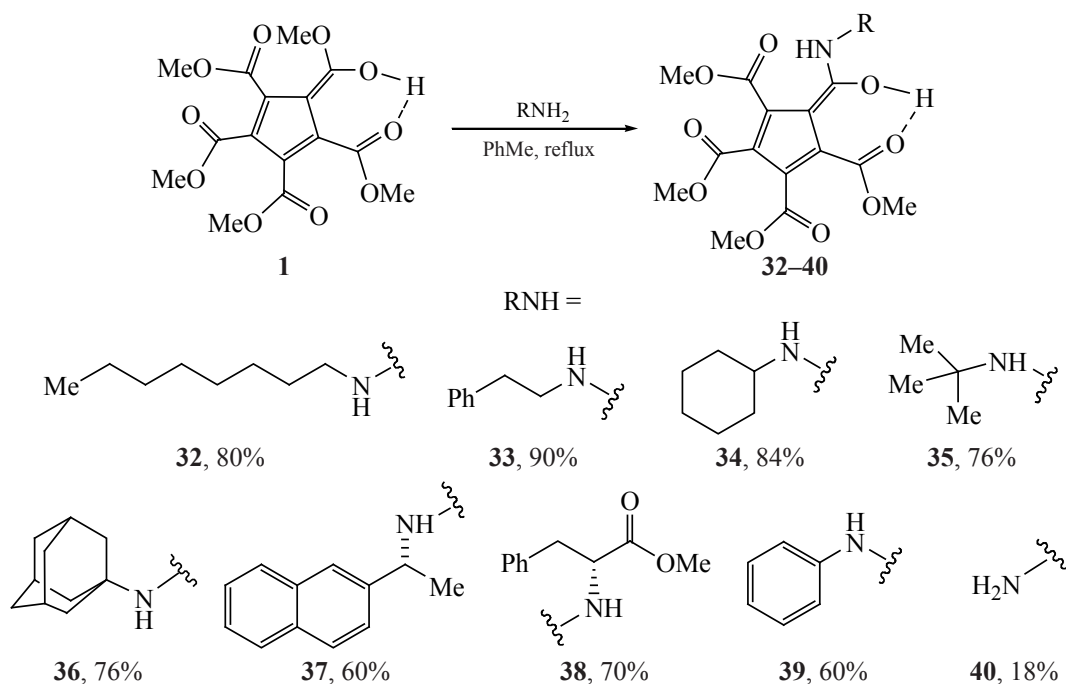
amido derivatives of PCCP. Thus, boiling PCCP **1** with primary amines produced monoamides in good yields (Scheme 8).

Derivatives **32–34** were prepared on the basis of aliphatic alcohols, PCCPs **35** and **36** were obtained from bulkier amines (*t*-BuNH$_2$ and 1-AdNH$_2$), and chiral derivatives **37** and **38** were synthesized from (*R*)-(+)-1-(1-naphthyl)ethylamine, and methyl ʟ-phenylalanine. It was found that the weakly nuclophilic aniline reacted to form PCCP monoamide **39** in 60% yield, and the

yield of the reaction with ammonia was as low as 18%. Secondary amines did not react by this procedure, and the reaction with 2 equiv of (*R*)-(+)-1-(1-naphthyl)-ethylamine gave 1,2-diamide derivative **41** in 30% yield (Scheme 9).

The molecular structures of monoamide **37** and diamide **41** were established by XRD analysis, according to which these compounds exist in the hydroxyfulve-ne form, and, therewith, each of the amido *N*–H bonds is H-bonded to the neighboring carbonyl group.

Scheme 9.

Scheme 10.

RO = (12), (42), Ar = 1-C$_{10}$H$_7$ (37), Ar = Ph (43).
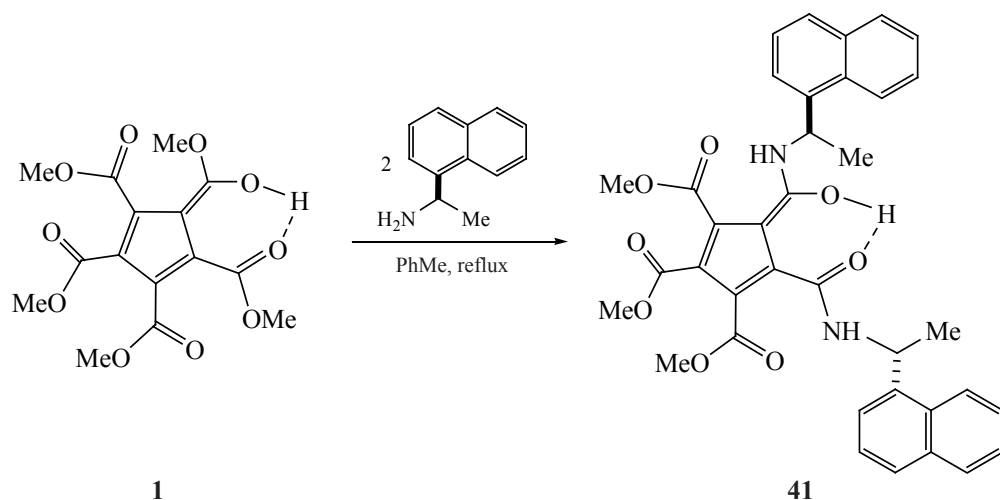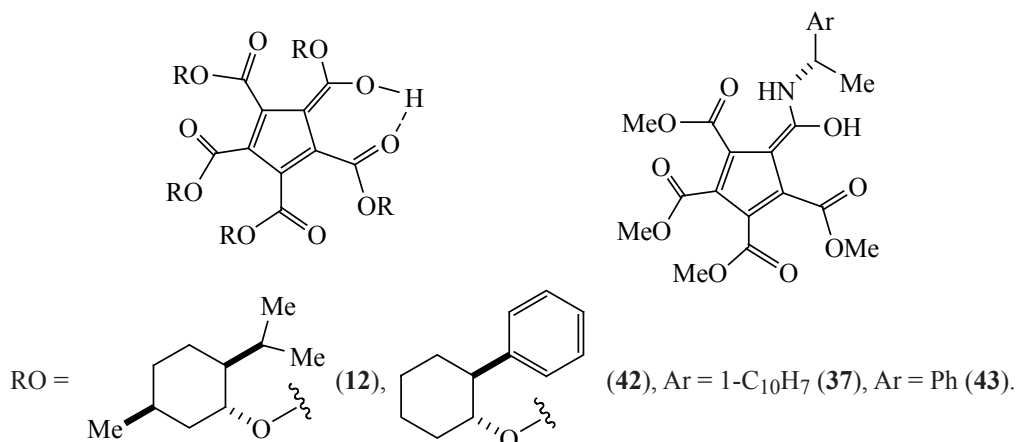
2. CHIRAL ACID PCCP CATALYSTS OF ENANTIOSELECTIVE REACTIONS

Chiral Brønsted acid catalysts are actively used for the synthesis of valuable chemical compounds in the enantioenriched form [47]. The most common such chiral catalysts are BINOL-derived ([1,1'-binaphthalene]-2,2'-diol) phosphoric acids [48], whose reactivity and selectivity are controlled by varying 3,3' substituents or the acid component, as well as phosphoric acids with other chiral cores, specifically VAPOL [49] and SPINOL [50]. However, to create the artificial chirality in such structures requires labor-consuming separation into enantiomerically pure compounds during synthesis, complicates their optimization, and limits their widespread use due to the high cost.
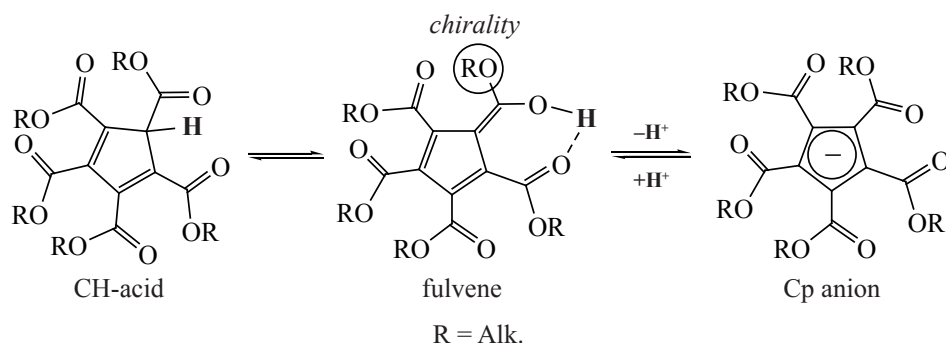
Another class of effective chiral Brønsted acid catalysts but not having the above-mentioned dis-advantages includes PCCPs **12** and **42**, recently synthesized by the derivatization of PCCP **1** with chiral alcohols, as well as its amido derivatives **37** and **43**, synthesized using simple chiral amines (Scheme 10) [30].

PCCPs **1**, **12**, and **42** are strong CH acids existing generally as fulvenes [27, 43, 44], and their deprotonation gives highly stable Cp anions. The aromatic stabilization of these anions, as well as the presence of 5 electron-acceptor alkoxycarbonyl groups significantly increase their acidity, making it comparable with the acidity of strong mineral acids and increasing the efficiency of such catalysts, the enantioselectivity of which is associated with the chiral alkoxy substituents (Scheme 11) [30, 51–53].
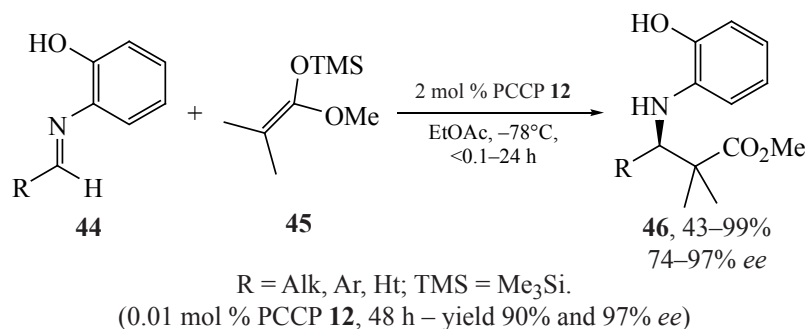
Chiral PCCPs **12**, **37**, **42**, and **43** were used to catalyze the Mukaiyama–Mannich reaction [30, 54] for the enantioselective addition to imines **44** of ketene acetal **45** (Scheme 12).

It was found that PCCP **12** not only outperforms in enantioselectivity (*ee*) (97% vs 89%) BINOL-phosphoric acid commonly used to catalyze this reaction, but also exhibits high activity, and, therefore, in concentration can be safely reduced to 0.01 mol % without sacrificing the enantioselectivity of adduct **46** formation, and monoamides **37** and **43** can also be used

Scheme 11.

R = Alk.

Scheme 12.

R = Alk, Ar, Ht; TMS = Me₃Si.
(0.01 mol % PCCP **12**, 48 h – yield 90% and 97% *ee*)

in this reaction as enantioselective catalysts, albeit with lower efficiency.

Furthermore, PCCP **12** was used for the enantioselective addition silylketene acetal **45** to oxocarbenium ions **47** (oxocarbenium Mukaiyama aldols [55]) generated in situ from acetals **48**, which allowed synthesis of alkoxy esters **49** with good yiedls and high enantioselectivity (Scheme 13).

It was shown that the aromatic Cp anion generated from PCCP catalyst **12** and stabilized by 5 CO_2R groups, which increase the acidity of the catalyst, plays a central role. According to XRD data for the Me_4N^+ salt of PCCP **12** [30], its ester groups have a propeller orientation relative to the planar Cp ring. In this case, the chiral menthyl substituents imparting enantioselectivity to the reaction are directed in one direction, forming a hydrophobic pocket, and the C=O groups are oriented in the opposite direction. The stereochemical non-rigidity of PCCP **12** allows realization, together with the reaction substrates, of suitable transition states to ensure that the catalytic process occurs in the desired direction.

The stereochemical rationale for the catalysis of the Mannich reaction includes the association of the protonated imine with one of the carbonyls of catalyst **12** through 2 H-bonds to form structure **50** (Scheme 14, *a*).

The carbonyl group is involved in this process, which leads to that the iminium ion turns to be located in the immediate vicinity of the neighboring carboxymenthyl group. The resulting blocking of the front side (reprochiral surface) of the iminium ion explains the observed stereochemistry.

A similar model was also proposed for the addition of the oxocarbenium ion to PCCP **12**; however, in this case, the binding is realized only through one H-bond between the *o*-phenolic group of the oxocarbenium ion and the Cp carbonyl (Scheme 14, *b*). In structure 51, additional stabilizing interactions occur between the C–H bonds adjacent to the oxocarbenium oxygen and the PCCP **12** carbonyl closest to the substrate and/or the Cp ring. In this case, blocking the π face of the substrate leads to a reaction across the *si* prochiral surface, which corresponds to the observed stereoselectivity for the *R*-enantiomer.

According the mechanism of the catalysis of the oxocarbenium aldol reaction of **12**, the initial protonation of acetal **48** with **12** leads to intermediate salt **52** (Scheme 15).

The addition of silylketene acetal **45** to the highly electrophilic oxocarbenium ion in salt **52** first leads to structure **53** and then to intermediate **54**. The subsequent reaction of the silyl group with the alcohol generated at

Scheme 13.

R = Alk; TMS = Me₃Si.
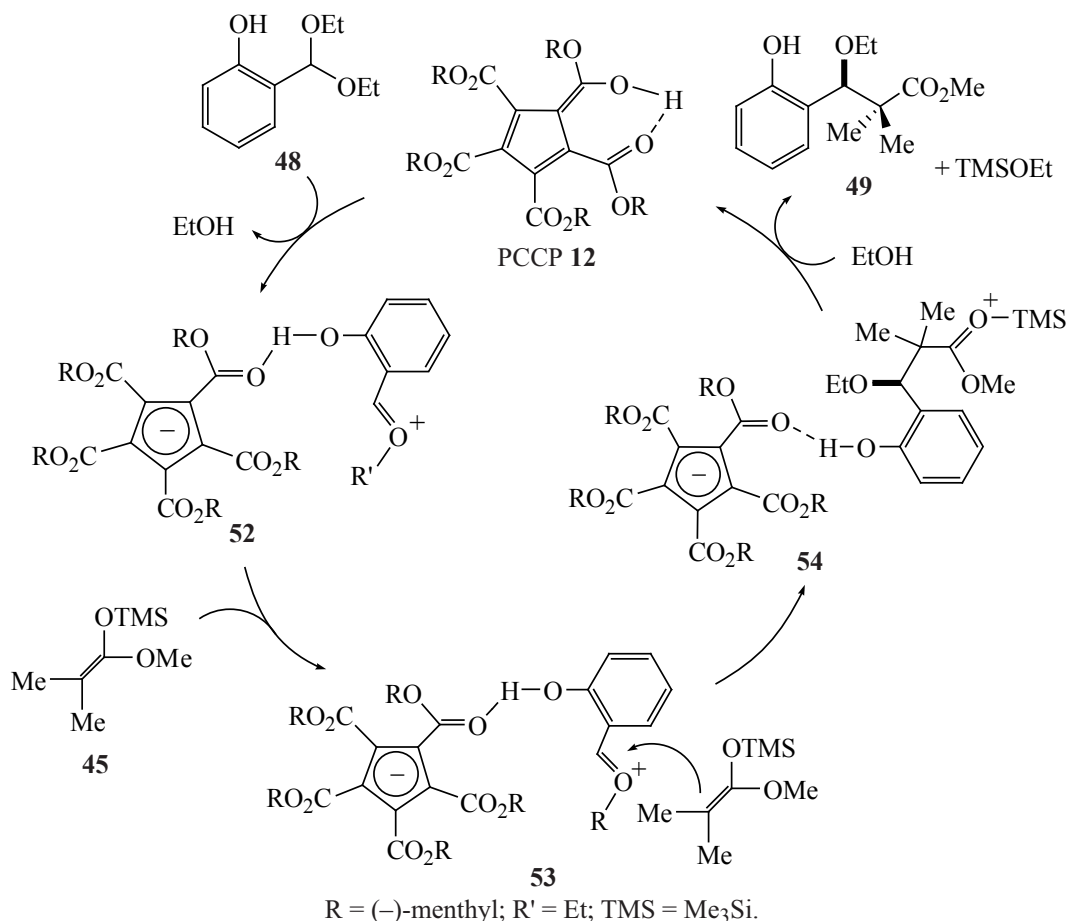
Scheme 14.

R = Alk.
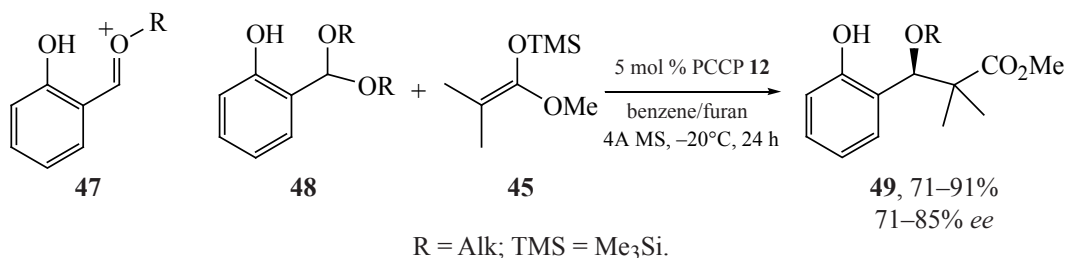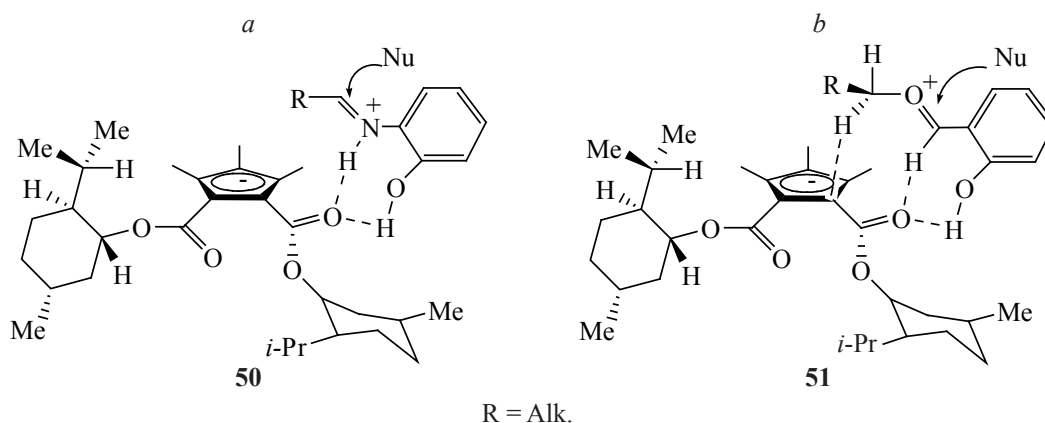
the initial stage of ionization leads to product **49** and return acid **12** in the catalytic cycle.

The tetrahydroquinoline fragment is contained in many biologically active natural compounds, as well as in a wide range of drugs [56], and this stimulates the development of synthetic approaches to these compounds. The most common method of synthesis involves the regioselective catalytic reduction of quinoline derivatives with hydrogen or its sources [57]. It is known that chiral phosphoric acids derived from BINOL catalyze the hydrogenation of quinolines with asymmetric transfer, when Hantzsch ester (HEH) 55 is used as a source of hydrogen [58].

Scheme 15.

R = (–)-menthyl; R' = Et; TMS = Me₃Si.
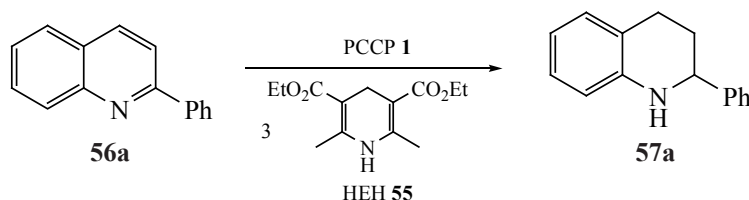
Scheme 16.

PCCP acids **1** and **12** were used as effective catalysts for the hydrogenation of 2-aryl(alkyl)quinolines **56** as a result of their activating protonation of the substrate and subsequent hydride transfer of from the Hantzsch ester to it (Scheme 16) [59].

We used the example of the reduction of 2-phenylquinoline (**56a**) to study the effect of the medium on the yields of product **57a**, which varied from moderate (33–46%; MeOH, DMF) to high (86–92%; toluene, CHCl$_3$). In polar media, the reaction yield decreased, probably due to the effect of the competitive reaction of the H-bonds between the solvent and the catalyst.

Taking into account that the highest yields of product **57a** were obtained in CHCl$_3$, the effect of PCCP **1** loading on the reaction yield was studied in this solvent. Thus, a decrease in the PCCP **1** loading from 5 to 1 mol % did not decrease the yield, while with a loading of 0.1–0.001 mol %, only traces of product **57a** formed. However, after raising the temperature to 60°C, product **57a** was isolated in good yield even with 0.001 mol % of PCCP **1**, but this reaction did not proceed without catalyst. When this reaction was carried out under the same conditions in the presence of diphenyl phosphate, product **57a** was obtained in a yield of only 61%, which indicates a higher activity of PCCP **1** compared to other catalysts.

Under the optimal conditions, we assessed the scope the PCCP **1**–catalyzed hydrogenation of 2-substituted quinolines **56b–56k** (Scheme 17).

It was found that quinolines **56b–56k** all were reduced in good to excellen yields.

In the asymmetric version of this reaction with chiral PCCP catalyst **12** (1 mol %), quinolines **56a**, and **56i** gave their reduction products with enantiomeric excesses of 34 and 43%, respectively (Scheme 18).

The asymmetric reduction of 3-substituted quinolines [60] was performed using chiral PCCPs **12** and **58** and various Hantzsch esters (HEH). Since chiral 3-substituted tetrahydroquinolines are the structural fragments of a wide range of biologically active compounds, as well as drugs, the development of methods of their synthesis is an urgent task [61].

It was found that the hydrogenation reaction of 3-methylquinoline **59a** proceeded with better enantioselectivity and yield with PCCP **12**, while acid **58** gave a racemic mixture of products and was excluded from further studies (Scheme 19).

The best reaction parameters were obtained with diethyl Hantzsch ester at 25°C in toluene. Decreasing the loading of PCCP **12** decreased the conversion and enantioselectivity, while increasing the loading (to 10 mol %) increased the yield and slightly increased enantioselectivity.

Scheme 17.
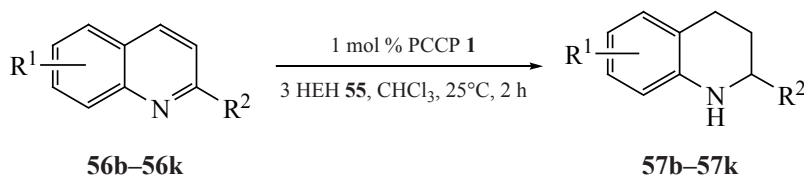
57b (R^1 = H, R^2 = 4-MeC$_6$H$_4$, yield 77%)
57c (R^1 = H, R^2 = 2,4-Me$_2$C$_6$H$_3$, yield 92%)
57d (R^1 = H, R^2 = 4-*i*-PrC$_6$H$_4$, yield 97%)
57e (R^1 = H, R^2 = 4-MeOC$_6$H$_4$, yield 93%)
57f (R^1 = H, R^2 = 2-FC$_6$H$_4$, yield 84%)

57g (R^1 = H, R^2 = 4-ClC$_6$H$_4$, yield 87%)
57h (R^1 = H, R^2 = 4-BrC$_6$H$_4$, yield 89%)
57i (R^1 = H, R^2 = Me, yield 91%)
57j (R^1 = 6-F, R^2 = Me, yield 98%)
57k (R^1 = 6-Cl, R^2 = Me, yield 94%)

Scheme 18.

56a, **56i**   **57a**, **57i**

R = Ph (yield 93%, *ee* 34%), Me (yield 94%, *ee* 43%)
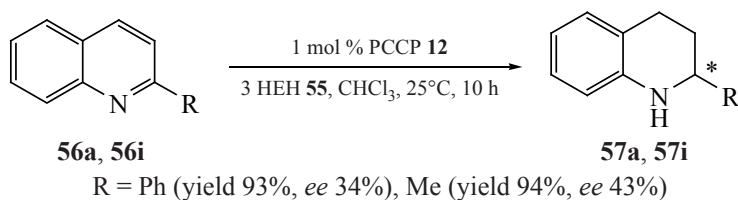
Under the optimal conditions, was assessed the scope of this PCCP **12**–catalyzed reaction for quinolines **59a–59j** (Scheme 20).

It was found that substrates **59a–59j** all were readily reduced, giving products **60a–60j** in moderate to good yields. In 3-alkylquinolines **59a–59f**, a steric substituent effect was observed. For example, compound **59e** containing a bulky cyclohexyl group reacted with a high enetioselectivity, but the reaction yield was than with quinolines **59a–59d**, and **59f**.

The catalytic enantioselective desymmetrization of mesoepoxides is an attractive method for the preparation of chiral alcohols [62], since mesoepoxide substrates are readily available compounds, and 1,2-difunctional products with two adjacent chiral centers are useful chemical structural blocks [63]. Various nucleophiles used in these reactions include amines, azides, alcohols, thiols, and halides, and, as a rule, the reactions are catalyzed by Lewis acids

[62]. The reaction was successfully accomplished with 2-sulfanylbenzothiazoles and a chiral BINOL-phosphoric acid [64]. Since chiral PCCP acids proved to be a good alternative to BINOL-phosphoric acids in terms of availability and efficiency, they were used for the enantioselective desymmetrization of mesoepoxides with 2-thiobenzothiazoles [65]. The ring opening reaction of cyclohexene oxide **61a** with benzothiazole **62a** in the presence of PCCP **12** was used as a model reaction to optimize its conditions (Scheme 21).

The reaction in the absence of PCCP **12** (CH$_2$Cl$_2$, 10°C, 12 h) gave a racemic product **63a** in 18% yield, while adding 2.5 mol % of PCCP **12** increased the yield to 93% and led to an enantiomeric ratio (*er*) of 57 : 43. The best result (99% yield, 72 : 28 *er*) was obtained in CHCl$_3$ at 22°C. The use of other sulfur and nitrogen nucleophiles in this reaction did not met with success, however, the addition of a catalytic amount of amine bases together with PCCP **12**, leading to H-bonded adducts or ammonium salts, had an effect on
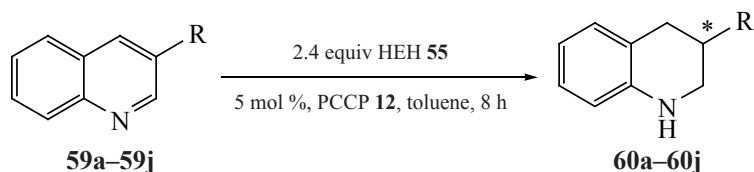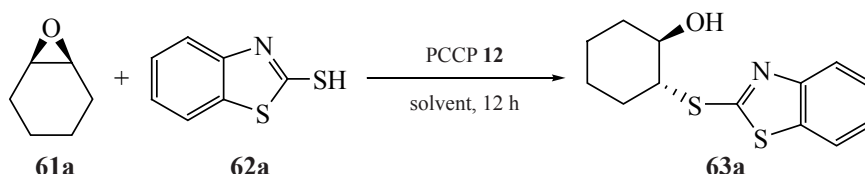
Scheme 19.

59a   **60a**
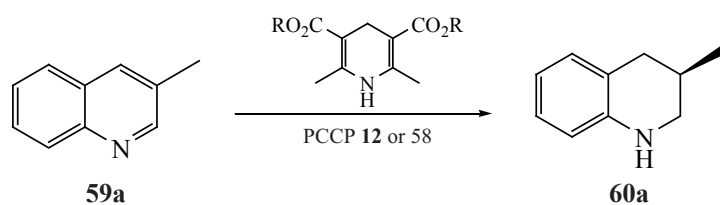
R = Me, Et, *t*-Bu, Bn, allyl.

Solvents: Et$_2$O, CH$_3$C$_6$H$_5$, C$_6$H$_6$, THF, dioxane, MeCN, CH$_2$Cl$_2$.
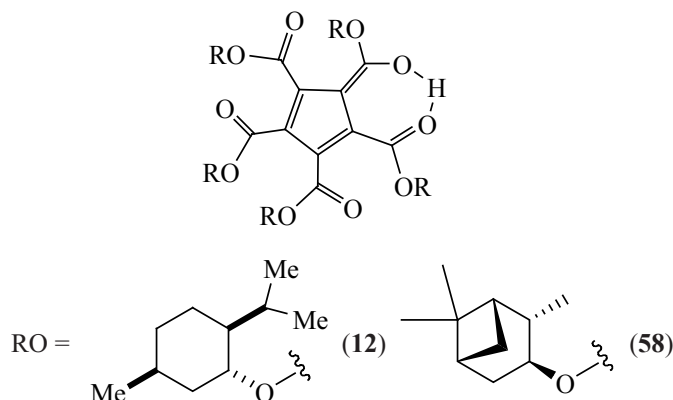
Scheme 20.

60a (R = Me, yield 77%, *ee* 46%)
60b (R = Et, yield 74%, *ee* 55%)
60c (R = Pr, yield 97%, *ee* 52%)
60d (R = *n*-Bu, yield 93%, *ee* 51%)
60e (R = Cy, yield 65%, *ee* 60%)

60f (R = Bn, yield 81%, *ee* 41%)
60g (R = 3,5-Me$_2$C$_6$H$_3$, yield 72%, *ee* 53%)
60h (R = 2-C$_{10}$H$_7$, yield 64%, *ee* 52%)
60i (R = 3-FC$_6$H$_4$, yield 70%, *ee* 60%)
60j (R = 4-FC$_6$H$_4$, yield 88%, *ee* 75%)

Scheme 21.

the reaction enantioselectivity and yields. Thus, Et$_3$N and *i*-Pr$_2$NH reduced yields and enantioselectivity, while derivatives of aniline (*i*-PrNHPh, Ph$_2$NH), pyridine (2,6-*t*-Bu$_2$C$_5$H$_3$N, 2,6-Ph$_2$C$_5$H$_3$N), and pyridine itself gave good yields and increased the enantioselectivity of the reaction compared to the reaction with PCCP **12** alone.

Probably, aniline or pyridine bases, when present, interacted with PCCP **12** to form, due to π-π-stacking interactions, stronger adducts than adducts of PCCP **12** with Et$_3$N and *i*-Pr$_2$NH (such stacking interaction

with aliphatic amines are impossible), which increased enantioselectivity. Further increase in enantioselectivity was achieved with a chiral PCCP catalyst **64**; in this case, product **63a** was obtained in a yield of 99% and an enantioselectivity of 89.5 : 10.5 *er*. The high steric hindrance in PCCP **64** improved its performance compared to PCCP **12**.

By varying the substituents in the aryl ring of benzothiazoles **62a–62j**, products **63a–63j** were obtained in moderate-to-good yields and enantioselectivity (Scheme 22).

Scheme 22.
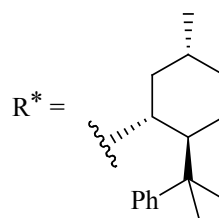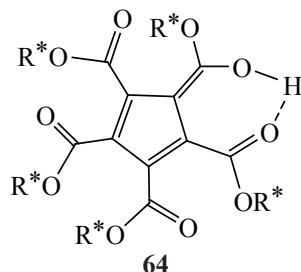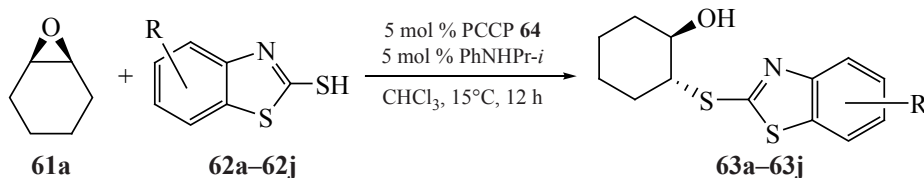
63a (R = H, yield 99%, *er* 89.5 : 10.5)
63b (R = 5-OMe, yield 86%, *er* 86 : 14)
63c (R = 5-OCF$_3$, yield 99%, *er* 90.5 : 9.5)
63d (R = 5-Me, yield 96%, *er* 88.5 : 11.5)
63e (R = 6-Me, yield 99%, *er* 89.5 : 10.5)

63f (R = 5-Cl, yield 61%, *er* 90.5 : 9.5)
63g (R = 6-Cl, yield 19%, *er* 82.5 : 17.5)
63h (R = 5-F, yield 92%, *er* 89.5 : 10.5)
63i (R = 5-CN, yield 51%, *er* 87 : 13)
63j (R = 5-NO$_2$, yield 32%, *er* 81 : 19)

Scheme 23.

61a–61h   **62a**   **63a–63h**

R–R = $(CH_2)_4$ (**a**), $(CH_2)_3$ (**b**), $(CH_2)_5$ (**c**), $CH_2CHCHCH_2$ (**d**),
1,2-$(CH_2)_2C_6H_4$ (**e**); R = Ph (**f**), Pr (**g**), CH_2 (**h**).
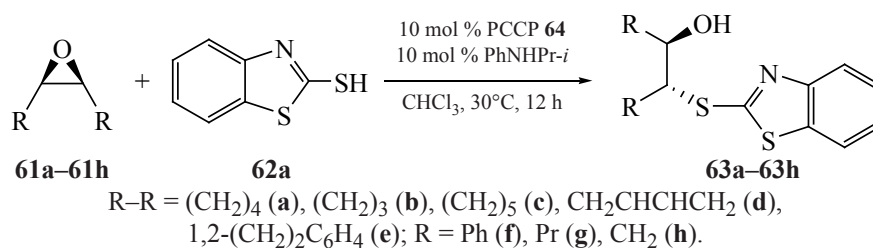
Table 1. Scope of mesoepoxides **61a–61h** and **63a–63h**

Compound		Yield, %	Enantioselectivity, *er*
structural formula	number		
	61a **63a**	93	90 : 10
	61b **63b**	73	81.5 : 18.5
	61c **63c**	74	87 : 13
	61d **63d**	80	86.5 : 13.5
	61e **63e**	93	81.5 : 18.5
	61f **63f**	62	68 : 32
	61g **63g**	90	85 : 15
	61h **63h**	49	89 : 11

With benzothiazole **62c**, product **63c** was obtained in a yield of 99% and an enantioselectivity of 90.5 : 9.5 *er*. Benzothiazoles with electron-donor and electroneutral substituents gave higher yields and enantioselectivities, than substrates with electron-acceptor groups.

The effect of the structure of mesoepoxides **61a–61h** on their desymmetrization with benzothiaozoles **62a**

was studied with the use of PCCP **64** (Scheme 23, Table 1).

The highest enantioselectivity for epoxides **61a–61h** was obtained at 15–30°C and decreased with increasing temperature. The epoxide ring opening products **63a**, **63c**, **63d**, and **63h** were obtained with a better enantioselectivity, while the results for compounds **63b**, **63e**, **63f**, and **63g** were moderate.

Scheme 24.

R* = (−)-menthyl; Ar = 2,4,6-(i-Pr)$_3$C$_6$H$_2$, 9-C$_{14}$H$_9$.
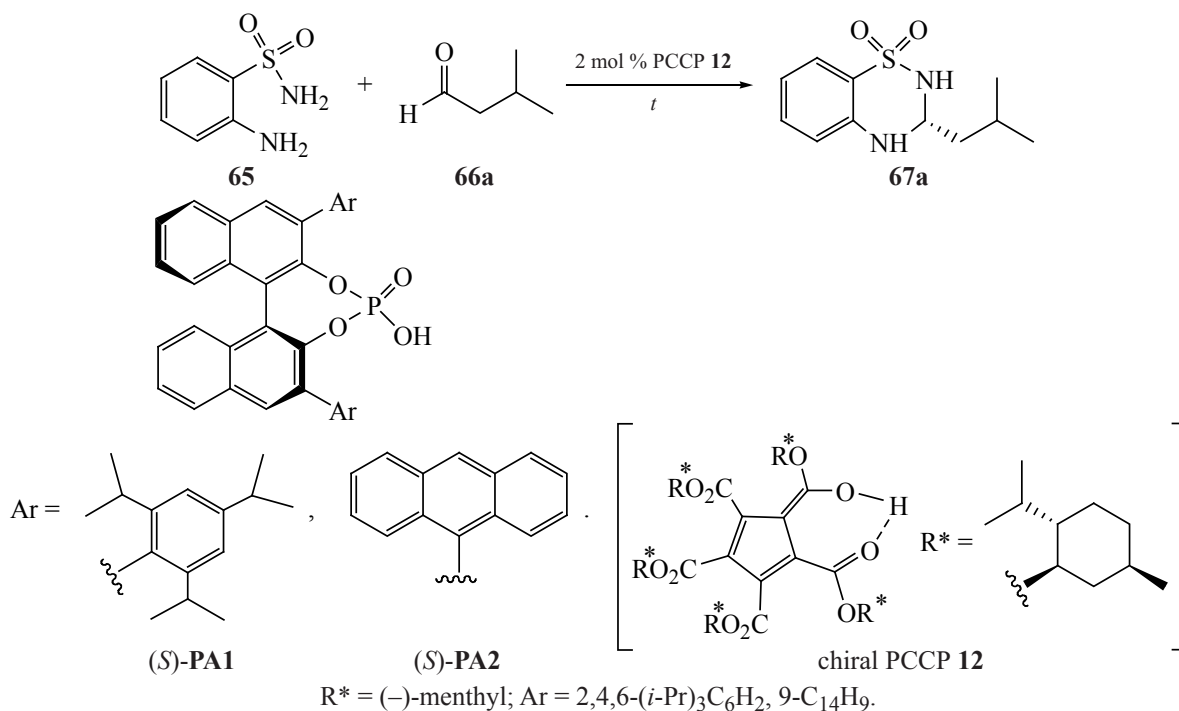
Cyclic aminals are often included as structural fragments in various drugs, for example, diuretics such as aquamox, thiabutazide, and bendroflumethiazide, which are widely used to treat hypertension [66]. However, their enantiomers have different biological activities [67], and drugs used in medical practice are still supplied in the form of a racemic mixture because of the lack of effective asymmetric methods for their synthesis.

To optimize the conditions of the enantioselective synthesis of cyclic amines, Sui et al. [68] chose the

reaction of sulfonamide 65 with aldehyde 66a (CH$_2$Cl$_2$, −20°C, 24 h) in the presence of 2 mol % PCCP 12 (Scheme 24, Table 2) as a model reaction.

Chiral acid PCCP 12 showed better results in enantioselectivity and reaction yield than chiral phosphoric acids based on BINOLs (S)-PA1 and (S)-PA2. It turned out that toluene gave the highest yield and the best enantioselectivity, while in other solvents, product 67a formed with good yields but with lower enantioselectivity. Decreasing the PCCP 12 loading from 2 to 1 mol % decreased the yield to

Table 2. Optimization of aminolyzation conditions

Catalyst	Solvent	T, °C	Yield, %	Enantioselectivity ee, %
(S)-PA1	CH$_2$Cl$_2$	−20	83	43
(S)-PA2	CH$_2$Cl$_2$	−20	82	38
PCCP 12	CH$_2$Cl$_2$	−20	96	64
PCCP 12	THF	−20	73	49
PCCP 12	EtOAc	−20	81	53
PCCP 12	toluene	−20	98	96
PCCP 12[a]	toluene	−20	73	93
PCCP 12	toluene	−45	97	98

[a] PCCP 12 concentration 1 mol %.

Scheme 25.
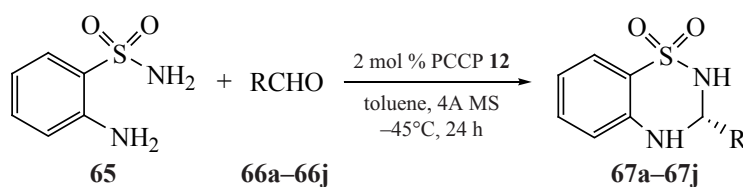
66a–66j, R = *i*-Bu (**a**), CH$_2$C(CH$_3$)$_3$ (**b**), *i*-Pr (**c**), *н*-Bu (**d**),
Pr (**e**), Et (**f**), Me (**g**), cyclopropyl (**h**), cyclopentyl (**i**), Cy (**j**).

67a (R = *i*-Bu, yield 95%, *ee* 98%)
67b [R = CH$_2$C(CH$_3$)$_3$, yield 92%, *ee* 94%]
67c (R = *i*-Pr, yield 91%, *ee* 93%)
67d (R = *n*-Bu, yield 92%, *ee* 94%)
67e (R = Pr, yield 94%, *ee* 90%)

67f (R = Et, yield 93%, *ee* 90%)
67g (R = Me, yield 92%, *ee* 85%)
67h (R = cyclopropyl, yield 88%, *ee* 72%)
67i (R = cyclopentyl, yield 90%, *ee* 93%)
67j (R = Cy, yield 93%, *ee* 88%)

73%. An increase in the temperature adversely affected enantioselectivity, and at –45°C it reached 98%. For the optimal conditions, the following parameters were chosen: 2 mol % PCCP **12**, –45°C, 70 mg of 4Å molecular sieves.

Using the optimal conditions, a wide variety of aldehydes **66a–66j** were introduced into this reaction to assess its substrate scope (Scheme 25).

For exampe, aliphatic aldehydes **66a–66f** gave aminals **67a–67f** in a yield of 91–95% and an enantioselectivity of 90–98%, and the enantioselectivity of the formation of aminal **67g** from acetaldehyde **66g** was as low as 85%. It was shown that the cycloalkanecarboxaldehyde ring size appreciably affetcs the reaction enantioselectivity. This, aminal **67i** was obtained from cyclopentanecarboxaldehyde **66i** with a high enantioselectivity (93%), whereas the respective values for aminals **67j** (*ee* 88%) and **67h** (*ee* 72%) obtained from cyclic aldehydes **66j** and **66h** are lower.

Scheme 26 depicts the plausible route of the reaction of 2-aminobenzenesuslfonamide **65** with aldehydes **66**, catalyzed by chiral PCCP acid **12**.

The protonation of aldehyde **66** with PCCP acid **12** gave compound **68**, further on the aldehyde condensed with sulfonamide **65** to form the enantiodetermining structure **69**, in which the chiral catalyst PCCP **12** combined the sulfonamido and imino groups via H-bonds. Because of this, the sulfonamido attacked the imine mainly from the sterically less loaded surface *Re*, imparting the *R*-configuration to product and regenerating PCCP 12 for the next catalytic cycle.

Ketones with α-heteroatomic substituents are of considerable interest due to their widespread use as building blocks in the synthesis of more complex structures. In addition, they are found as key substructures in many biologically active compounds and drugs, for example, in bupropion [69] and brephedrone [70], drugs used in the therapy of psychiatric disorders.

A one-step asymmetric synthesis of α-heterosubstituted ketones via sulfur-mediated bifunctionalization of internal alkynes is shown in Scheme 27 [71].

According to this scheme, alkyne **70** was attached by Tf$_2$O activated with Ph$_2$SO to give vinylsulfonium intermediate **71**, whose hydrolysis formed α-sulfonium ketone **72**. At the last, enantiodetermining step of this reaction, chiral PCCP catalyst **12** was added, leading to compound **73**, after which aniline was added as a nucleophile to the latter at –20°C to obtain α-aminoketone **74** in a yield of 67% and an enantioselectivity of 75 : 25 *er*. This result points that the use of chiral catalysts makes it possible to prepare enantioenriched α-aminoketones directly from alkynes.

The asymmetric protonation of prochiral enolates is a simple and reliable method for the preparation of optically active α-substituted carbonyl compounds [72]. Stable prochiral silylenol ethers often used for this purpose are protonated with an excess of an achiral proton source in the presence of chiral Lewis or Bronsted acids [73].

Li et al. [74] reported the asymmetric protonation of silyl enol ethers using chiral PCCP catalysts and water (methanol) as a source of protons. To select the most efficient catalyst for this reaction, silyl enol ester **75a**

Scheme 26.

chiral PCCP **8**
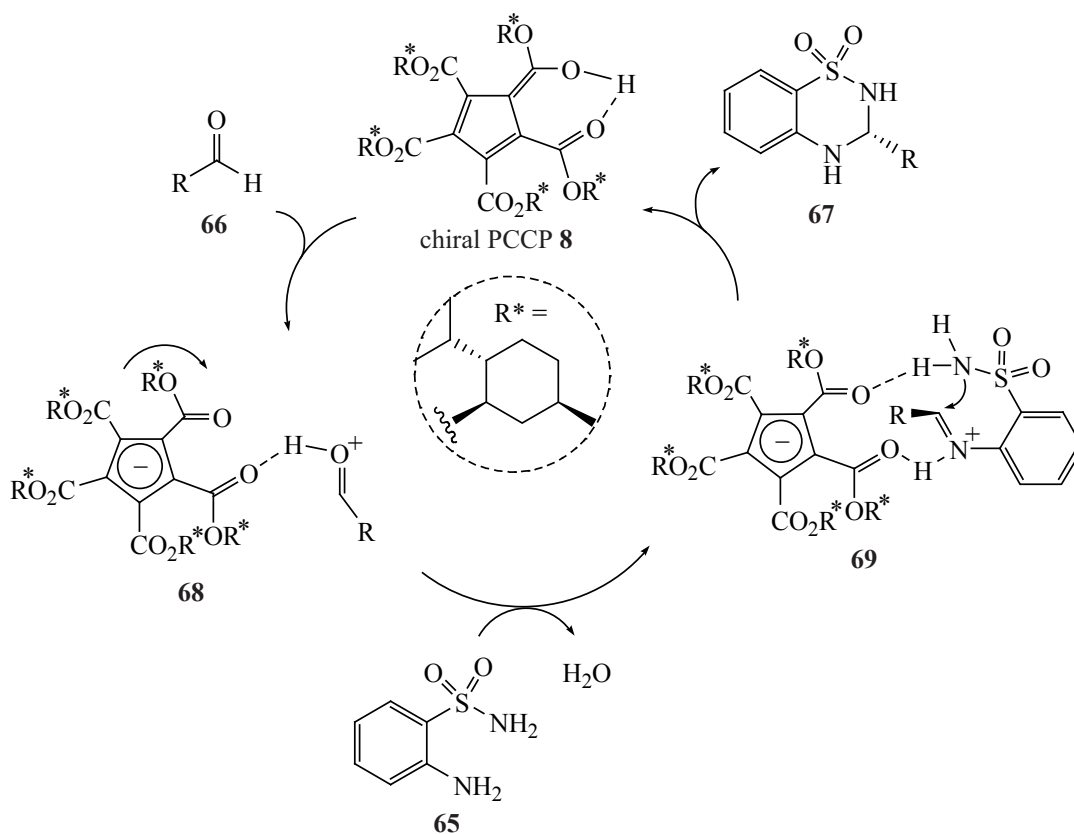
and chiral acids PCCP **12**, **58**, **64**, **77** and **78** were tested, and methanol was chosen as the source of protons (Scheme 28).

The best results were obtained with PCCP **77** (yield of **76a** 88%, enantioselectivity 28%), and it was

used for further research (Table 3). To increase the stereoselectivity of the reaction, optimization of its conditions was performed.

It was shown that phenols cannot be used as sources of protons, because the reaction was nonstereoselective

Scheme 27.

74
67%, *er* 75/25
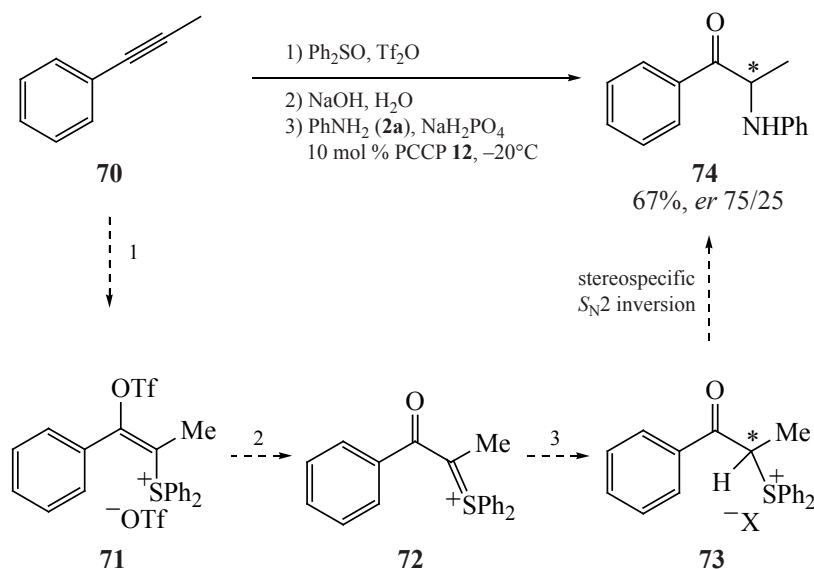
Scheme 28.

and provided low yields of the target products. Good results were obtained with methanol, but the best result was obtained with H_2O (xylene, –10°C, yield 99% and enantioselectivity 74%). A decrease in temperature did not lead to an increase in the selectivity of the reaction.
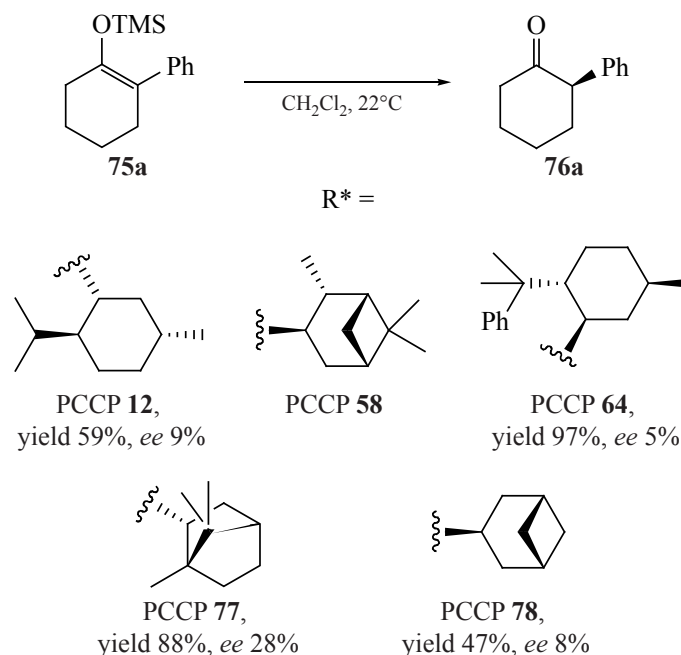
The aza-Piancatelli reaction is one of the popular methods for the synthesis of nitogen-substitued polyfunctional cyclopentenes **85** from readily available 2-furylcarbinols **79** (Scheme 29) [75].

It was shown that the products of this reaction have a *trans* bond between the substituents on C^4 and C^5 [76], and the stage of conrotatory 4π electrocyclization, which converts cation **83** formed during this reaction into product **85**, is responsible for controlling the relative

diastereoselectivity in this cascade rearrangement (Scheme 30).

To control the absolute stereochemistry of this reaction, Cai et al. [77] used chiral phosphoric acids, which are capable of controlling clockwise or counter-clockwise rotation in the key stage of 4π-electrocyclization as an enantioselectivity inducing element.

To expand the range of catalysts for this reaction, chiral PCCP acid **12** was tested to find that the reaction of furylcarbinol **79a** with aniline **80a** in the presence of this catalyst gave 4-aminocyclopentenone **85a** with a yield of 78% and enantioselectivity of 65% (Scheme 31) [78].

Table 3. Optimization of the conditions of the asymmetric protonation of silyl enol ether **75a**, catalyzed by PCCP **77**

Proton source (equiv)	Solvent	T, °C	Time, h	Yield, %	Enantioselectivity *ee*, %
2,6-Dimethylphenol (2)	CH_2Cl_2	25	24	traces	–
Phenol (2)	CH_2Cl_2	25	24	51	0
EtOH (10)	CH_2Cl_2	25	12	74	16
MeOH (1.1)	toluene	–20	8	91	62
H_2O (1.1)	toluene	–20	8	94	67
H_2O (1.1)	xylene	–10	8	99	74
H_2O (1.1)	xylene	–30	8	99	74

Scheme 29.

R^1, R^2 = Ar.

Scheme 30.

enantiodetermining 4π electrocyclization

R^1, R^2 = Ar.
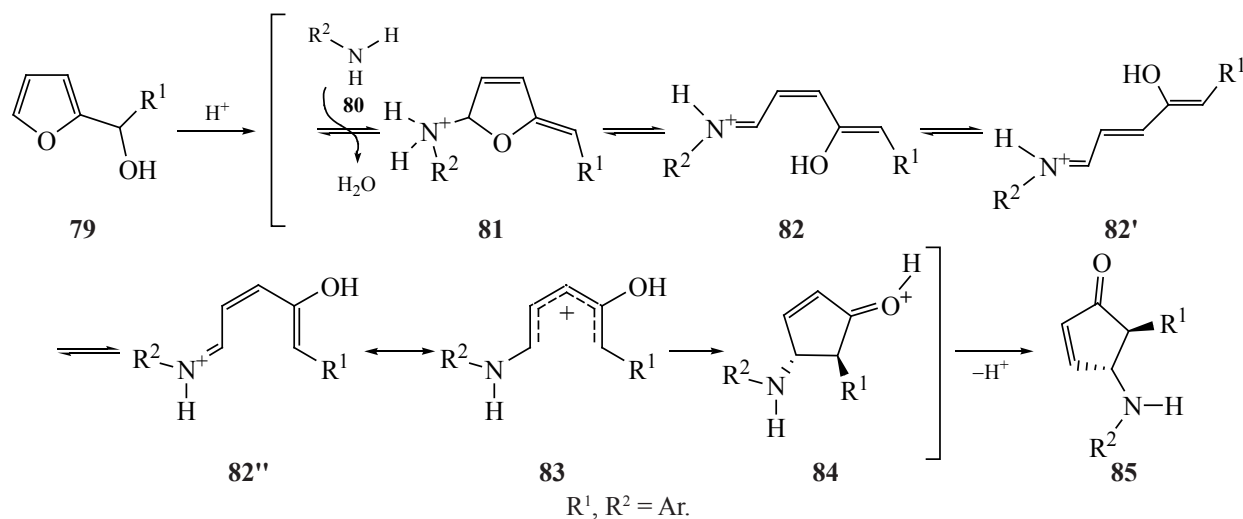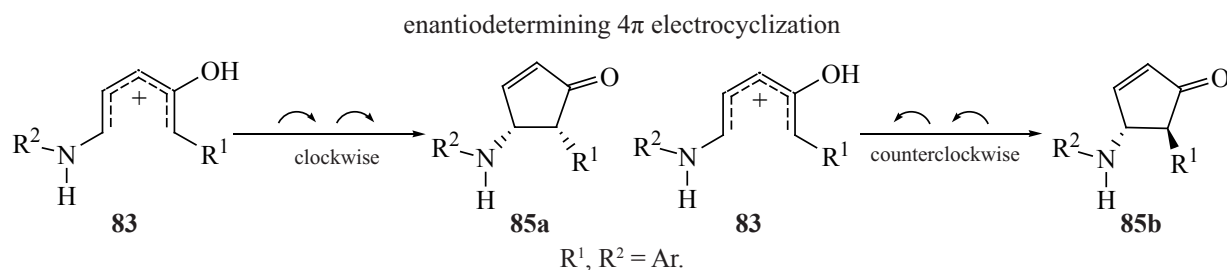
At 30°C (*ee* 73%) and 22°C (*ee* 78%), the selectivity increased by the yield dropped, but it proved possible to increased by prolonging the reaction time from 48 to 120 h. Of the solvent, CH_2Cl_2 was found to be the most suitable. The following optimal conditions were chosen for further research: 5 mol % PCCP **12**, CH_2Cl_2, 22°C, 48 h (Scheme 32).

Anilines with electron-acceptor groups in the *p*-position ensured a balance between the yields of products **85a–85e** and the enantioselectivity of the

Scheme 31.
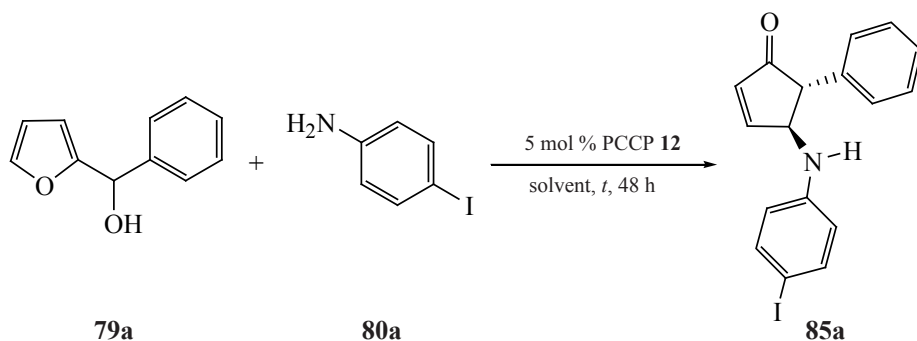
Solvent	t, °C	Yield, %	*ee*, %
CH_2Cl_2	40	78	65
CH_2Cl_2	30	46	73
CH_2Cl_2	22	26	78
$1,2\text{-}(CH_2)_2Cl_2$	22	23	68
FC_6H_5	22	20	76
MeC_6H_5	22	12	75

Scheme 32.

79a   **80a–80h**   **85a–85h**

85a (R = 4-I, yield 70%, *ee* 75%)
85b (R = 4-CN, yield 50%, *ee* 71%)
85c (R = 4-CF$_3$, yield 64%, *ee* 76%)
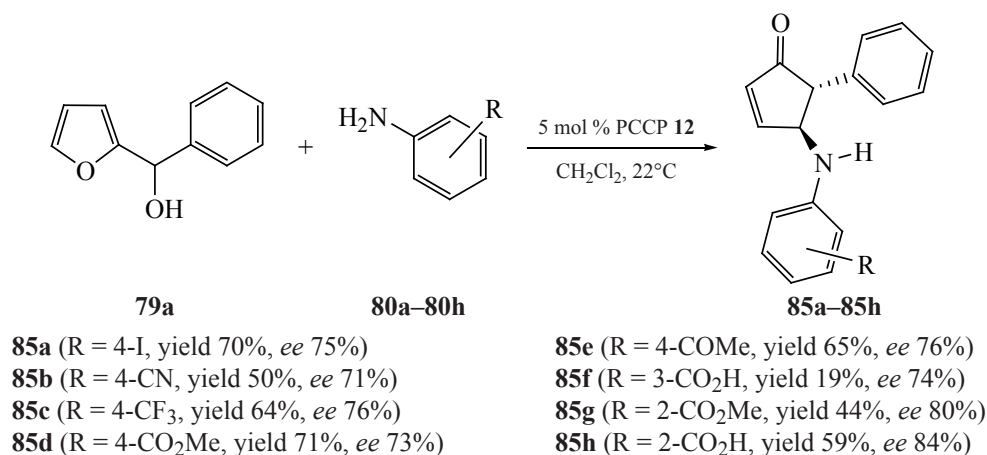**85d** (R = 4-CO$_2$Me, yield 71%, *ee* 73%)

85e (R = 4-COMe, yield 65%, *ee* 76%)
85f (R = 3-CO$_2$H, yield 19%, *ee* 74%)
85g (R = 2-CO$_2$Me, yield 44%, *ee* 80%)
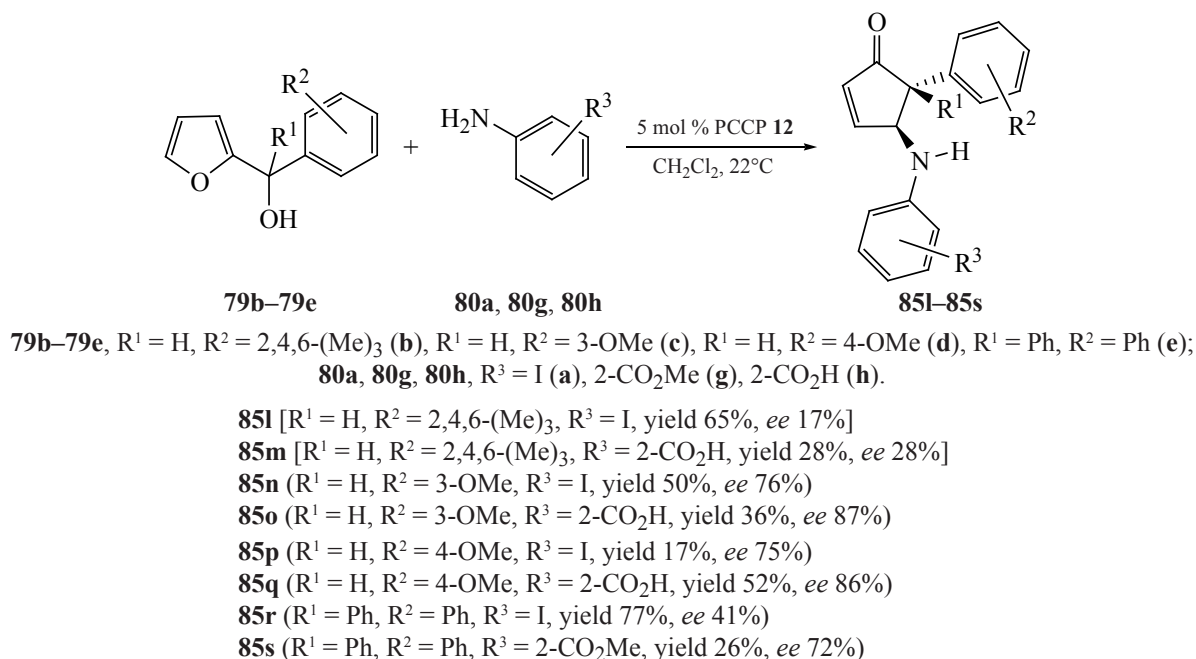**85h** (R = 2-CO$_2$H, yield 59%, *ee* 84%)

reaction. Therewith, *o*-aminobenzoic acid with an additional group of H-bonds gave the highest selectivity (**85h**, *ee* 84%). Slightly lower selectivities were observed with *m*-aminobenzoic acid (**85f**, *ee* 74%) and methyl *o*-aminobenzoate (**85g**, *ee* 80%).

To the scope of the aza-Piancatelli reaction, the dependence of its yields and enantioselectivity of nature of substitution in furylcarbinols **79b–79e** was studied (Scheme 33).
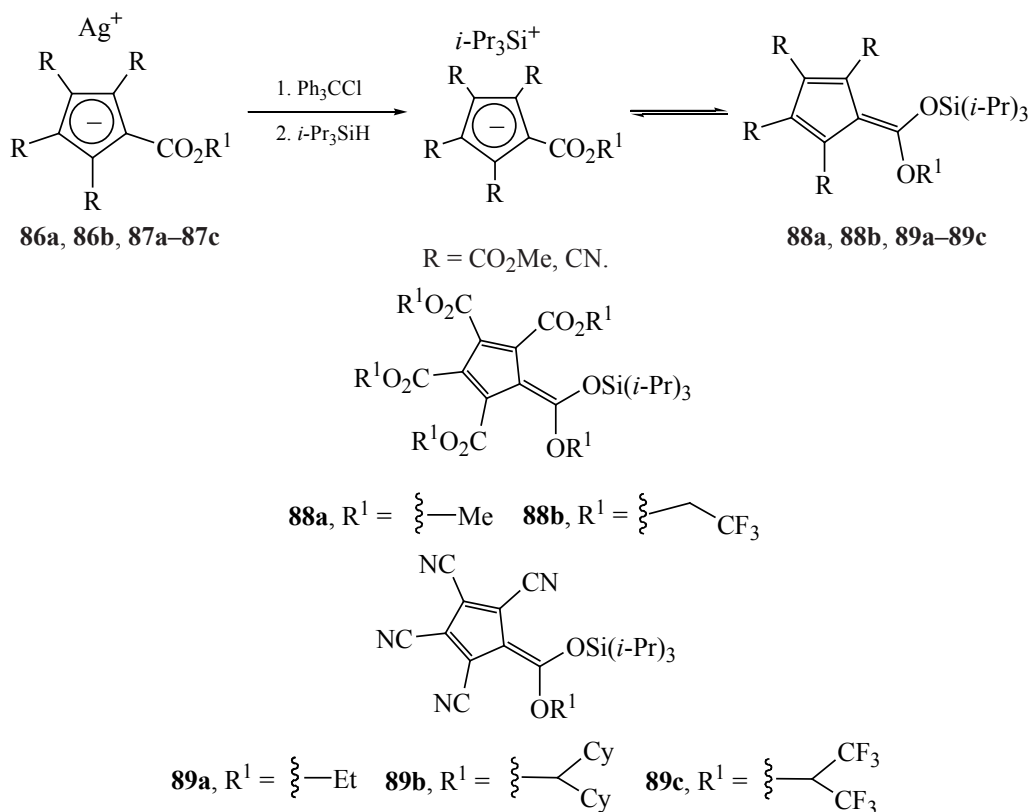
An all cases, *o*-aminobenzoic acid **80h** gave a higher enantioselectivity compared to *p*-iodoaniline **80a**, which provides evidence for the importance of the additional ability of the CO$_2$H group to bind hydrogen. On the contrary, except to compounds **85p**, **85q**, and **85a**, a lower yield was obtained with acid **80h**, probably due to an increase in the steric volume of aniline, which slows down the initial nucleophilic attack on the furan ring necessary to initiate the cascade sequence. With tertiary furylcarbinol **79e**, a noticeable difference in the selectivity of the formation of products **85r** and **85s** was observed. In this case, methyl benzoate **80g** led to a product with good enantioselectivity (72%), while aniline **80a** gave only 41% enantioselectivity for compound **85r**.

Scheme 33.

79b–79e   **80a, 80g, 80h**   **85l–85s**

79b–79e, R^1 = H, R^2 = 2,4,6-(Me)$_3$ (**b**), R^1 = H, R^2 = 3-OMe (**c**), R^1 = H, R^2 = 4-OMe (**d**), R^1 = Ph, R^2 = Ph (**e**);
80a, 80g, 80h, R^3 = I (**a**), 2-CO$_2$Me (**g**), 2-CO$_2$H (**h**).

85l [R^1 = H, R^2 = 2,4,6-(Me)$_3$, R^3 = I, yield 65%, *ee* 17%]
85m [R^1 = H, R^2 = 2,4,6-(Me)$_3$, R^3 = 2-CO$_2$H, yield 28%, *ee* 28%]
85n (R^1 = H, R^2 = 3-OMe, R^3 = I, yield 50%, *ee* 76%)
85o (R^1 = H, R^2 = 3-OMe, R^3 = 2-CO$_2$H, yield 36%, *ee* 87%)
85p (R^1 = H, R^2 = 4-OMe, R^3 = I, yield 17%, *ee* 75%)
85q (R^1 = H, R^2 = 4-OMe, R^3 = 2-CO$_2$H, yield 52%, *ee* 86%)
85r (R^1 = Ph, R^2 = Ph, R^3 = I, yield 77%, *ee* 41%)
85s (R^1 = Ph, R^2 = Ph, R^3 = 2-CO$_2$Me, yield 26%, *ee* 72%)

Scheme 34.

R = CO$_2$Me, CN.

88a, R^1 = $\S$—Me   **88b**, R^1 = $\S$—CH$_2$CF$_3$

89a, R^1 = $\S$—Et   **89b**, R^1 = $\S$—CH(Cy)$_2$ **89c**, R^1 = $\S$—CH(CF$_3$)$_2$

Silicon Lewis acids are widely used in various catalytic processes [79]. One of the methods of their activation is the binding of the silicon center to a stabilized conjugated base, whose role can be played by electron-deficient pentacyanocyclopentadienide anions, the silyl complexes of which showed good results [80]. However, no attempts have been made to modify them to increase the catalytic activity. Silicon Lewis acids were obtained from cyclopentadienes with ester groups, the presence of which made it possible to modify these acids in order to increase their catalytic activity [81].

Treatment of silver salts **86a**, **86b**, and **87a–87c** with Ph$_3$CCl followed by the reaction with *i*-Pr$_3$SiH gave silyl derivatives **88a**, **88b**, and **89a–89c** (Scheme 34).

To compare the catalytic activities of silicon Lewis acids **88a**, **88b**, and **89a–89c**, the allylation of

4-(trifluoromethyl)benzaldehyde **90** in the presence of these acids was studied (Scheme 35).

Catalyst **88a** did not show any activity, and, by-contrast, Lewis acid **88b** containing the electron-acceptor CF$_3$CH$_2$ groups catalyzed allylation to result in a 90% conversion less than within 6 h, and silicon complexes **89a–89c** exhibited the highest activity. The most active of them, complex **89a**, catalyzed complete conversion of compound **90** to **91** less than within 5 min.
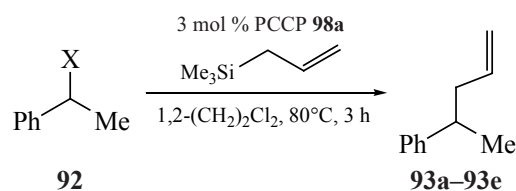
In view of the high electrophilicity of complex **89a**, its ability to split off halides to form phenylethyl cations that are trapped by the silane was studied (Scheme 36).

Ether **92a** and fluoride **92b** proved to be the most active, which meets the expectation of their silyl-enhanced nucleofugacity. Bromide **92d** showed

Scheme 35.
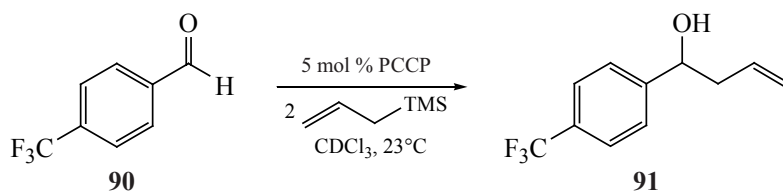
Scheme 36.

93	X	conversion, %
93a	MeO	>95%
93b	F	>95%
93c	Cl	15%
93d	Br	67%
93e	I	20%

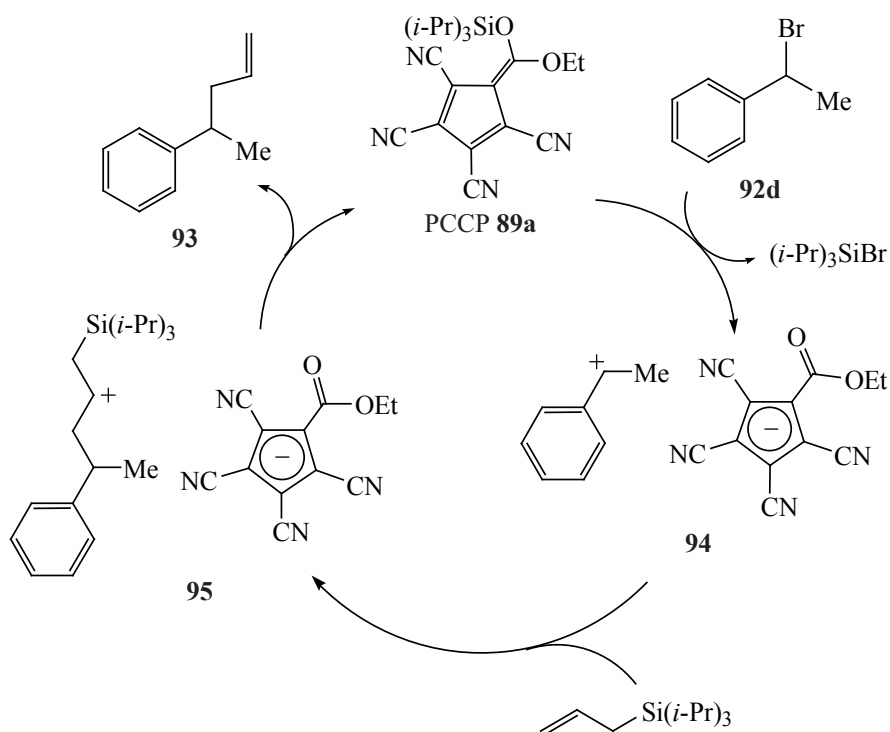moderate activity, whereas chloride **92c** and iodide **92e** gave low yields.

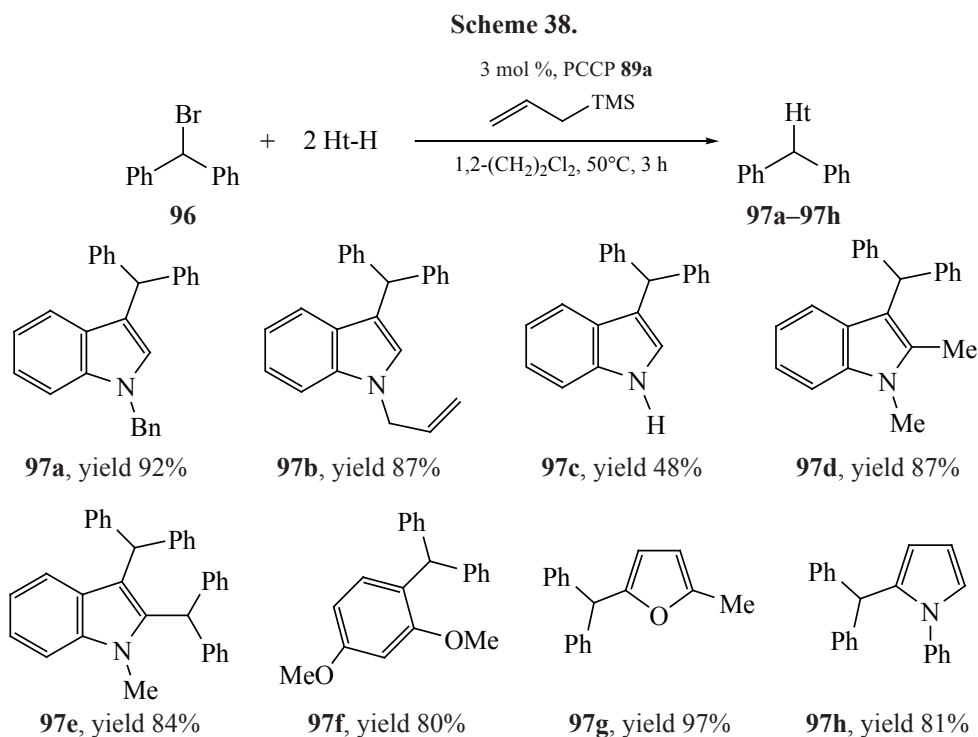The mechanism of catalytic allylation is shown in Scheme 37.

The reaction of PCCP catalyst **89a** with bromide **92d** led to ionization due to the elimination of triisopropylsilyl bromide. The resulting carbenium Cp salt **94** was then reacted allylsilane to form intermediate **95**, and its desilylation provided allylated adduct **93** and regenerated silyl catalyst **89a**, thereby completing the catalytic cycle.

The high electrophilicy of the resulting carbocationic compounds allowed this reaction to be used for other nucleophilic substitutions (Scheme 38).

Radtkea and Lambert [81] showed that *N*-benzyl- and *N*-allylindoles reacted with high yields, whereas the yield with indole intelf was moderate. The alkylation of 1,3-dimethoxybenzene led to product **97f** with a yield of 80%. Even though furan itself failed to react, 2-methylfural gave product **97g** with a yield of 97%. The reaction with *N*-phenylpyrrole gave product **97h** with good yield as a 4 : 1 mixture of 2- and 3-substituted pyrroles. It was found that substrates with electron-

Scheme 37.

Scheme 38.

97a, yield 92%   **97b**, yield 87%   **97c**, yield 48%   **97d**, yield 87%

97e, yield 84%   **97f**, yield 80%   **97g**, yield 97%   **97h**, yield 81%

acceptor substituents (Ac, Ts) on nitrogen did not enter this reaction.

The introduction of an aminomethyl group into organic compounds is an urgent task, because this group is widely present in natural products and in pharmaceuticals [82], as well as because aminomethylated products are used as universal building blocks in the synthesis of biologically active compounds. Although many aminomethylation methods have been developed [83], most of them are racemic versions, and only a few asymmetric aminomethylation reactions have been described so far [84].

Kang et al. [85] developed a new three-component stereoselective aminomethylation reaction, involving a diazo compound, an alcohol, and an α-aminomethyl ether and initiated by asymmetric counteranion directed catalysis (ACDC), was developed [85], which opened up a convenient synthetic approach to optically active α-hydroxyl-β-amino acids (Scheme 39).

In this reaction, enolate **102a** formed in situ from α-diazo ester **98a** and alcohol **99a** under the action of a Pd catalyst, entered into stereoselective addition with a tight ion pair of methyleneimine cation **103a** generated in situ from α-aminomethyl ether **100a** with chiral counteranion of PCCP **12**, which ensured trapping intermediate **102a** and led to enantioselective aminomethylation [86].

Chiral PCCPs **12** and **77** gave with good yield (88–92%) and high enantioselectivity (84–96%) product 101a, in contrast to BINOL phosphoric acids, which gave moderate enantioselectivity with good yields. Control experiments and DFT calculations showed that the chiral Cp anion is responsible for asymmetric induction due to its electrostatic interaction with intermediate compounds and the formation of H-bonds with them.
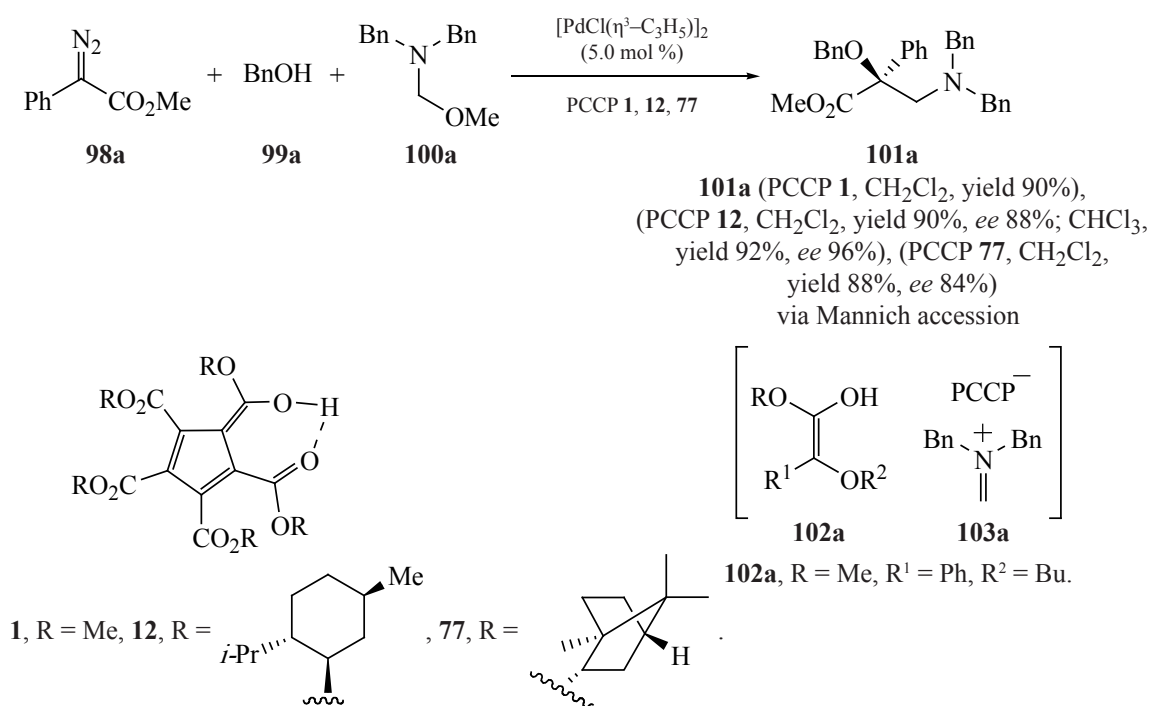
Chiral PCCP catalysts were used in the enantioselective inverse electron demand Diels–Alder cycloaddition of ethyl vinyl ethers **104** to oxocarbenium ions **47** (Scheme 40) [41].

The importance of this reaction from a practical point of view is that it leads to 2,4-dialkoxychromanes **105** contained as structural units in biologically active natural substances, including the antitumor agent berkelic acid [87], antibiotic pecylospiron [88], and anti-HIV agent calanolide A [89].

To select the optimal catalyst for the reaction of diethyl acetal **48a** with ethyl vinyl ether **104a**, the effect of chiral PCCP catalysts **12**, **20**, **24**, **42**, and **106–116** with various alkoxy substituents on its parameters was studied (Table 4).

The reaction with 5 mol % PCCP in C_6H_6 at 22°C gave cycloadduct **105a** with a diastereoselectivity higher than 20 : 1 in all cases, and catalysts **114** and

Scheme 39.

98a + BnOH **99a** + **100a** → **101a**

[PdCl(η³–C₃H₅)]₂ (5.0 mol %)

PCCP **1**, **12**, **77**

101a (PCCP **1**, CH₂Cl₂, yield 90%),
(PCCP **12**, CH₂Cl₂, yield 90%, *ee* 88%; CHCl₃,
yield 92%, *ee* 96%), (PCCP **77**, CH₂Cl₂,
yield 88%, *ee* 84%)
via Mannich accession

102a, R = Me, R¹ = Ph, R² = Bu.

1, R = Me, **12**, R = [structure], **77**, R = [structure].

115 containing respectively the *p*-CH₃O and *p*-CH₃S substituents in the benzene ring turned out to be the most effective in terms of both yield and enantioselectivity. Based on its activity and availability, PCCP catalyst 114 was chosen for further work.

Using PCCP 114, the effect of structural changes in the starting compounds on the reaction products was studied (Scheme 41).

It turned out that the replacement of Et by *i*-Pr in the acetal moiety led to products 105a and 105b with almost equal enantioselectivity. Methyl substitution in aryl did not decrease enantioselectivity unless it was orthogonal to the phenolic group 105d–105f. The introduction of halogen into the aryl ring had a significant effect on the enantioselectivity of the reaction. Thus, fluorine-substituted diethyl acetal 105g

and its fluorine-unsubstituted analog 105a showed the same enantioselectivity, and the transition to chlorine 105h and especially to bromine 105i resulted to a sharp decrease in enantioselectivity. Varying the structure of the vinyl ester showed that its β-substitution leads to compounds 105j and 105k with 3 stereogenic centers in each, and β-substitution reduces the yield of product 105j and the enantioselectivity of its formation.

To establish the structure and mechanism of action of PCCP 114, an X-ray diffraction analysis of its NMe₄⁺ salt was carried out, according to which all CO₂R* groups are strongly linked to each other and formed a chiral helical structure. Each carboxyl is directed at an angle from 28° to 57° to the Cp ring plane, and the C=O atoms are arranged on one side and 2-arylcyclohexyl groups on the other. Such arrangement is not related
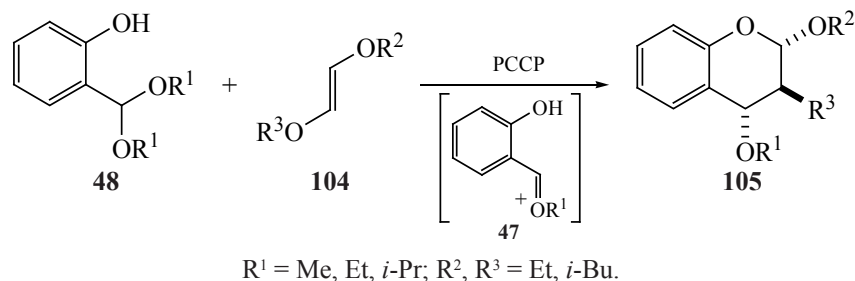
Scheme 40.

48 + **104** → **105**

PCCP

R¹ = Me, Et, *i*-Pr; R², R³ = Et, *i*-Bu.

Table 4. Optimization of the structure of the PCCP catalyst for the addition of salicylaldehyde diethyl acetal **48a** to ethyl vinyl ether **104a**
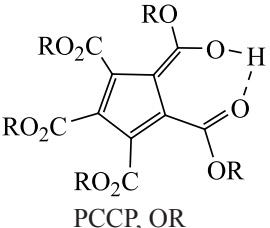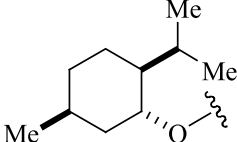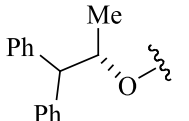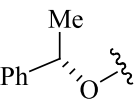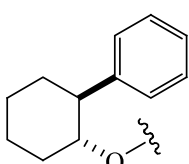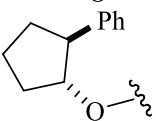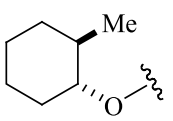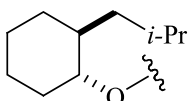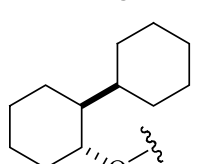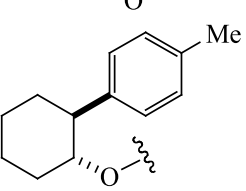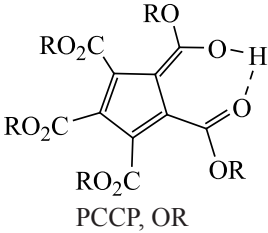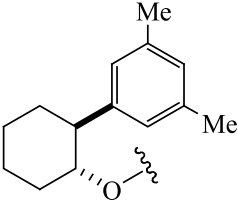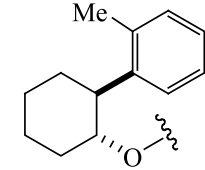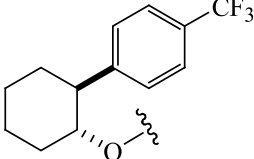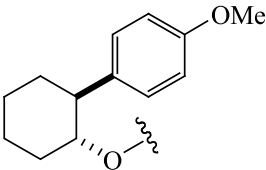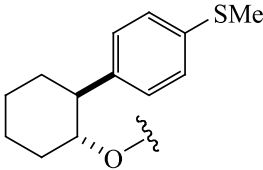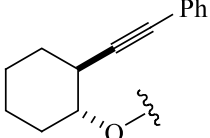
Compound		nimber	Yield, %	Enantioselectivity, *er*
PCCP, OR				
		PCCP **12**	69	85 : 15
		PCCP **20**	58	89 : 11
		PCCP **24**	79	67 : 33
		PCCP **42**	63	92 : 8
		PCCP **106**	69	59 : 41
		PCCP **107**	60	91 : 9
		PCCP **108**	65	82 : 18
		PCCP **109**	69	85 : 15
		PCCP **110**	11	93 : 7

Table 4. (Contd.)

Compound	number	Yield, %	Enantioselectivity, *er*
PCCP, OR			
PCCP **111**	PCCP **111**	10	84 : 16
PCCP **112**	PCCP **112**	no reaction	
PCCP **113**	PCCP **113**	78	83 : 17
PCCP **114**	PCCP **114**	78	94 : 6
PCCP **115**	PCCP **115**	78	94 : 6
PCCP **116**	PCCP **116**	90	50 : 50

to crystal packing, since the lowest energy B3LYP/6-31G* transition structures **117** and **118** for the reaction between the oxacarbenium cation–PCCP anion complex and vinyl ether had exactly the same helical conformation of the C=O groups (Scheme 42).

In view of the lack of difference between steric interactions in the compounds **117** and **118**, the fact that the TS$_{(S,S)}$ structure is energetically preferred TS$_{(R,R)}$ can

be explained by better stabililization of the transition state by noncovalent interactions in TS$_{(S,S)}$ than in TS$_{(R,R)}$. From this it follows that the helical conformation of the anion of PCCP **114** decreases its energy, thereby minimizing conformational interactions between chiral CO$_2$R* groups. Therewith, the point chirality of the CO$_2$R* substituents induces the helical chirality of the PCCP anion as a whole, which leads to a decrease in the

Scheme 41.

48a–48c   **104a**, **104b**   **105a–105l**

R^1 = Me, Et, *i*-Pr; R^2 = Et, *i*-Bu; R^3 = H, Me.

105a
yield 78%, 94 : 6

105b
yield 87%, 94 : 6

105c
yield 76%, 90 : 10

105d
yield 94%, 94 : 6

105e
yield 84%, 94 : 6

105f
yield 96%, 80 : 20

105g
yield 71%, 94 : 6

105h
yield 78%, 88 : 12

105i
yield 68%, 62 : 38

105j
yield 77%, 89 : 11

105k
yield 78%, 93 : 7

105l
yield 50%, 83 : 17
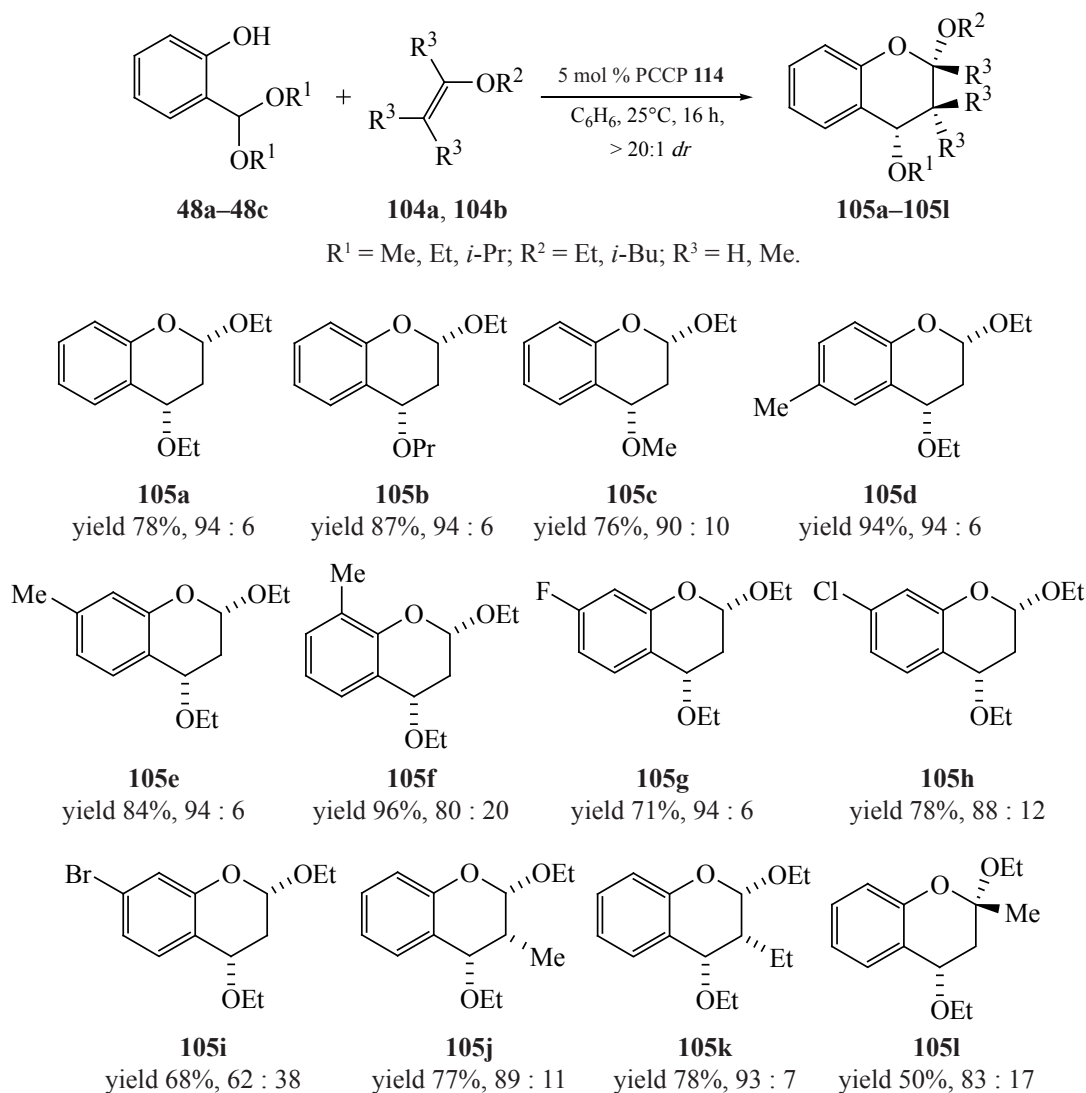
energy of the enantiodetermining TS. This conclusion made it possible to explain the observed structure–activity relationships (SAR) for PCCP **12**, **20**, **24**, **42**, and **106–116** (Table 4). Thus, chiral groups that enhance helical organization lead to high enantioselectivity (PCCP **114**), while helix-destabilizing substituents are less effective either due to steric volume (PCCP **109**, **111**, and **112**) or length (PCCP **116**).

The mechanism of the enantioselective inverse electron demand Diels–Alder cycloaddition of ethyl vinyl ether **104a** to oxocarbenium ion **47a** is shown in Scheme 43.

According to Scheme 43, PCCP **114** induces ionization of acetal **48a** to form salt **119** (oxocarbenium and PCCP anion), after which the latter takes up ether **104a**

through TS **117**, where the absolute stereochemistry of the product is dictated by the helical chirality of the Cp anion transmitted through a network of H-bonds, C–H⋯O interactions, and aryl CH interactions. Subsequently, the deprotonation of resulting intermediate **120** with the PCCP anion affords final chroman product **105a** and regenerates catalyst **114**.

3. PCCP-CATALYZED CONTROLLED CATIONIC POLYMERIZATION OF VINYL ETHERS

"Live" ionic polymerizations is an abundant class of reactions that allow the synthesis of macromolecules with a high level of control [90]. However, the field of application of these processes is limited due to their sensitivity to impurities and harsh conditions. Thus, controlled cationic polymerization should be carried

Scheme 42.

TS$_{(S,S)}$ **117**
E_{rel} 0 kcal/mol

TS$_{(R,R)}$ **118**
E_{rel} 2.8 kcal/mol

R =
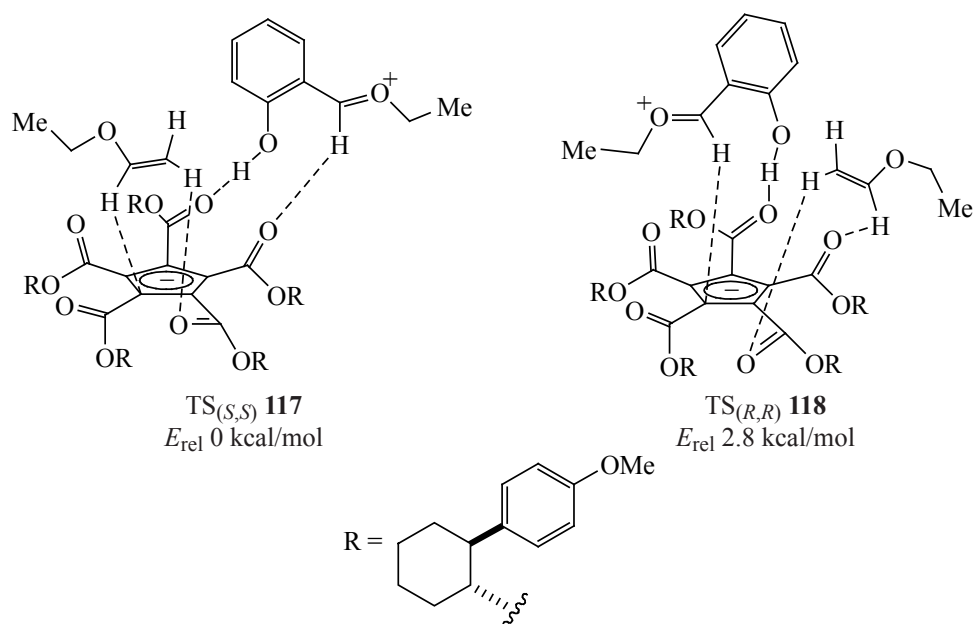
out at low temperatures in an inert atmosphere using thoroughly purified monomers and catalysts [91], which limits its widespread use [92].

Kottisch et al. [93] undertook a search for catalysts that would allow cationic polymerizations to be performed under milder conditions. The close interaction of the end of the cationic chain with a well-chosen counter anion will presumably allow cationic polymerizations at room temperature and to selectively add a monomer to the reaction mixture, even if it contains nucleophilic impurities, without causing chain termination or transfer. The choice of PCCP **1** as a catalyst for this reaction was made taking into account the fact that it forms a stable anion upon dissociation [30], and its complexes with oxocarbenium ions react with vinyl ethers through TSs, in which noncovalent interactions arise between key reacting C–H bonds, both with the Cp ring and with the carbonyls of the anion [41]. In this case, the mechanism of PCCP **1** catalysis of cationic polymerization would involve the reaction of vinyl ether **121** with the catalyst, resulting in covalent compound **122**, which exists in equilibrium with salt **123** containing compound **122**, and the end of the growing chain (Scheme 44).

In this case, the addition of monomers to salt **123** would take place through TS **124**. Due to the high reactivity of the oxocarbenium ion, the end of the chain would be mainly in the covalent form **122**, which would provide controlled polymerization at ambient temperature. This mechanism would eliminate the need for highly purified reagents, an inert atmosphere, and low temperatures. To test this mechanism, the authors of the cited work studied the polymerization of isobutyl vinyl ether (IBVE) with PCCP **1** at 22°C in the absence of an inert atmosphere, solvent, and additional purification of IBVE. As a result, the polymerization with 50 equiv of IBVE led to complete consumption of the monomer after 16 h and gave a polymer with M_n^{exp} 5.1 kg/mol and Đ 1.1 (Table 5, experiment 1).

Therewith, the experimental molar mass (M_n^{exp}) fitted well the theoretical value (M_n^{theor}), indicating that the polymer chain was initiated by each PCCP **1** molecule, whereas the low dispersities Đ indicated an effective protonation of IBVE by PCCP **1**. From this it followed that the events of chain termination and transfer did not play an important role in this reaction. Moreover, the relatively low polymerization rate observed in this case was associated with a strong interaction between the Cp anion and the chain end of the oxocarbenium ion, arising from the formation of a strong ion pair between these two species or due to the presence of a dynamic covalent bond between them. By varying the ratio of PCCP **1** to IBVE ratio and the target polymers with a higher molar mass (Table 5, runs 2 and 3), polymers with narrow dispersities Đ were obtained in all cases, and the M_n^{exp} values were slightly lower than M_n^{theor}, but nevertheless agreed well with each other. This indicated

Scheme 43.
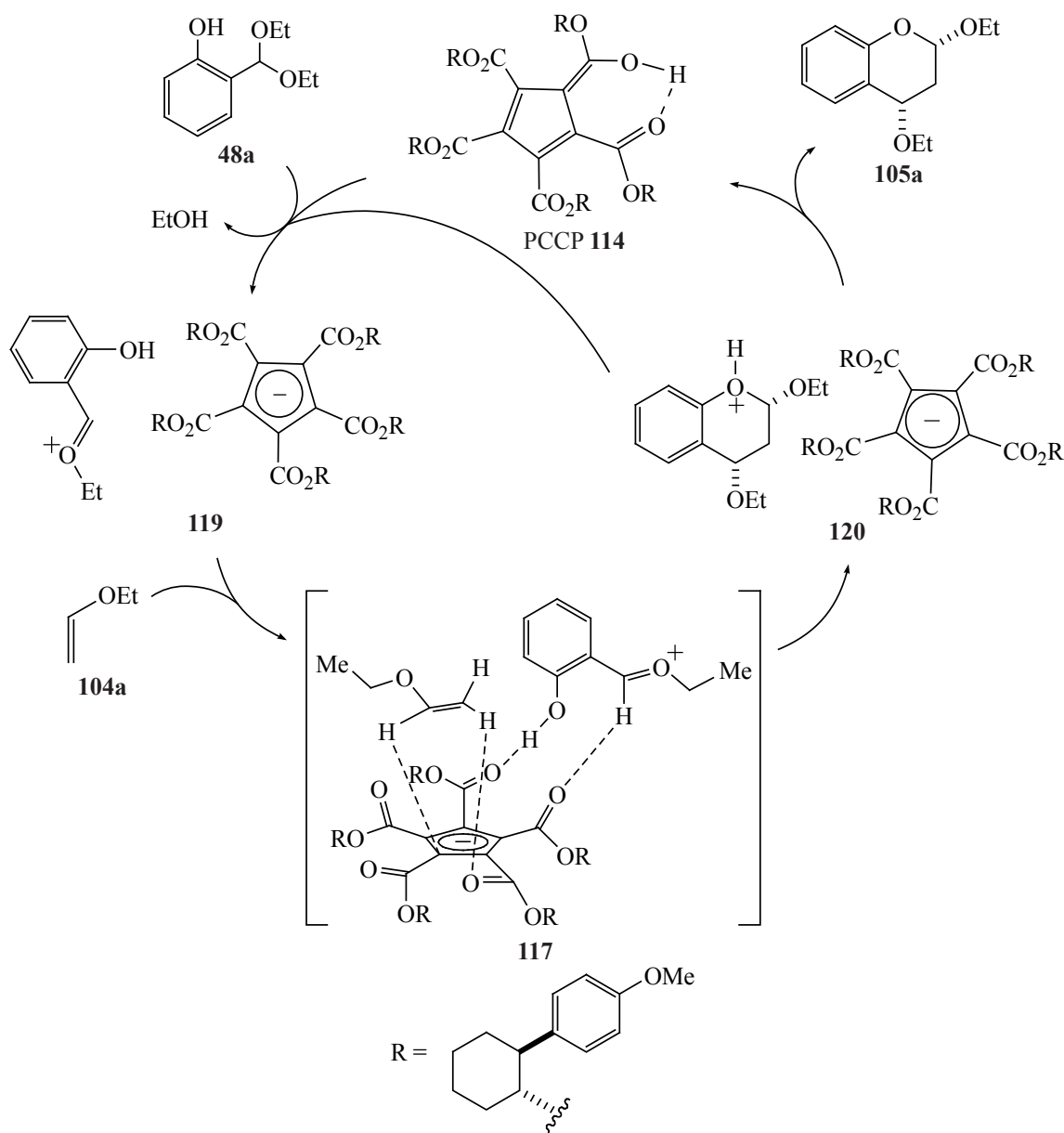
a minimal effect of chain transfer on the polymerization process if transfer took place.

When these reactions were performed in an inert atmosphere with well purified IBVE, almost the same results were obtained, which made it possible to carry out the reactions catalyzed by PCCP **1** without thorough purification and dehydration of the reagents. Dihydrofuran monomer **121d**, the starting material for poly(DHF) with a high glass temperature (126°C), polymerized under standard conditions, but the M_n^{exp} of the resulting polymer was lower than expected, and the dispersity $Đ$ was broad (test 6).

The activity and chain-end fidelity of this reaction was investigated in the synthesis of diblock copolymers (Scheme 45).

For the first block, poly(EVE) with M_n^{exp} 4.0 kg/mol was obtained from purified monomers in an N_2 atmosphere, and then, after 95% conversion, IBVE was added to obtain poly(EVE-b-IBVE) diblock polymer with M_n^{exp} 8.2 kg/mol. The SEC plot of the polymer after chain elongation showed a shift toward higher Mn while maintaining a narrow dispersity ($Đ$ = 1.2), which indicated the formation of a diblock polymer. When the reaction was let to proceed to complete

Scheme 44.

PCCP **1**　　　　　　　　**122**　　　　　　　　**123**

124

R = Et, *i*-Bu.
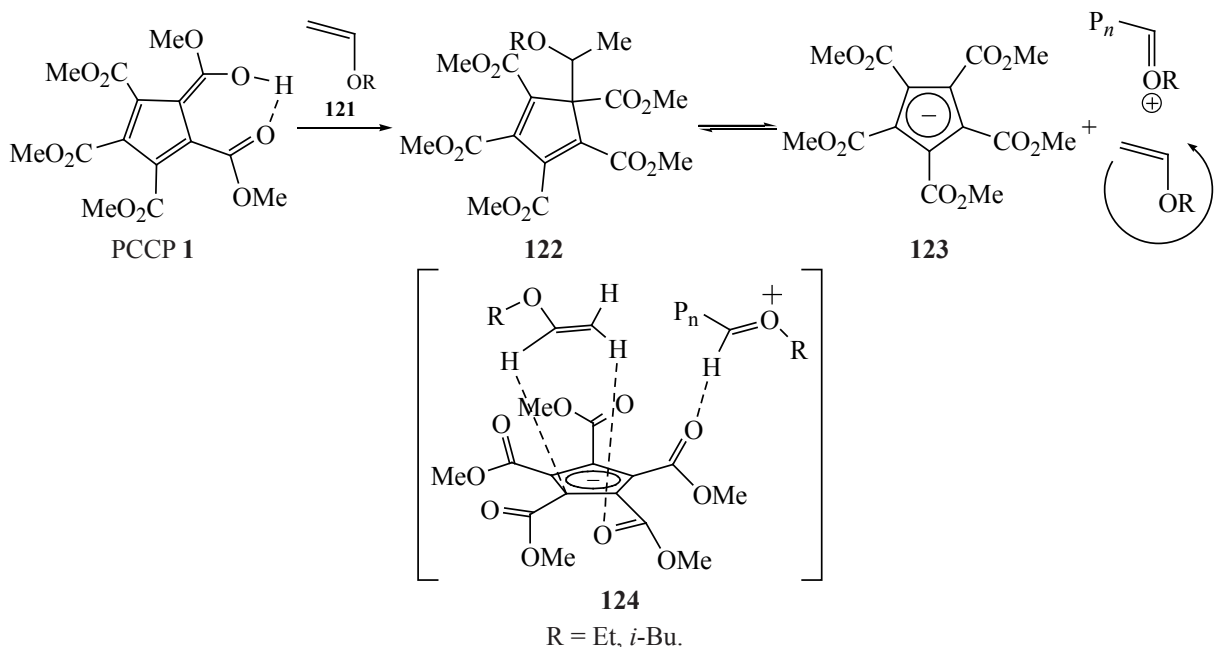
conversion before the second monomer was added, the chain was terminated by nucleophilic impurities, and chain termination became competitive at a high degree of monomer conversion.

To extend the range of application of the developed polymerization methods, polymers were functionalized at the end of the chain by quenching the propagating oxocarbenium ion with alcohols after complete conversion of the monomer. Thus, the addition of

5 equiv of various alcohols and Et$_3$N to poly(IBVE) gave polymers with the desired acetal group at the end of the chain with a yield of more than 95% (Scheme 46, *a*).

In addition, the ends of the oxocarbenium chains were efficiently trapped by the dithiocarbamate salt to form macroinitiator poly(**127a**), which opens access to the multiblock material through chain elongation (Scheme 46, *b*). The use of FcBF$_4$ as a chemical

Table 5. Cationic polymerization of vinyl ethers **121a–121d** activated with PCCP **1**

121a–121d　　　　*poly*(**121a–121d**)　**121a 121b**　**121c 121d1**

Monomers

R^1 = H, R^2 = *i*-Bu, Et, *t*-Bu.
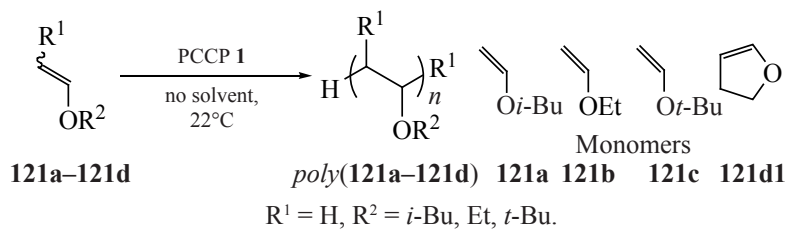
Experiment	Monomer	Time, h	M_n^{theor}, kg/mol	M_n^{exp}, kg/mol	Đ
1	IBVE	16	5.0	5.1	1.11
2	IBVE	16	9.3	7.2	1.27
3	IBVE	16	23.0	18.1	1.15
4	EVE	3	3.4	2.5	1.06
5	TBVE	0.1	8.1	6.2	1.25
6	DHF	5	33.6	34.1	1.20

Scheme 45.

R = fragments of nucleophilic impurities contained in the monomer

Scheme 46.

a

R = Et, *i*-Bu, Bn.

b
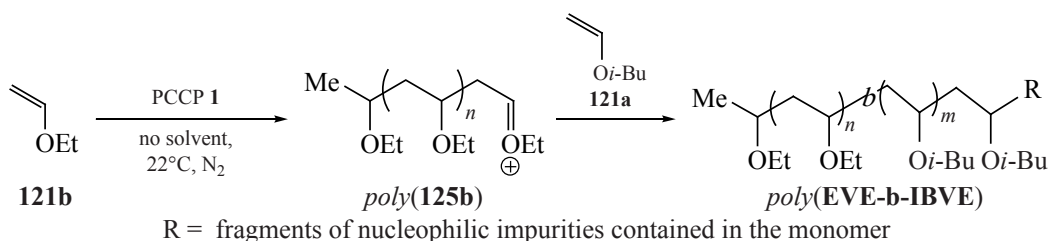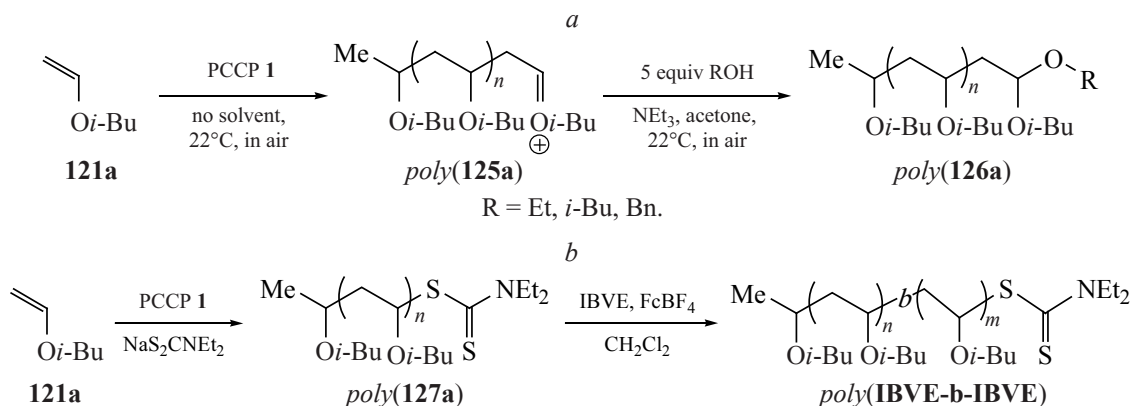
mediator for poly(**127a**) effectively lengthened the chain by cationic reversible addition-fragmentation-chain transfer polymerization (RAFT) to obtain poly(IBVE-b-IBVE), which indicates the possibility of efficient control of chain ends after polymerization, as well as extending the chain using other methods.

Attempts to obtain polymers with a degree of polymerization greater than 100 from monomers **121** using PCCP **1** gave products with lower M_n and broadened dispersity Đ. The loss of control over this process was associated with a high level of elimination at the end of the chain and its subsequent transfer through the PCCP anion (Scheme 47) [94].

The close location of the PCCP **1** anion to the last-by-one C–H bond of the chain in compound **128** promoted intramolecular deprotonation to form a strong acid PCCP **1**, which protonated an additional monomer and initiated growth of a new poly(**121**) chain, the transfer of which led to low M_n values and broad dispersities Đ (Scheme 47).

Scheme 47.

Polymeric chain transfer via intramolecular deprotonation

R = Alk, P*n* – fragment of the polymeric chain

Scheme 48.

Decreasing basicity by H-bond formation

129

R = Alk, P_n – fragment of the polymeric chain

faster polymerization
$M_n > 50$ kg/mol
mild polymerization conditions
moisture resistance

121
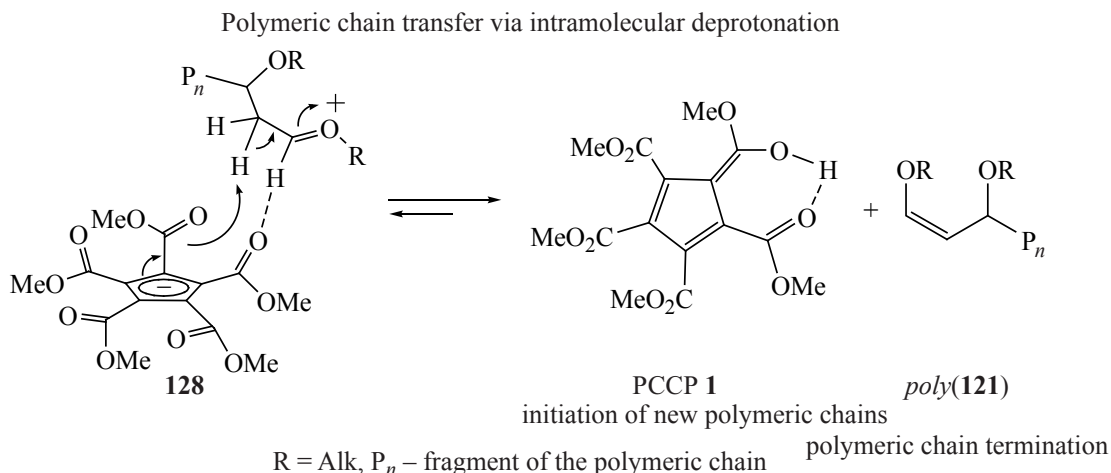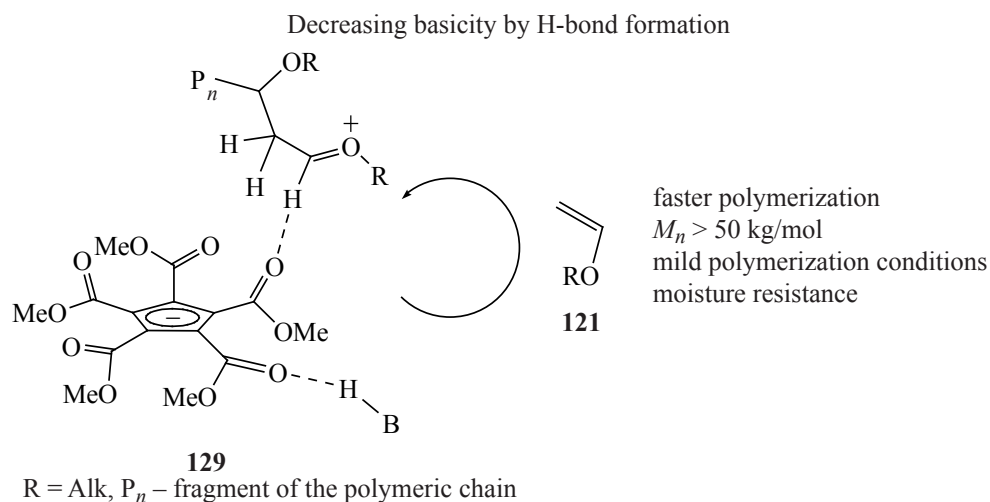
To solve this problem, the basicity of the PCCP **1** anion was lowered by adding H-bond donors (HBD) to it, and this inhibited chain transfer through interaction with one or more carbonyl groups of the Cp anion (Scheme 48).

When used as effective polymerization cocatalysts, HBD must firmly bind to the PCCP **1** anion, reducing its basicity, and remain close to the end of the polymer chain throughout the reaction to prevent its termination by nucleophiles. Based on these requirements, a number of different HBDs **130–135** were selected, and their effect on IBVE polymerization studied (Scheme 49).

Among H-bond donors (HBD **130–135**), thio-phosphoramide **133** turned out to be the best in the polymerization of IBVE. When it was used in the PCCP **1**-catalyzed cationic polymerization of vinyl ethers, it was possible to obtain polyvinyl ethers with a

molar mass of up to 60 kg/mol even in the surrounding atmosphere, thereby maintaining control over M_n and narrow dispersities Đ, which indicates an improvement in the previously described method [93].

The interactions between HBD **133**, the PCCP **1** anion, and the oxocarbenium ion chain end were simulated by DFT calculations (Scheme 50).

The resulting geometry-optimized transition structure **136** revealed several important interactions that facilitate polymerization. In structure **136** hydrogen bond donor HBD **133** located above the PCCP **1** anion in structure **136** is slightly displaced relative to the center and forms 2 H-bonds with neighboring carbonyls of the anion, and the third N–H bond is coordinated with the π system of this anion. The growing polymer chain is located in a pocket between HBD **133** and the PCCP **1** anion, protruding from it, while the monomer

Scheme 49.

130   **131**   **132**

133   **134**   **135**
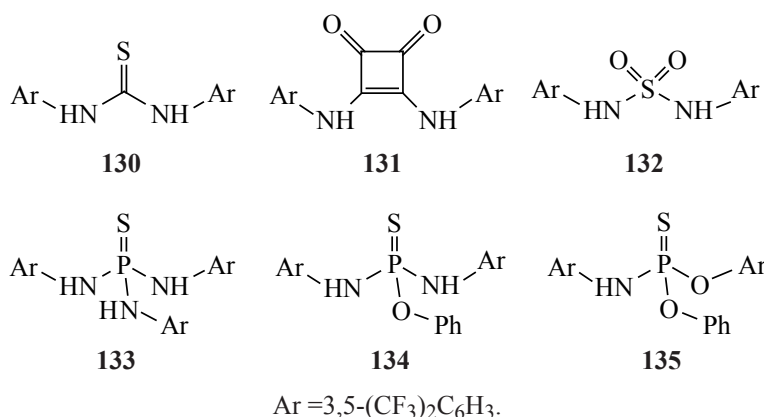
Ar = 3,5-(CF$_3$)$_2$C$_6$H$_3$.

Scheme 50.
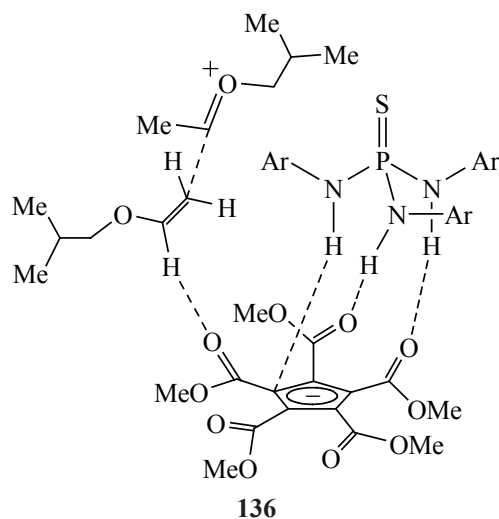
136

Ar = 3,5-(CF$_3$)$_2$C$_6$H$_3$.

moves inward, forming the key C–H···O interaction between the vinyl α-C–H bond and another PCCP **1** carbonyl. This model also determines the resistance of polymerization to external nucleophiles, because the gap between HBD **133** and the anion can protect the chain end from external nucleophiles, minimizing chain transfer.

4. REARRANGEMENT OF ORGANIC AND ORGANOELEMENT GROUPS AND HALOGENS IN THE PCCP SYSTEM

Wilkinson and Piper were the first to describe in 1956 [95] an extremely rapid migration of the Fe(η^5-C$_5$H$_5$)(CO)$_2$ and Hg(η^1-C$_5$H$_5$) groups along the Cp ring in the unsubstituted Cp. To date, rapid circular migrations along the perimeter of the Cp ring have been found for many metal-centered groups formed by transition and non-transition metals [96, 97], as well as for σ-derivatives of Cp with migrants liked with the Cp ring through Group 13–17 elements of the Periodic Table [31, 98–100]. Since organometallic derivatives and PCCP **1** complexes are mainly characterized by the coordination of the metals to the carbonyl groups, only circular migrations of element-centered substituents were observed in them, and such migrations are mainly carried out as 1,5-sigmatropic shifts. However, due to the stability of its Cp anion, this system in some alkyl and arylazo derivatives features migrations that occur as a result of dissociation–recombination through the formation of tight ion pairs.

The displacement of alkyl groups in the unsubstituted or permethylated Cp ring occurs at $t > 300°C$ [31]. The electron-acceptor CO$_2$Me groups into the Cp ring decreased the energy barrier for the shift of the alkyl substituents in the Cp ring and significantly accelerated the shifts of the 4-nitrobenzyl group in compounds **137a–137c** (Scheme 51) [101].

Isomers **137a–137c** were preparatively isolated, and from the dynamics of their ^{1}H NMR spectra,
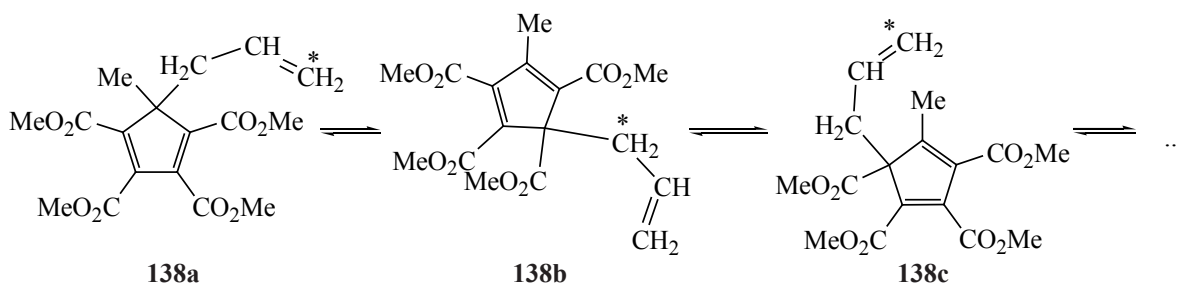
Scheme 51.
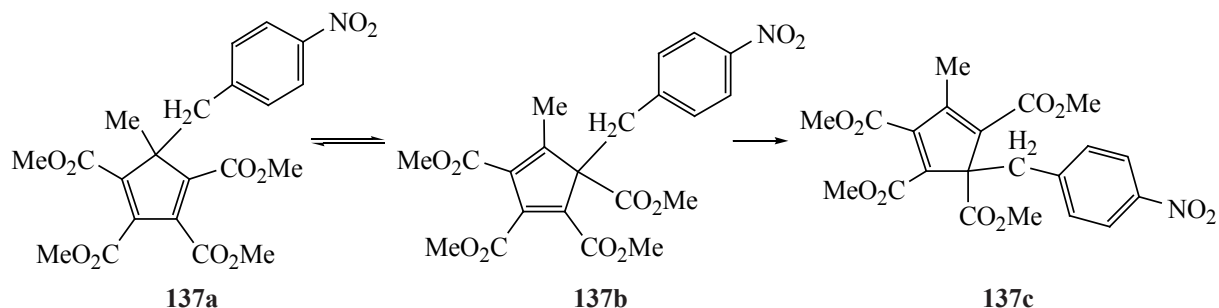
137a　　　　　　**137b**　　　　　　**137c**

Scheme 52.

intramolecular 1,5-shifts of the 4-nitrobenzyl group along the Cp ring were revealed, with $\Delta G^{\neq}_{120°C}$: **137a** → **137b** 29.5 kcal/mol, **137b** → **137a** 30.0 kcal/mol, and **137b** → **137c** 33.6 kcal/mol.

Allyl group migrations along the Cp ring were studied in allyl derivatives **138a–138c**. For preparatively isolated isomers **138a–138c**, analysis of the time dependence of their ^{1}H NMR spectra at 80–130°C showed that they interconverted due to 3,3-sigmatropic shifts of the allyl group along the perimeter of the Cp ring with $\Delta G^{\neq}_{25°C}$: **138a** → **138b** 28.5 kcal/mol, **138b** → **138a** 29.7 kcal/mol, **138b** → **138c** 30.2 kcal/ mol, and **138c** → **138b** 30.3 kcal/mol (Scheme 52) [102].

The mechanism of 3,3-sigmatropic shifts was confirmed by the DFT B3LYP/6-311++G(d,p) method on the example of allyl derivative **139**, in which degenerate migrations of the allyl group along the perimeter of the Cp ring also proceeded along the Cope rearrangement pathway through transition states with a *chair* (TS **140**) or a *boat* (TS **141**) six-membered ring conformations

with close barriers ($\Delta G^{\neq}_{25°C}$ 27.4 and 27.7 kcal/mol, respectively) (Scheme 53).

At the same time, the alternative 1,5-shifts of the allyl group in the PCCP **139** ring should proceed with a higher barrier ($\Delta G^{\neq}_{25°C}$ 30.8 kcal/mol).

Jefferson and Warkentin [103] showed that, in polar media, the rearrangement of alkyl derivatives **142** proceeded by the ionization–recombination mechanism through the heterolysis of the R–Cp bond (Scheme 54).

Thus, in a methanol solution, compound **142** dissociate to give ion pairs **143**, whose collapse forms covalent isomers **142**. The latter undergo degenerate circular rearrangement competing with an irreversible reaction with the solvent.

In cyclopentadienes **144–146**, the energy barrier for the 1,5-sigmatropic shifts of the methoxycarbonyl group was estimated at $\Delta G^{\neq}_{100°C}$ 24.1–29.9 kcal/mol (Scheme 55) [104].

Scheme 53.

Scheme 54.

R = CH$_2$OMe, CHPh$_2$, CH$_2$C$_6$H$_4$OMe-4, 1Ad.

Scheme 55.

R=NMe$_2$, NHPh, CN, OMe, Ph, CH$_2$CO$_2$Me, Me, Et, i-Pr, SMe, Cl.
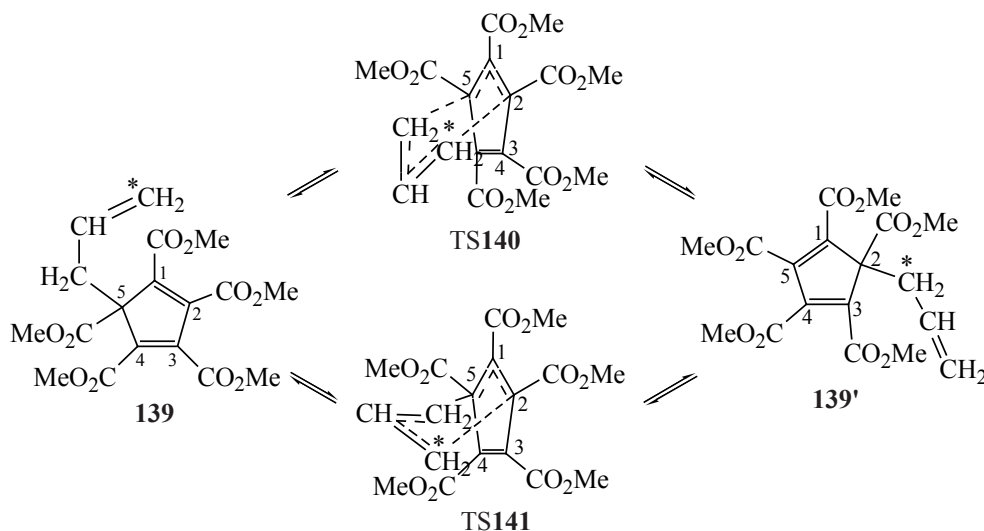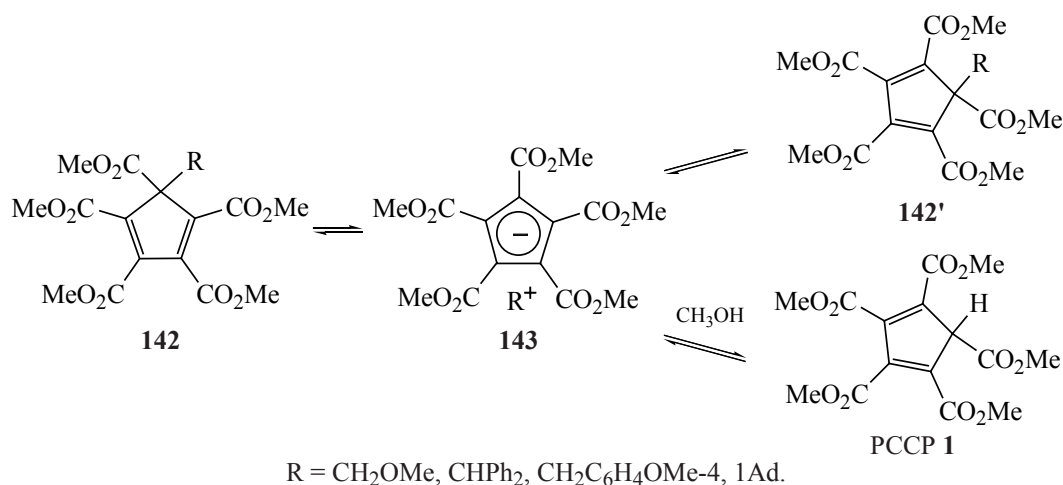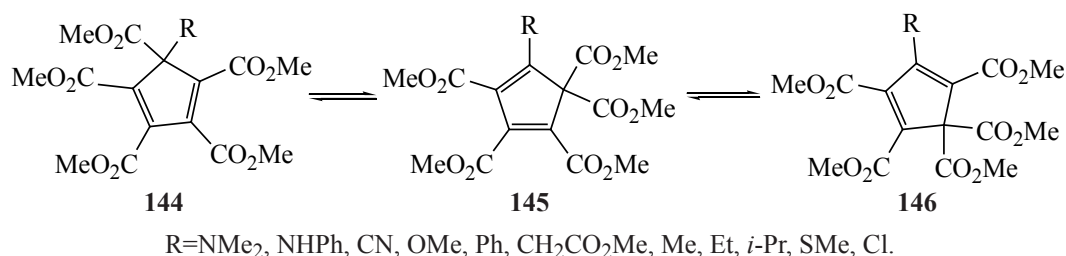
Substituents in the Cp ring appreciably affected the rate of the shift of the methoxycarbonyl group. The rearrangement **144 → 145** occurred at room temperature at R = NMe$_2$ ($\Delta G^{\neq}$ 24.1 kcal/mol), while R = Cl migration occurred at 150–190°C ($\Delta G^{\neq}$ 25.7 kcal/mol).

The dynamics of the NMR spectra (–30 ÷ 30°C) of aryl derivatives **147a–147l** provided evidence showing that the arylazo groups migrate along the Cp ring due to randomization and forms a tight ion pair **148** with a barrier of $\Delta G^{\neq}_{25°C}$ 12.9–16.0 kcal/mol (Scheme 56) [31, 105].

Electron-acceptor substituents in the aryl ring decreased the migration rate due to destabilization of cations **148a–148l**, while electron-donor substituents increased. Thus, in going from compound **148d** with one NO$_2$ group in the aryl ring to compound **147j** with 3 NO$_2$ groups in the aryl ring, the migration marrier $\Delta G^{\neq}_{25°C}$ increased by 2.6 kcal/mol.

In was established by IR spectroscopy and XRD analysis that, it was found that compounds with one NO$_2$ or CF$_3$SO$_2$ substituent in the aryl ring exist exclusively as aryldiazonium salts **148a–148g**, and **148k**, while compounds with two NO$_2$ substituents in

Scheme 56.

Ar = 2-MeO,4-O$_2$NC$_6$H$_3$ (**a**); 2-Me,4-O$_2$NC$_6$H$_3$ (**b**); 4-O$_2$NC$_6$H$_4$ (**c**); 2-O$_2$NC$_6$H$_4$ (**d**); 2-I,4-O$_2$NC$_6$H$_3$ (**e**);
2-Br,4-O$_2$NC$_6$H$_3$ (**f**); 2-Cl,4-O$_2$NC$_6$H$_3$ (**g**); 2,4-(O$_2$N)$_2$C$_6$H$_3$ (**h**); 2,6-(O$_2$N)$_2$C$_6$H$_3$ (**i**); 2,4,6-(O$_2$N)$_3$C$_6$H$_2$ (**j**);
2-CF$_3$SO$_2$C$_6$H$_4$ (**k**); 2,4-(CF$_3$SO$_2$)$_2$C$_6$H$_3$ (**l**).

Scheme 57.

Ar = 2-MeO,4-$O_2NC_6H_3$ (**a**); 4-$O_2NC_6H_4$ (**c**); 2-I,4-$O_2NC_6H_3$ (**e**); 2-Br,4-$O_2NC_6H_3$ (**f**);
2-Cl,4-$O_2NC_6H_3$ (**g**); 2,4-$(O_2N)_2C_6H_3$ (**h**); Ph (**m**); 4-$MeOC_6H_4$ (**n**).
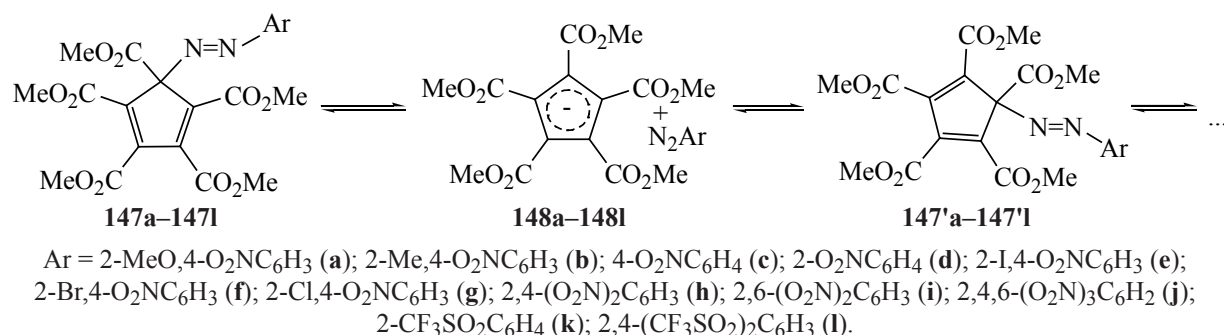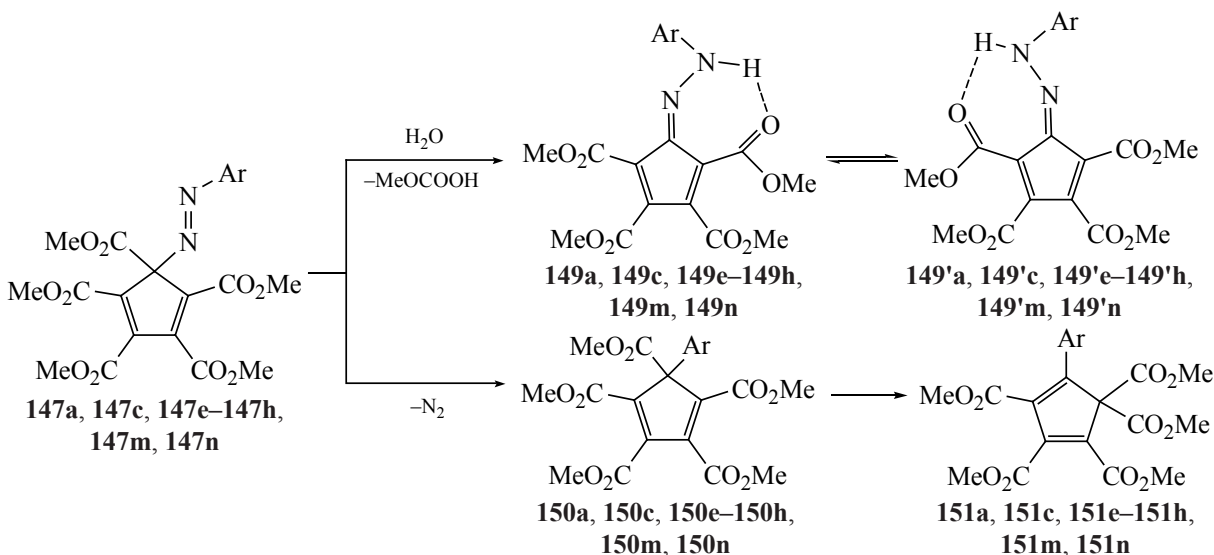
the aryl ring exist in 2 forms: covalent azo compounds **147h** and aryldiazonium salts **148h** and **148i**, while compounds with three NO_2 substituents (**147j**) or two CF_3SO_2 substituents (**147l**) are stable only in the form of azo compounds. The molecular and crystal structures of compounds **148c** and **147h** were determined by XRD analysis [105]. Crystals of compound **148c** are built of ion pairs lying in almost parallel planes, and the molecular structure of **147h** is a covalent 2,4-dinitrophenylazo derivative.

Compounds **147** decompose on heating (Scheme 57) [106].

The reaction proceeds along 2 channels: the first involves the elimination of the CO_2Me group to form hydrazones **149** and the second involves the elimination of nitrogen to form arylcyclopentadienes **150**, which then undergoes the 1,5-shift of the CO_2Me group, leading to products **151**. In arylhydrazones **149**, hydrogen is bonded to the hydrazone nitrogen and

coordinated to the carbonyl of the neighboring CO_2Me group. We earlier studied the *syn–anti* isomerization with respect to the double C=N bond in hydrazones **149** ($\Delta G^{\neq}_{25°C}$ 20.7–25.1 kcal/mol) by dynamic ^{1}H and ^{13}C NMR spectroscopy [106].

In nitrocyclopentadienes **152a–152d**, nondegenerate 1,5-sigmatropic shifts of the nitro group along the perimeter of the Cp ring were found and investigated (Scheme 58) [31, 107].

Isomers **152a–152d** and **153a–153d** were obtained as an equilibrium mixture and isolated preparatively. The structure of nitro derivatives **152a** and **153a** was confirmed by XRD. According to ^{1}H NMR, isomers **152a–152d** and **153a–153d** interconvert with $\Delta G^{\neq}_{25°C}$ 23.9–26.0 kcal/mol.

The interconversion of isomers **152a** and **153a** was studied by quantum-chemical calculations at the B3LYP/6-311++G** level (Scheme 59) [108].

Scheme 58.

R = Me (**a**), *i*-Pr (**b**), CH_2CO_2Me (**c**), CH_2COMe (**d**).

Scheme 59.

152a   **TS155**   **154a**

TS156   **153a**
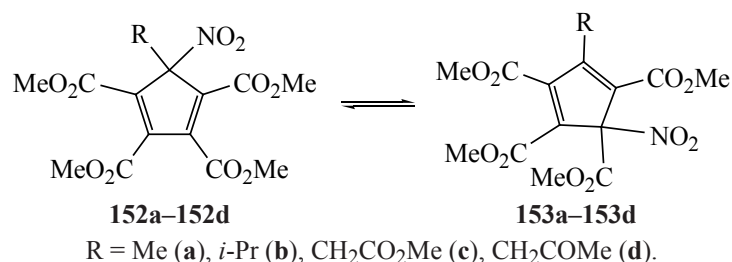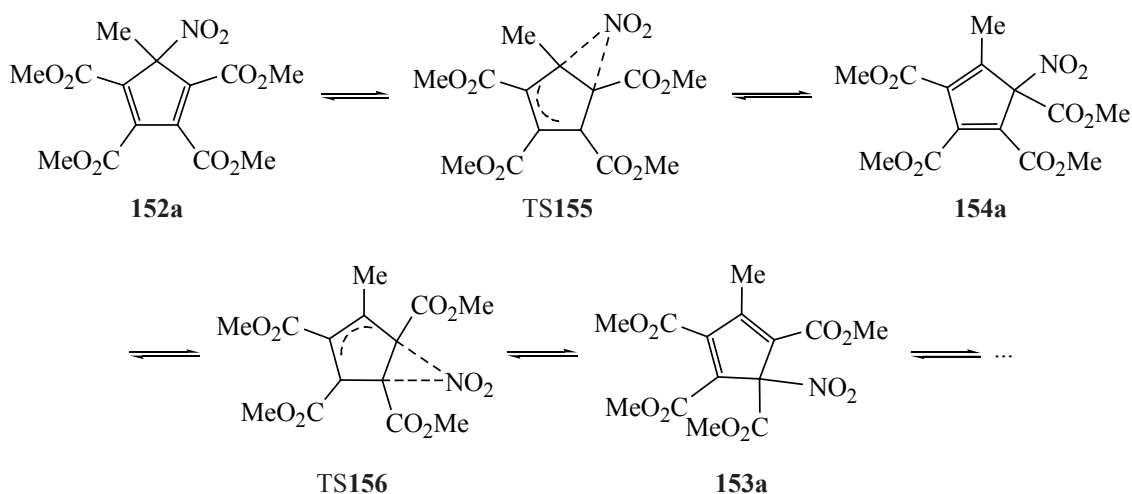
It was shown that these interconversions occur by the way of 1,3-shift of the nitro group along the perimeter of the Cp ring, which is impossible to detect on the NMR scale, and, according to the principle of the conservation of orbital symmetry, via consecutive 1,5-sigmatropic shifts of the nitro group and formation of an unstable isomer **154a**. According to the gas-phase calculations, isomer **154a** is less stable than **152a** by ΔE_{ZPE} 3.6 kcal/mol, and the barrier for the step process **152a → 153a** is 24.5 kcal/mol, which agrees with the NMR data [107].

Dynamic ^{1}H NMR was used to study fast and reversible migrations of the arylthio groups along the perimeter of the Cp ring in arylthiocyclopentadienes **157a–157g** (Scheme 60) [31, 109, 110].

According to the XRD analysis, compound **157d** exists in a conformation, in which the aryl ring is arranged over the the Cp moiety, forming with the former a dihedral angle of 50.0°. The dynamics of the NMR spectra of compounds **157a–157g** in the range
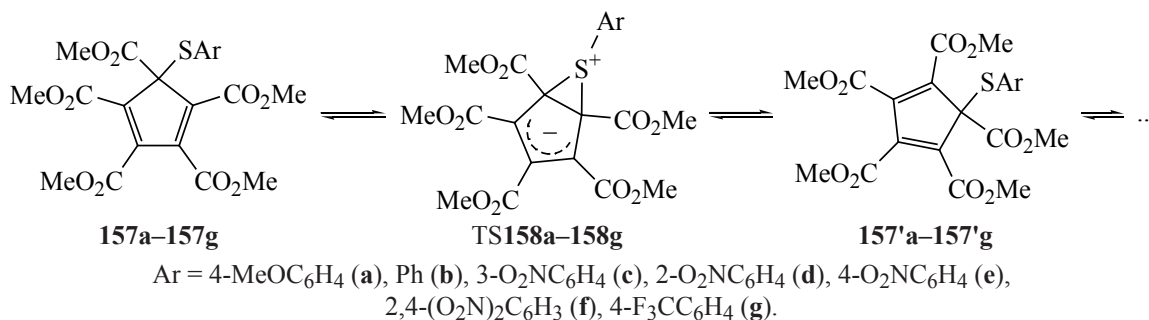
30–100°C are indicative of 1,5-sigmatropic shifts of the arythio group along the perimeter of the Cp ring ($\Delta G^{\neq}_{25°C}$ 16.0–20.9 kcal/mol). In going from compound **157a** with an electron-donor substituent in the aryl ring to compounds **157c–157g** with electron-acceptor substituents, the barrier for migration of the arylthio group increased substantially, which gave evidence for the formation of betaine structures **158a–158g**, in which the positive charge is localized on the sulfur atom, and the negative charge, on the Cp ring.

The reaction of potassium cyclopentadienides **159a** and **159b** with selenyl chloride formed selenium derivatives **160a–160c** (Scheme 61) [31, 110].

Since selenyl chloride can also act as halogenative agents, chlorine derivatives **161a–161c**, diselenides **162**, and dimers **163** were isolated. The dynamic ^{1}H NMR spectra of compounds **160a–160c** revealed fast intramolecular degenerate and nondegenerate 1,5-sigmatripic shifts of the seleno groups along the Cp ring with a barrier of $\Delta G^{\neq}_{25°C}$ 16.3–17.1 kcal/mol, which

Scheme 60.

157a–157g   **TS158a–158g**   **157'a–157'g**

Ar = 4-MeOC$_6$H$_4$ (**a**), Ph (**b**), 3-O$_2$NC$_6$H$_4$ (**c**), 2-O$_2$NC$_6$H$_4$ (**d**), 4-O$_2$NC$_6$H$_4$ (**e**), 2,4-(O$_2$N)$_2$C$_6$H$_3$ (**f**), 4-F$_3$CC$_6$H$_4$ (**g**).
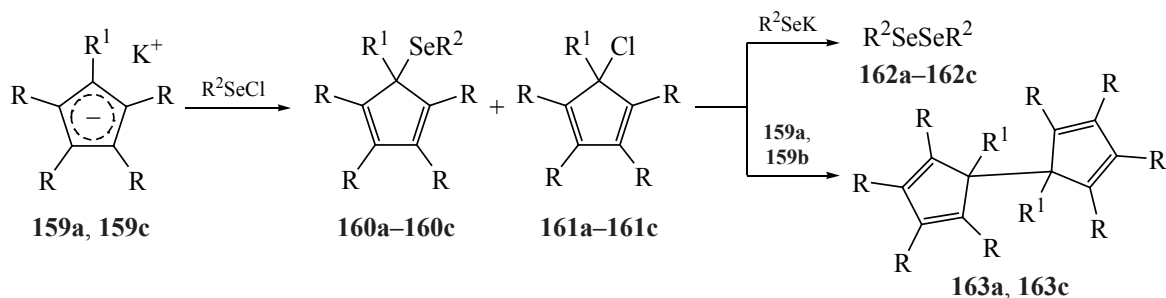
Scheme 61.

159, R = R^1 = CO$_2$Me (**a**); R = CO$_2$Me, R^1 = Me (**b**);
160, R = R^1 = CO$_2$Me, R^2 = 2,4-(O$_2$N)$_2$C$_6$H$_3$ (**a**), CF$_3$ (**b**); R = CO$_2$Me, R^1 = Me, R^2 = 2,4-(O$_2$N)$_2$C$_6$H$_3$ (**c**).

Scheme 62.

160a–160c ⇌ **160'a–160'c** ⇌ **160''a–160''c** ⇌ ...
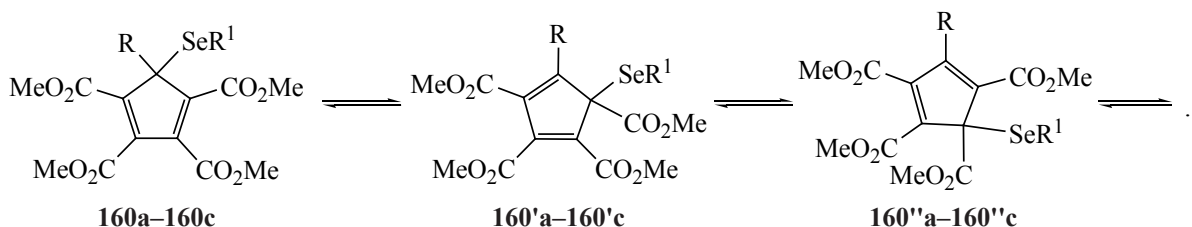
R = CO$_2$Me, R^1 = 2,4-(O$_2$N)$_2$C$_6$H$_3$ (**a**), CF$_3$ (**b**); R = Me, R^1 = 2,4-(O$_2$N)$_2$C$_6$H$_3$ (**c**).

is 3–5 kcal/mol lower than for the respective thio groups (Scheme 62).

The reaction of PCCP⁻Ag⁺ with aryltellurenyl bromides was used to prepare air-resistant aryltellurenyl cyclopentadienes **164a–164c**, evidence for the η^1 structure of which, both in crystal and in solution, as well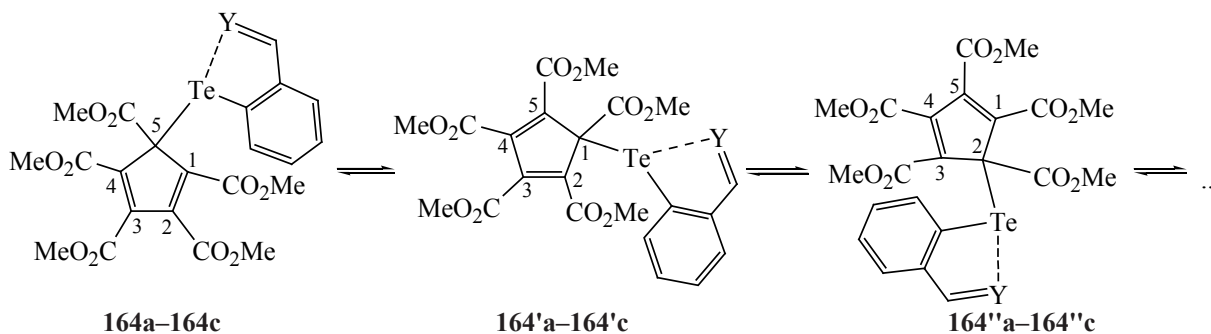 as the intramolecular Te···O and Te··N coordination in them was obtained by IR and NMR spectroscopy (Scheme 63) [111, 112].

The ^{1}H and ^{13}C NMR spectra of compound **164a** (Y = O) at low temperatures display diastereotopic splitting of signals from the sp^2-C atoms of the Cp ring and substituents on them, due to the asymmetric arrangement of the tellurium substituent relative to this ring. The dynamics of the ^{1}H and ^{13}C NMR spectra of compound **164a** in the temperature range 25–65°C indicates fast intramolecular 1,5-sigmatropic shifts of the aryltellurenyl group along the Cp ring ($\Delta G^{\neq}_{25°C}$ 13.4 kcal/mol). In azomethine derivatives **164b** and **164b** (Y = NAr), the migrations of the tellurenyl group occur much faster and are too fast to be detectable on the ^{1}H and ^{13}C NMR time scales even at –90°C; the energy barrier for these migrations is 6.0 ± 2.0 kcal/mol. Thus, the migratory capacity of thio, seleno, and telluro groups in the PCCP **1** system increases in the order S < Se <Te, which is associated with a decrease in the energy of the C5–chalcogen bond with an increase in

Scheme 63.

164a–164c ⇌ **164'a–164'c** ⇌ **164''a–164''c** ⇌ ...

Y = O (**a**), NPh (**b**), NC$_6$H$_4$Me-2 (**c**).

Scheme 64.

R = CO$_2$Me, R^1 = Me (**a**), *i*-Pr (**b**), CH$_2$Ph (**c**).

165a–165c ⇌ **166a–166c**
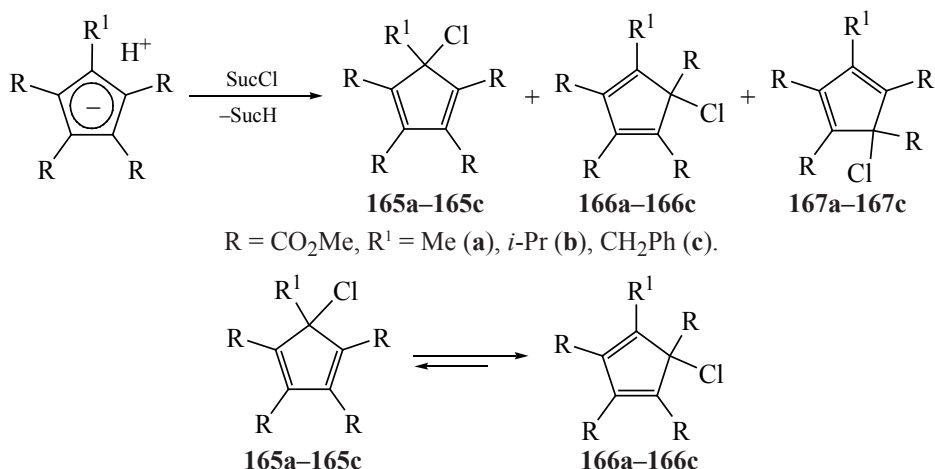
the atomic number of the central atom of the migrating group.

Halocyclopentadienes are an important class of precursors of Cp compounds and their metal complexes [15, 16, 113–116]. According to DFT calculations, the iodocyclopentadiene molecule in a rotating electric field is a prototype of a molecular rotary motor with a fast ($k_{25°C}$ 630 s^{-1}) unidirectional movement of iodine along the Cp ring [117].

Dynamic ^{1}H and ^{13}C NMR spectroscopy revealed reversible intramolecular 1,5-shifts of Cl and Br along the perimeter of the penta(alkyltetra)methoxy-carbonylcyclopentadiene ring (Alk = Me, *i*-Pr, CH$_2$Ph, CH$_2$CO$_2$CH$_3$), with proceeding with $\Delta G^{\neq}_{25°C}$ 25.7–27.3 (Cl) and 16.2–22.9 (Br) kcal/mol [118, 119]. Chlorocyclopentadienes **165a–165c** and **167a–167c** were obtained as mixtures of isomers by the reaction of the corresponding cyclopentadienes with *N*-chlorosuccinimide (Scheme 64).

Upon heating *o*-dichlorobenzene solutions of preparatively isolated isomers **165a–165c** at 70–100°C for 0.5–2.5 h resulted in the formation of the following

equilibrium mixtures: **165a** : **166a** = 0.11 : 0.89, **165b** : **166b** = 0.35 : 0.65, and **165c** : **166c** = 0.25 : 0.75.

A similar reaction with NBS led to an equilibrium mixture of bromocyclopentadienes **168a–168c** and **170a–179c**, the dynamics of the ^{1}H and ^{13}C NMR spectra of which at 25–140°C indicated 1,5-shifts of bromine along the Cp ring with $\Delta G^{\neq}_{25°C}$ 16.2–22.9 kcal/mol (Scheme 65) [120].

Quantum-chemical calculations at the (B3LYP/6-311++G(d,p) and B3LYP/Gen, 6-311++G(d,p)/SDD) levels showed that compounds **171a–171d** prefer 1,5-sigmatropic shifts of halogens along the perimeter of the Cp ring to 1,3-shifts and estimated the effect of the halogens on the activation barriers for their migrations (Scheme 66) [119].

The calculated barriers for symmetry-allowed 1,5-shifts of halogens through TS **172** are $\Delta E^{\neq}_{ZPE}$ 42.9(F), 26.9(Cl), 19.8(Br), and 15.4(I) kcal/mol (Scheme 66, *a*), and they are lower those for 1.3-shifts through TS **173** [$\Delta E^{\neq}_{ZPE}$ 65.4(F), 47.6(Cl), 38.1(Br), and 34.2(I) kcal/mol] (Scheme 66, *b*). The calculated barrier fit well the experimental values. The migration

Scheme 65.

168   **169**   **170**

R = Me (**a**), *i*-Pr (**b**), CH$_2$COMe (**c**).

Scheme 66.

a

171a–171d   TS**172**   **171'a–171'd**

b

171a–171d   TS**173**   **171''a–171''d**

Hlg = F (**a**), Cl (**b**), Br (**c**), I (**d**).
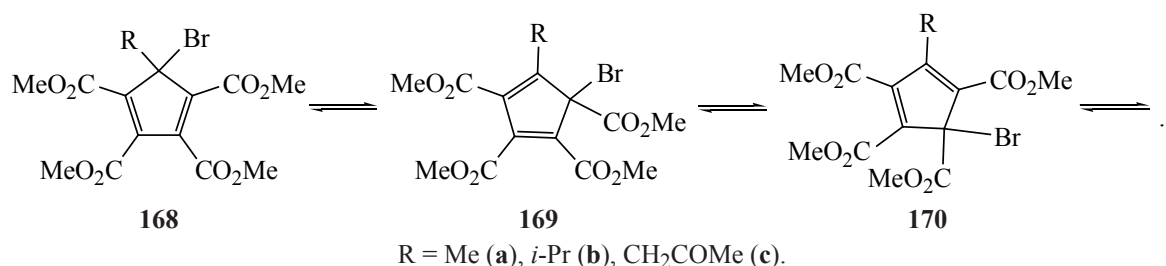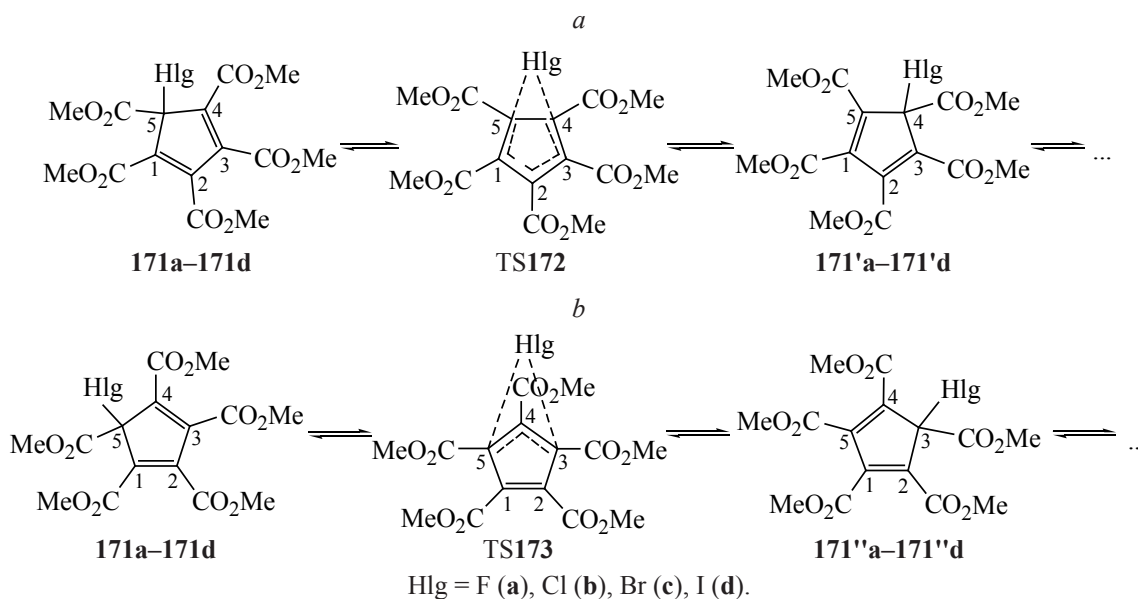
ability of halogens in the corresponding derivatives of PCCP **1** strongly increases in the series F < Cl < Br < I, with increasing atomic number of the halogen.

5. EFFECTIVE CARRIERS OF FUNCTIONAL GROUPS BASED ON FLUCTUATING PCCP

It was shown that arylazo derivatives **147** are convenient reagent for introducing the aryl azo group in compounds containing N- and C-nuclephilic centers, because compounds readily enter the azo coupling reaction with such centers in organic media at 22°C (Scheme 67).

For example, arylazo derivatives **147** react with *N,N'*-diarylbenzamidines **174a** and **174b** [121], react with 2-methylindole, *N,N*-diethylaniline, and malononitrile, as well as with aniline and secondary amines to form C–azo coupling products (**176**, **178**, **179**) and triazenes (**175**, **177**) [122, 123].

The reaction of compound **147a**, which contains one NO₂ substituent in the aryl ring, with Cp* leads to isomer **180** with the arylazo substituent in the Cp* ring, whereas 2,4-dinitrophenyl azo derivative **147b** the diazonium cation generated from 2,4-dinitrophenyl azo derivative **147b** attacks both the methyl substituent and the Cp* ring (Scheme 68) [124].

The reaction of arylzocyclopentadiene **147a** with compound **183** involves the azo coupling product at the carbon atom of the Cp ring with the substitution of the CO₂Me group (Scheme 69) [125].

In this cascade reaction, the CO₂Me group undergoes a 1,5-shift to the nitrogen of the amidine triad, followed by hydrolysis of the imido group to give product **184**.

Air oxygen- and moisture-resistant arylthiocyclopentadienes **157a** and **157b** are convenient sulfenylating reagents, giving arylthio derivatives in reactions (22°C, 2–48 h) with amidines (**185**), primary and secondary amines (**186**, **187**), and compounds with activated carbon centers (**188**, **189**) (Scheme 70) [124, 126, 127].

6. TETRACARBOMETOXYCYCLOPENTADENYL LIGAND SYSTEMS AND THEIR METAL COMPLEXES

The nucleophilic substitution of the nitro group in compound **191** by the amine nitrogen atom of amidines **190** allowed the synthesis of a wide range of bidentate amidinylcyclopentadienyl ligands **194a–194f** (Scheme 71) [32–34, 128–131].

This reaction involves the 1,4-sigmatropic shift of the CO₂Me group to the amidine imino nitrogen to give Cp ylides **193a–193f**, and HNO₂ released during reaction nitrosylated amidine **191** (double excess), yielding *N*-nitrosoamidene **192**. Treatmeny of ylides **193a–193f** with methanolic NaOH resulted in the elimination of the N–CO₂Me group, and subsequent acidification with HCl led to ligands **194a–194f**.

Potassium and Tl(I) complexes complexes **195a–195f** and **196a–196c**, respectively, were prepared

Scheme 67.

Ar = 4-NO$_2$C$_6$H$_4$ (**a**), 2,4-(NO$_2$)$_2$C$_6$H$_3$ (**b**); Ar' = 4-MeC$_6$H$_4$.
R^2 = Et$_2$, (CH$_2$)$_5$, (CH$_2$)$_2$O(CH$_2$)$_2$.
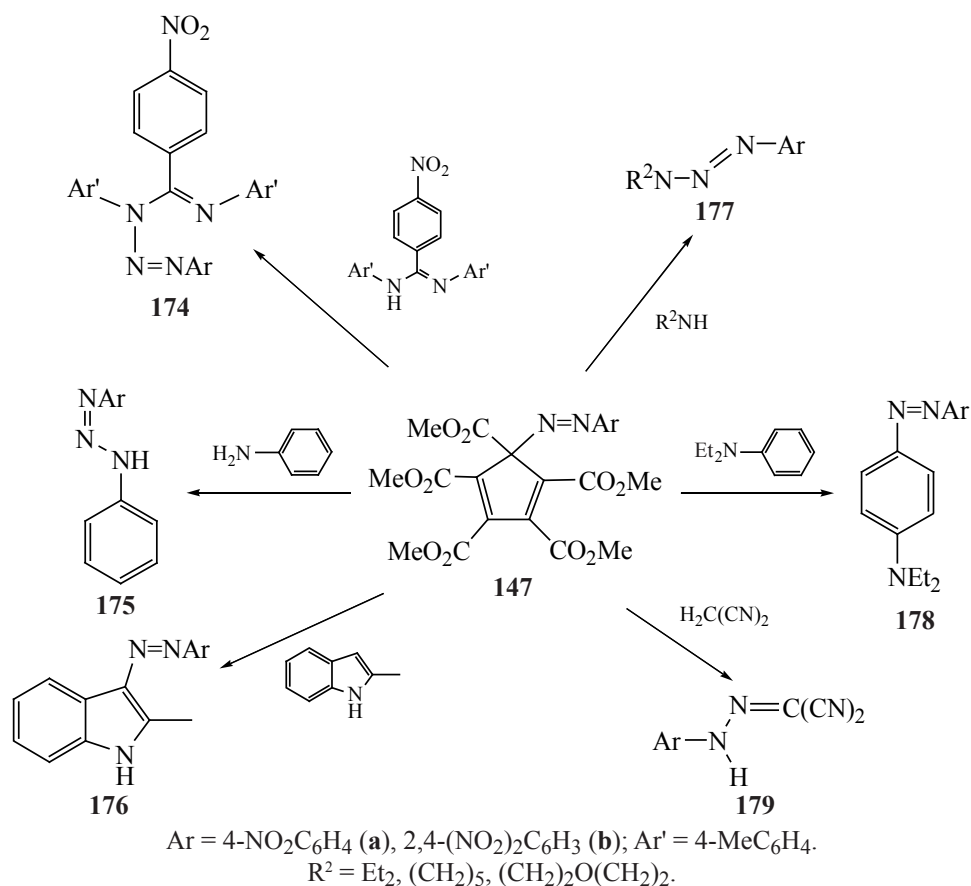
by treatment of ylides **193** with methanolic KOH and TlOH, respectively (Scheme 72) [33, 34, 132].

The reaction of compounds **195a**, **195b**, and **195f** with (Ph$_3$P)AuCl in MeCN gave Au(I) complexes **197a**, **197b**, and **197f** (Scheme 73) [31, 32].

The reaction of ligands **194a** and **194b** with 4-Me$_2$NC$_6$H$_4$HgOCOMe in methanol resulted in the synthesis of arylmercury complexes **198a** and **198b** (Scheme 74) [32].

It was shown that ligands **194** and metal complexes **195–198** have a zwitter ionic structure, with the positive charge localized in the amidine triade and the negative charge in the Cp ring. The metals in complexes **195–198** are coordinated to the terminal nitrogen and additionally coordinated to the π-system of the Cp. Ligands or K, Tl(I), Au(I), and Hg(II) complexes with axially asymmetric α-naphthyl or *o*-substituted Ar' groups in the amidine triad characteristically have a chiral structure, which is associated with high barriers for rotation of the aryl groups about the C–C bond and of the amidinium fragment about the C$_{Cp}$–N bond.

The cascade reactions of potassium cycloheptatrienyl **199** with organic azides were used to prepare similar β-aminovinyl Cp anions **200** (Scheme 75) [133].

Therewith, the formation of the Cp fragment involved C–C bond cleavage and CO$_2$Me migration. The structure of N–Ms complex **200** was confirmed by XRD analysis, which showed that the K$^+$ or Na$^+$ ions are coordinated to two CO$_2$Me carbonyl groups on the Cp ring and vinyl group. Complex **200** gave stable salts with organic cations [134].

7. PUSH−PULL CHROMOPHORES WITH HYDRAZONE PCCP FRAGMENTS FOR ORGANIC PHOTOVOLTAICS

It was shown that the reaction between *N*-mesyl complex **200** and aryldiazonium followed by hydrolysis and decarboxylation of one CO$_2$Me leads to isomeric 3- and 4-aminovinyl-5-hydrazonocyclopentadienes **201** and **202**, which undergo cyclization on silica gel to form pyridazine **203** (Scheme 76) [135].

Scheme 68.

Scheme 69.

Scheme 70.

Ar = 2-NO$_2$C$_6$H$_4$ (**a**), 4-NO$_2$C$_6$H$_4$ (**b**); Ar' =4-MeC$_6$H$_4$, 4-MeOC$_6$H$_4$.

Scheme 71.

R = CO$_2$Me, Ar' = 1-C$_{10}$H$_7$, Ar = 4-MeC$_6$H$_4$ (**a**), 3-MeC$_6$H$_4$ (**b**);
R = CO$_2$Me, Ar' = 4-MeC$_6$H$_4$, Ar = Ph (**c**), 2-MeOC$_6$H$_4$ (**d**), 2-ClC$_6$H$_4$ (**e**), 2-BrC$_6$H$_4$ (**f**).

Scheme 72.

195, Ar = 4-MeC$_6$H$_4$, Ar' = Ph (**a**), 1-C$_{10}$H$_7$ (**b**), 2-BrC$_6$H$_4$ (**c**), 2-ClC$_6$H$_4$ (**d**), 2-MeOC$_6$H$_4$ (**e**); Ar = 3-MeC$_6$H$_4$,
Ar' = 1-C$_{10}$H$_7$ (**f**); **196**, Ar = 4-MeC$_6$H$_4$, Ar' = 1-C$_{10}$H$_7$ (**a**), 2-ClC$_6$H$_4$ (**b**), 2-Cl,6-MeC$_6$H$_3$ (**c**).

Scheme 73.

195a, **195b**, **195f**   **197a**, **197b**, **197f**

Ar = 4-MeC$_6$H$_4$, Ar' = Ph (**a**); Ar' = 1-C$_{10}$H$_7$ (**b**); Ar = 3-MeC$_6$H$_4$, Ar' = 1-C$_{10}$H$_7$ (**f**).

Scheme 74.

194a, **194b**   **198a**, **198b**

R = CO$_2$Me, Ar = 4-MeC$_6$H$_4$, Ar" = 4-Me$_2$NC$_6$H$_4$; Ar' = Ph (**a**), 1-C$_{10}$H$_7$ (**b**).

Scheme 75.

199

200

R = Ms, Ts, CO$_2$Et, C(O)*cyclo*-C$_3$H$_5$, C(O)Ph, C(O)C$_6$H$_4$F-4, C(O)C$_6$H$_4$NO$_2$-4.

Scheme 76.

Ar = 4-MeOC$_6$H$_4$ (**a**), 2,5-Me$_2$C$_6$H$_3$ (**b**), 4-FC$_6$H$_4$ (**c**), 4-O$_2$NC$_6$H$_4$ (**d**), 1-C$_{10}$H$_7$ (**f**).

Hydrazines **201** and **202** strongly absorb in the range 400–600 nm and are of interest for dye-sensitized solar cells. X-ray diffraction analysis of hydrazone **201c** revealed a short N–N in it, which indicates strong conjugation between the donor and acceptor parts of the molecules. The polarized Cp–hydrazone fragment is of interest as an acceptor substituent for chromophores of the D–π–A type. The short N–N bond characteristic of these structures, the length of which corresponds to a greater extent to the bond length in azo compounds than in hydrazones, indicates polarization of hydrazones **201** and **202**, similar to fulvenes. The developed

synthetic approach of the azafulvene fragment can be in demand in the preparation of D–π–A chromophores for photovoltaics and nonlinear optics and for the creation of organic light-emitting diodes and field-effect transistors.

The reaction of cyclopentadienone **204** with arylhydrazine hydrochlorides gave stable arylhydrazones **205** (Scheme 77) [35].
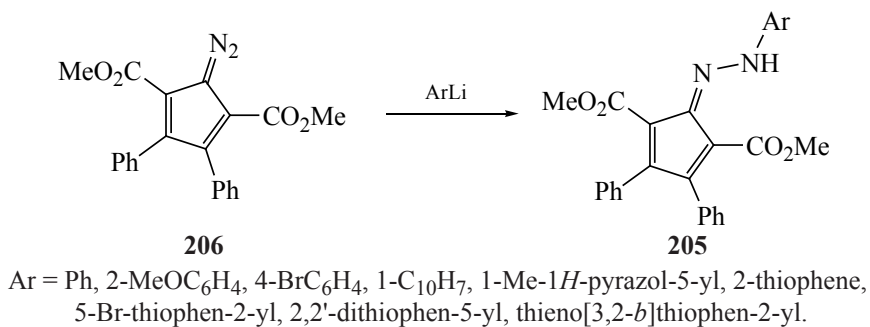
The range of D–A chromophores with hydrazin-ylidene acceptors **205** was expanded by the action of organolithium reagents on cyclic diazo compounds **206**, which made it possible to introduce thiophene fragments

Scheme 77.
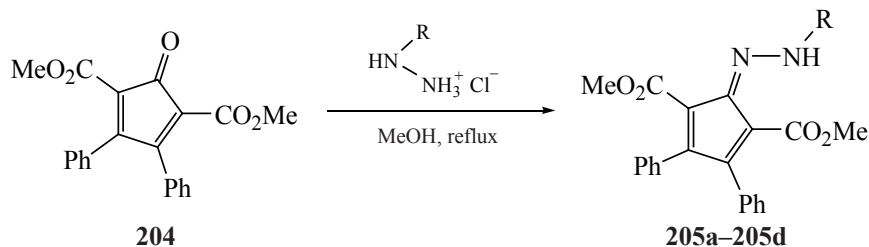
R = XC$_6$H$_4$ (X = H, 4-Me, 3-Me, 4-MeO, 4-F, 4-Br, 2-CF$_3$), 1-Me-1*H*-pyrazol-5-yl.

Scheme 78.

Ar = Ph, 2-MeOC$_6$H$_4$, 4-BrC$_6$H$_4$, 1-C$_{10}$H$_7$, 1-Me-1*H*-pyrazol-5-yl, 2-thiophene,
5-Br-thiophen-2-yl, 2,2'-dithiophen-5-yl, thieno[3,2-*b*]thiophen-2-yl.

into the chromophore to create planar molecules (Scheme 78) [136].

Arylhydrazones **205** intensely absorbed visible light in the 373–562 nm range with extinction coefficients (ε) up to 36500 M^{-1} cm^{-1}, while thiophene derivatives had the longest absorption compared to other hydrazones.

Compounds with an acceptor hydrazone Cp fragment, a π-conjugated phenylene spacer, and an electron-donor triphenylamine substituent **207a** and **207b** were also obtained and exhibited optical, electrochemical, and photoelectric properties, due to which these compounds have a high potential for use in organic photovoltaics (Scheme 79) [137].

Despite their non-coplanar structure, hydrazones **207a** and **207b** showed semiconducting properties and were capable of intramolecular charge separation. Hydrazone **207a** as donor components of photovoltaic layers of organic solar cells were found to have the highest efficiency (up to 1.85%), which opens up the prospects for the use of hydrazone Cp fragments in the design of polarized chromophores for photovoltaics.

A new A–D–A chromophore **209** with the indacenodithienothiophene core linked to 2 terminal acceptor hydrazone Cp groups was obtained by the reaction
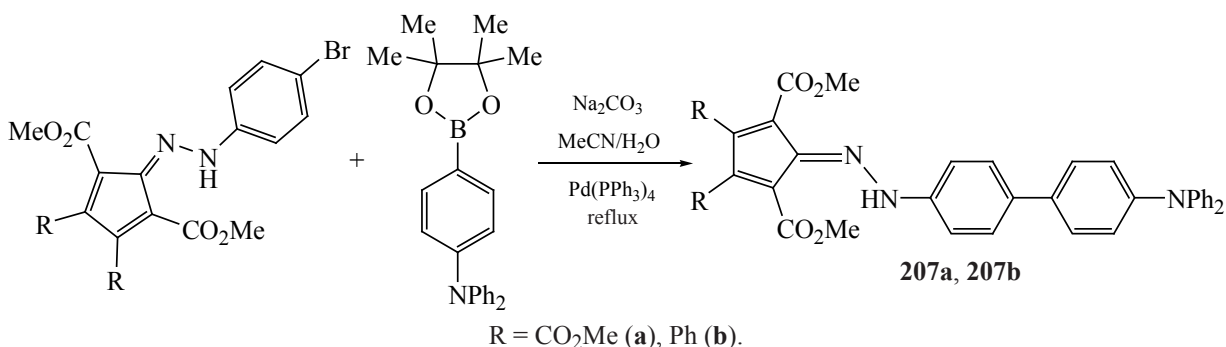
of dilithium indacenodithienothiophene **208** with diazo derivative **206** (Scheme 80) [138].

Chromophore **209** intensely absorbed in the range 500–800 nm, with a maximum ε value of 86700 M^{-1}·cm^{-1} at 669 nm. Its absorption spectrum in the film had a similar maximum, which indicated the absence of significant molecular organization and amorphous structure in it. The optical band gap for chromophore **209** in the film was estimated from the absorption edge (800 nm) as 1.55 eV. The energies of the boundary orbitals were estimated at –5.42 (HOMO) and –3.80 (LUMO) eV. These data allowed the conclusion that compound **209** is suitable for use as an acceptor material in organic solar cells (OSC).

Based on the synthetically available dimethyldibromosuccinate **210**, a new method for the synthesis of pyridinium cyclopentadienolate **211** (Scheme 81) was developed [139].

It was shown that salt **211** is as reactive toward arylhydrazines as cyclopentadienones, giving arylhydrazonecyclopentadienes **212**. Thus, compounds **212** were introduced in intramolecular cyclization reactions, which made it possible to obtain chromophores **213**–**215** (Scheme 82).

Scheme 79.

R = CO$_2$Me (**a**), Ph (**b**).

Scheme 80.

208

209

Scheme 81.

210   **211**

212

Ar = Ph, 4-MeOC$_6$H$_4$, 4-MeC$_6$H$_4$, 4-BrC$_6$H$_4$, [1,1'-biphenyl]-4-yl

Scheme 82.

R = H, MeO, Me, Br, Ph.
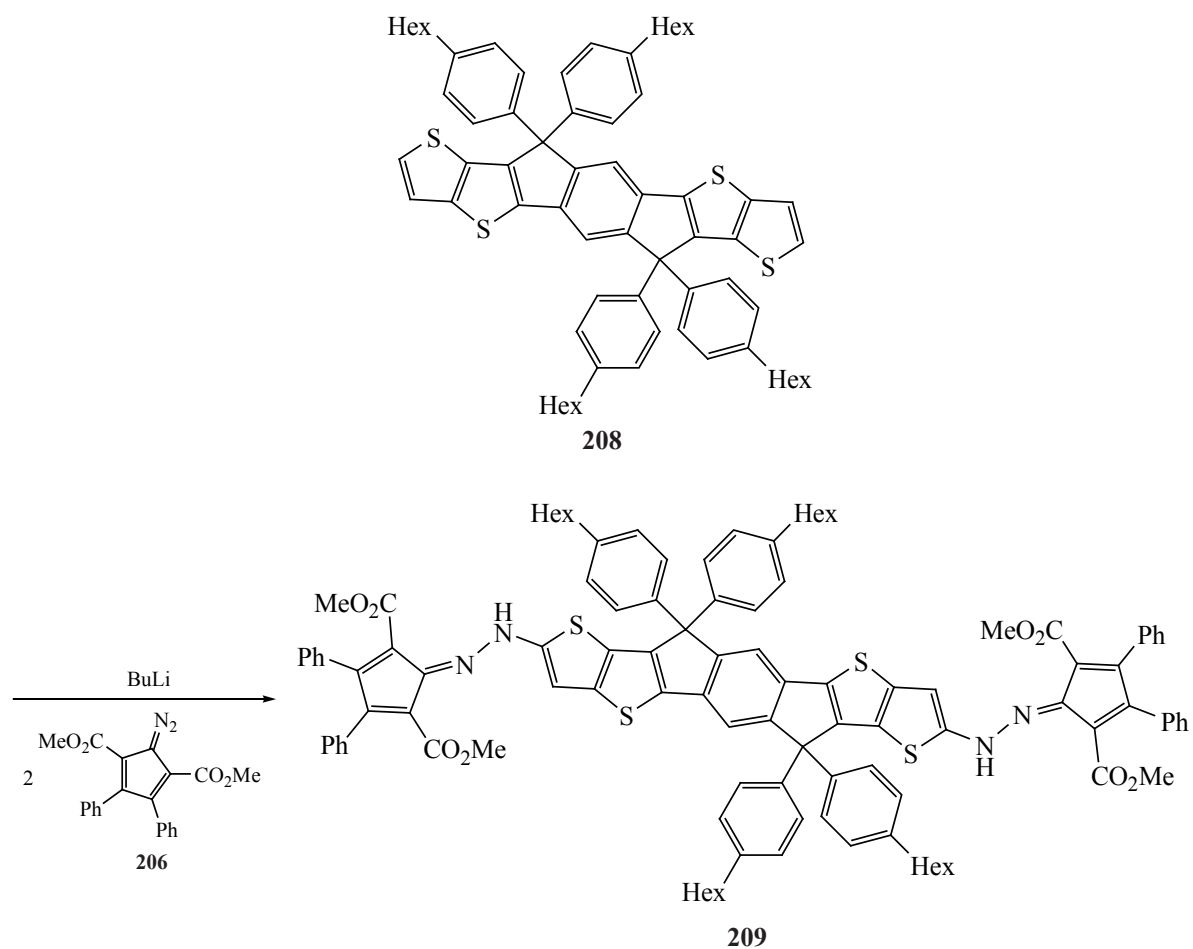
CONCLUSIONS

Despite the fact that (pentamethoxycarbonyl)-cyclopentadiene (**1**) and a number of its derivatives were obtained in the middle of the last century, the chemistry of these compound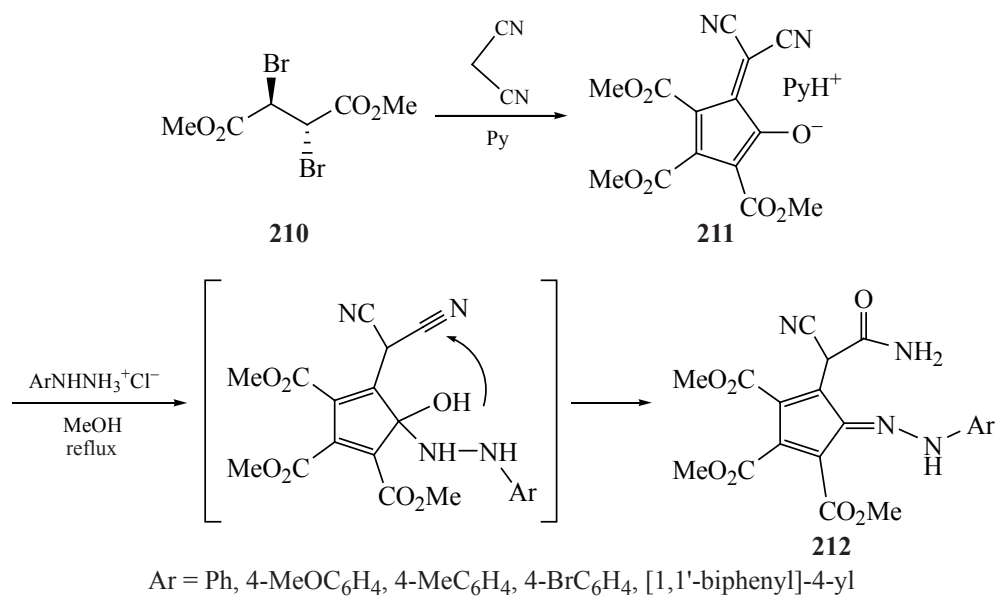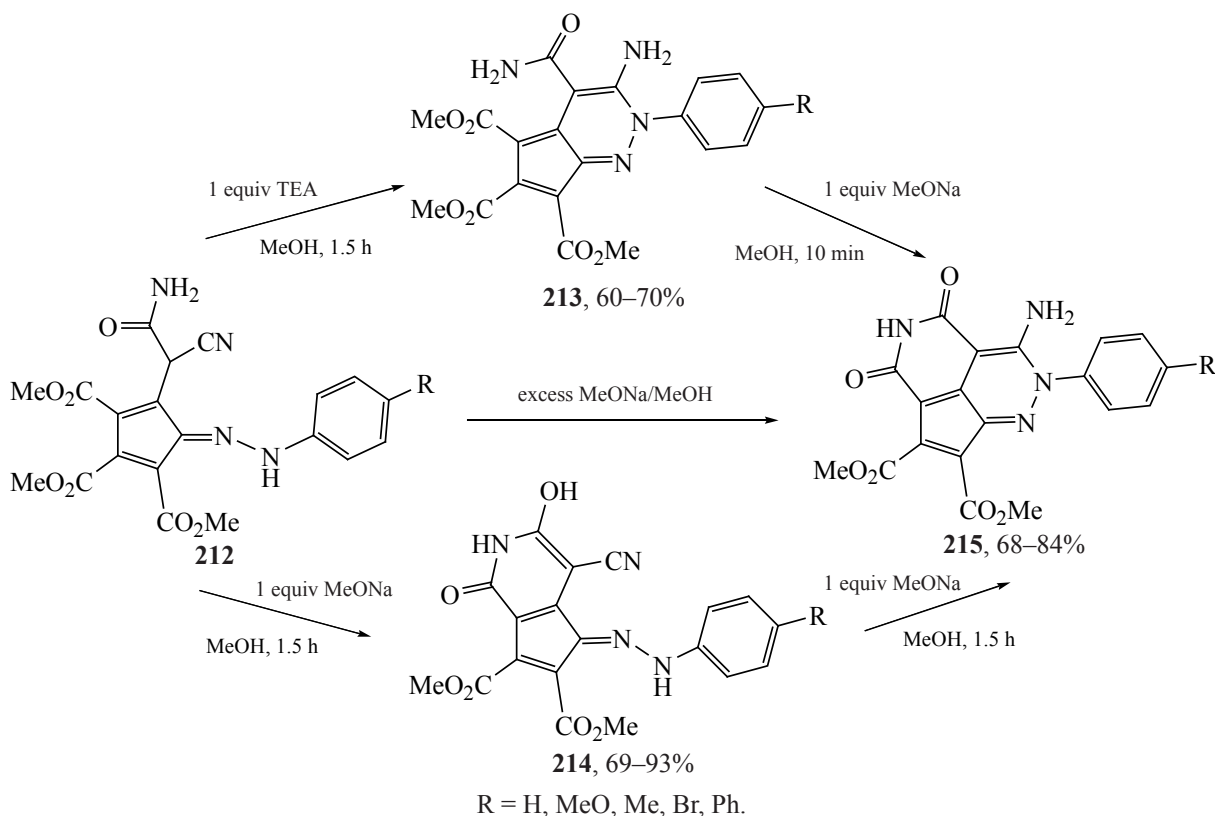s continues to evolve at present, which is due to the synthetic availability and unique properties of these compounds. In particular, the extremely high acidity of PCCP makes it possible to use these compounds as highly efficient enantioselective Bronsted catalysts, due to their fulvic structure favors the formation of a wide range of metal complexes, and the ester groups in their composition allows functionalization, which leads to a wide range of derivatives. Of particular note is the unusual propeller orientation of the chiral ester groups in these compounds relative to the Cp ring, which allows enantioselective control of reactions with their participation.

Together the ability of these groups to act as H-bond acceptors and of the Cp anion to participate in intermolecular interactions with substrates favors the formation of suitable transition states for the chemical reactions to take the desired direction. A high potential of PCCP derivatives as enantioselective catalysts for a wide range of reactions and as effective carriers of arylazo and arylthio groups, in the preparation of push-pull chromophores for organic photovoltaics and in the creation of new pharmaceuticals, including anticarcinogenic ones was revealed. This review aims to draw further attention to this interesting and promising class of compounds.

FUNDING

AUTHOR INFORMATION

I.E. Mikhailov, ORCID: http://orcid.org/0000-0003-1820-4012

G.A. Dushenko, ORCID: http://orcid.org/0000-0002-5455-8419

V.I. Minkin, ORCID: http://orcid.org/0000-0001-6096-503X

CONFLICT OF INTEREST

The authors declare no conflict of interest.

REFERENCES

1. Sk, M.R., Bera, S.S., Basuli, S., Metya, A., and Maji, M.S., *Asian J. Org. Chem.*, 2020, vol. 9, p. 1701.
https://doi.org/10.1002/ajoc.202000367

2. Wang, S., Chen, S.Y., and Yu, X.Q., *Chem. Commun.*, 2017, vol. 53, p. 3165.
https://doi.org/10.1039/c6cc09651d

3. Ye, B. and Cramer, N., *Acc. Chem. Res.*, 2015, vol. 48, p. 1308.
https://doi.org/10.1021/acs.accounts.5b00092

4. Doerksen, R.S., Hodik, T., Hu, G.Y., Huynh, N.O., Shuler, W.G., and Krische, M.J., *Chem. Rev.*, 2021, vol. 121, p. 4045.
https://doi.org/10.1021/acs.chemrev.0c01133

5. Yamamoto, Y., *Tetrahedron Lett.* 2017, vol. 58, p. 3787.
https://doi.org/10.1016/j.tetlet.2017.08.040

6. Ehm, C., Vittoria, A., Goryunov, G.P., Izmer, V.V., Kononovich, D.S., Samsonov, O.V., Di, Girolamo, R., Budzelaar, P.H.M., Voskoboynikov, A.Z., Busico, V., Uborsky, D.V., and Cipullo, R., *Polymers*, 2020, vol. 12, p. 1005.
https://doi.org/10.3390/polym12051005

7. Zaccaria, F., Cipullo, R., Budzelaar, P.H.M., Busico, V., and Ehm, Ch., *J. Polym. Sci.*, *Part A: Polym. Chem.*, 2017, vol. 55, p. 2807.
https://doi.org/10.1002/pola.28685

8. Greene, D.L., Chau, A., Monreal, M., Mendez, C., Cruz, I., Wenj, T., Tikkanen, W., Schick, B., and Kantardjieff, K., *J. Organometal. Chem.*, 2003, vol. 682, p. 8.
https://doi.org/10.1016/S0022-328X(03)00637-5

9. Dewangan, S., Barik, T., Parida, R., Mawatwal, S., Dhiman, R., Giri, S., and Chatterjee, S., *J. Organometal. Chem.*, 2019, vol. 904, p. 120999.
https://doi.org/10.1016/j.jorganchem.2019.120999

10. Kelbysheva, E.S., Telegina, L.N., Strelkova, T.V., Ezernitskaya, M.G., Smol'yakov, A.F., Borisov, Yu.A., Lokshin, B.V., Konstantinova, E.A., Gromov, O.I., Kokorin, A.I., and Loim, N.M., *Organometallics*, 2019, vol. 38, p. 2288.
https://doi.org/10.1021/acs.organomet.9b00165

11. Sturala, J., Etherington, M.K., Bismillah, A.N., Higginbotham, H.F., Trewby, W., Aguilar, J.A., Bromley, E.H.C., Avestro, A.-J., Monkman, A.P., and McGonigal, P.R., *J. Am. Chem. Soc.*, 2017, vol. 139, p. 17882.
https://doi.org/10.1021/jacs.7b08570

12. Suta, M., Kuehling, M., Liebing, P., Edelmann, F.T., and Wickleder, C., *J. Luminescence*, 2017, vol. 187, p. 62.
https://doi.org/10.1016/j.jlumin.2017.02.054

13. Long, J., Tolpygin, A.O., Cherkasov, A.V., Lyssenko, K.A., Guari, Y., Larionova, J., and Trifonov, A.A., *Organometallics*, 2019, vol. 38, p. 748.
https://doi.org/10.1021/acs.organomet.8b00901

14. Guo, F.S., Day, B.M., Chen, Y.C., Tong, M.L., Mansikkamaki, A., and Layfield, R.A., *Science*, 2018, vol. 362, p. 1400.
https://doi.org/10.1126/science.aav0652

15. Field, L.D., Lindall, C.M., Masters, A.F., and Clentsmith, G.K.B., *Coord. Chem. Rev.*, 2011, vol. 255, p. 1733.
https://doi.org/10.1016/j.ccr.2011.02.001

16. Stefak, R., Sirven, A.M., Fukumoto, S., Nakagawa, H., and Rapenne, G., *Coord. Chem. Rev.*, 2015, vol. 287, p. 79.
https://doi.org/10.1016/j.ccr.2014.11.014

17. Muller, C., Vos, D., and Jutzi, P., *J. Organomet. Chem.*, 2000, vol. 600, p. 127.
https://doi.org/10.1016/S0022-328X(00)00060-7

18. Jutzi, P. and Burford, N., *Chem. Rev.*, 1999, vol. 99, p. 969.
https://doi.org/10.1021/CR941099T

19. Siemeling, U., *Chem. Rev.*, 2000, vol. 100, p. 1495.
https://doi.org/10.1021/cr990287m

20. Frei, A., *Chem. Eur. J.*, 2019, vol. 25, p. 7074.
https://doi.org/10.1002/chem.201900276

21. Deck, P.A., *Coord. Chem. Rev.*, 2006, vol. 250, p. 1032.
https://doi.org/10.1016/j.ccr.2005.11.001

22. Yoshino, T., Satake, S., and Matsunaga, S., *Chem. Eur. J.*, 2020, vol. 26, p. 7346.
https://doi.org/10.1002/chem.201905417

23. Sünkel, K. and Nimax, P.R., *Dalton Trans.*, 2018, vol. 47, p. 409.
https://doi.org/10.1039/c7dt03862c

24. Day, B.M., Guo, F.-S., and Layfield, R.A., *Acc. Chem. Res.*, 2018, vol. 51, p. 1880.
https://doi.org/10.1021/acs.accounts.8b00270

25. Loginov, D.A., Shul'pina, L.S., Muratov, D.V., and Shul'pin, G.B., *Coord. Chem. Rev.*, 2019, vol. 387, p. 1.
https://doi.org/10.1016/j.ccr.2019.01.022

26. Cookson, R.C., Henstock, J.B., Hudec, J., and Whitear, B.R.D., *J. Chem. Soc. C*, 1967, p. 1986.
https://doi.org/10.1039/J39670001986

27. Bruce, M.I., and White, A.H., *Aust. J. Chem.*, 1990, vol. 43, p. 949.
https://doi.org/10.1071/CH9900949

28. Cramer, N., Mas-Roselló, J., Herraiz, A.G., Audic, B., and Laverny, A., *Angew. Chem. Int. Ed.*, 2021, vol. 60, p. 13198.
https://doi.org/10.1002/anie.202008166

29. Shaaban, S., Davies, C., and Waldmann, H., *Eur. J. Org. Chem.*, 2020, vol. 42, p. 6512.
https://doi.org/10.1002/ejoc.202000752

30. Gheewala, C.D., Collins, B.E., and Lambert, T.H., *Science*, 2016, vol. 351, p. 961.
https://doi.org/10.1126/science.aad0591

31. Minkin, V.I., Mikhailov, I.E., Dushenko, G.A., and Zschunke, A., *Russ. Chem. Rev.*, 2003, vol. 72, p. 867.
https://doi.org/10.1070/RC2003v072n10ABEH000848

32. Dushenko, G.A., Mikhailov, I.E., Zschunke, A., Reck, G., Schulz, B., Mugge, C., and Minkin, V.I., *Mendeleev Commun.*, 1999, p. 67.
https://doi.org/10.1070/mc1999v009n02abeh001064

33. Dushenko, G.A., Mikhailov, I.E., Reck, G., Schulz, B., Zschunke, A., and Minkin, V.I., *Russ. Chem. Bull.*, 2001, vol. 50, p. 890.
https://doi.org/10.1023/A:1011323629390

34. Mikhailov, I.E., Dushenko, G.A., Reck, G., Schulz, B., Zschunke, A., and Minkin, V.I., *Dokl. Chem.*, 2007, vol. 412, p. 49.
https://doi.org/10.1134/S0012500807020073

35. Salikov, R.F., Trainov, K.P., Platonov, D.N., Davydov, D.A., Lee, S., Gerasimov, I.S., Medvedev, M.G., Levina, A.A., Belyy, A.Yu., and Tomilov, Yu.V., *Dyes Pigm.*, 2019, vol. 161, p. 500.
https://doi.org/10.1016/j.dyepig.2018.09.040

36. Jayanty, S., Kumar, D.B.K., and Radhakrishnan, T.P., *Synthetic Metals*, 2000, vol. 114, p. 37.
https://doi.org/10.1016/S0379-6779(00)00204-6

37. Griffin, P.J., Freyer, J.L., Han, N., Geller, N., Yin, X., Gheewala, C.D., Lambert, T.H., Campos, L.M., and Winey, K.I., *Macromolecules*, 2018, vol. 51, p. 1681.
https://doi.org/10.1021/acs.macromol.7b02546

38. Jayanty, S. and Radhakrishnan, T.P., *J. Mater. Chem.*, 1999, vol. 9, p. 1707.
https://doi.org/10.1039/a901661i

39. Micallef, L.S., Loughrey, B.T., Healy, P.C., Parsons, P.G., and Williams, M.L., *Organometallics*, 2010, vol. 29, p. 6237.
https://doi.org/10.1021/om100645y

40. Gheewala, C.D., Radtke, M.A., Hui, J., Hon, A.B., and Lambert, T.H., *Org. Lett.*, 2017, vol. 19, p. 4227.
https://doi.org/10.1021/acs.orglett.7b01867

41. Gheewala, C.D., Hirschi, J.S., Lee, W.-H., Paley, D.W., Vetticatt, M.J., and Lambert, T.H., *J. Am. Chem. Soc.*, 2018, vol. 140, p. 3523.
https://doi.org/10.1021/jacs.8b00260

42. Radtke, M.A., Dudley, C.C., O'Leary, J.M., and Lambert, T.H., *Synthesis*, 2019, vol. 51, p. 1135.
https://doi.org/10.1055/s-0037-1611650

43. Lei, Y.X., Cerioni, G., and Rappoport, Z., *J. Org. Chem.*, 2000, vol. 65, p. 4028.
https://doi.org/10.1021/jo000046a

44. Mikhailov, I.E., Dushenko, G.A., Minkin, V.I., and Olekhnovich, L.P., *Zh. Org. Khim.*, 1984, vol. 20, p. 1657.

45. Dushenko, G.A., Mikhailov, I.E., Mikhailova, O.I., Minyaev, R.M., and Minkin, V.I., *Dokl. Chem.*, 2017, vol. 476, p. 230.
https://doi.org/10.1134/S0012500817100020

46. Dushenko, G.A., Mikhailov, I.E., Mikhailova, O.I., Minyaev, R.M., and Minkin, V.I., *Dokl. Chem.*, 2016, vol. 471, p. 350.
https://doi.org/10.1134/S0012500816120028

47. Parmar, D., Sugiono, E., Raja, S., and Rueping, M., *Chem. Rev.*, 2014, vol. 114, p. 9047.
https://doi.org/10.1021/cr5001496

48. Akiyama, T. and Mori, K., *Chem. Rev.*, 2015, vol. 115, p. 9277.
https://doi.org/10.1021/acs.chemrev.5b00041

49. Rowland, G.B., Zhang, H., Rowland, E.B., Chennamadhavuni, S., Wang, Y., and Antilla, J.C., *J. Am. Chem. Soc.*, 2005, vol. 127, p. 15696.
https://doi.org/10.1021/ja0533085

50. Xu, F., Huang, D., Han, C., Shen, W., Lin, X., and Wang, Y., *J. Org. Chem.*, 2010, vol. 75, p. 8677.
https://doi.org/10.1021/jo101640z

51. Fleischer, I., *Angew. Chem. Int. Ed.*, 2016, vol. 55, p. 7582.
https://doi.org/10.1002/anie.201603672

52. Lyons, D.J.M., Crocker, R.D., Blümel, M., and Nguyen, T.V., *Angew. Chem. Int. Ed.*, 2017, vol. 56, p. 1466.
https://doi.org/10.1002/anie.201605979

53. Preethalayam, P., Krishnan, K.S., Thulasi, S., Chand, S.S., Joseph, J., Nair, V., Jaroschik, F., and Radhakrishnan, K.V., *Chem. Rev.*, 2017, vol. 117, p. 3930.
https://doi.org/10.1021/acs.chemrev.6b00210

54. Akiyama, T., Itoh, J., Yokota, K., and Fuchibe, K., *Angew. Chem. Int. Ed.*, 2004, vol. 43, p. 1566.
https://doi.org/10.1002/anie.200353240

55. Ratjen, L., García-García, P., Lay, F., Beck, M.E., and List, B., *Angew. Chem. Int. Ed.*, 2011, vol. 50, p. 754.
https://doi.org/10.1002/anie.201005954

56. Katritzky, A.R., Rachwal, S., and Rachwal, B., *Tetrahedron*, 1996, vol. 52, p. 15031.
https://doi.org/10.1016/S0040-4020(96)00911-8

57. Bartoszewicz, A., Ahlsten, N., and Martín-Matute, B., *Chem.-Eur. J.*, 2013, vol. 19, p. 7274.
https://doi.org/10.1002/chem.201202836

58. Rueping, M., Sugiono, E., Steck, A., and Theissmann, T., *Adv. Synth. Catal.*, 2010, vol. 352, p. 281.
https://doi.org/10.1002/adsc.200900746

59. Qiao, X., El-Shahat, M., Ullah, B., Bao, Z.B., Xing, H.B., Xiao, L., Ren, Q.L., and Zhang, Z.G., *Tetrahedron Lett.*, 2017, vol. 58, p. 2050.
https://doi.org/10.1016/j.tetlet.2017.04.038

60. Zhao, X.F., Xiao, J.L., and Tang, W.J., *Synthesis*, 2017, vol. 49, p. 3157.
https://doi.org/10.1055/s-0036-1589012

61. Sridharan, V., Suryavanshi, P.A., and Menendez, J.C., *Chem. Rev.*, 2011, vol. 111, p. 7157.
https://doi.org/10.1021/cr100307m

62. Meninno, S. and Lattanzi, A., *Chem.-Eur. J.*, 2016, vol. 22, p. 3632.
https://doi.org/10.1002/chem.201504226

63. Zhu, Y., Wang, Q., Cornwall, R.G., and Shi, Y., *Chem. Rev.*, 2014, vol. 114, p. 8199.
https://doi.org/10.1021/cr500064w

64. Wang, Z., Law, W.K., and Sun, J., *Org. Lett.*, 2013, vol. 15, p. 5964.
https://doi.org/10.1021/ol402797v

65. Yuan, C., Li, J., and Li, P.F., *ACS Omega*, 2018, vol. 3, p. 6820.
https://doi.org/10.1021/acsomega.8b01207

66. Verdel, B.M., Souverein, P.C., Egberts, A.C.G., and Leufkens, H.G.M., *Ann. Pharm.*, 2006, vol. 40, p. 1040.
https://doi.org/10.1345/aph.1G642

67. Chinigo, G.M., Paige, M., Grindrod, S., Hamel, E., Dakshanamurthy, S., Chruszcz, M., Minor, W., and Brown, M.L., *J. Med. Chem.*, 2008, vol. 51, p. 4620.
https://doi.org/10.1021/jm800271c

68. Sui, Y.B., Cui, P., Liu, S.S., Zhou, Y.M., Du, P., and Zhou, H.F., *Eur. J. Org. Chem.*, 2018, vol. 2018, p. 215.
https://doi.org/10.1002/ejoc.201701561

69. Perrine, D.M., Ross, J.T., Nervi, S.J., and Zimmerman, R.H., *J. Chem. Educ.*, 2000, vol. 77, p. 1479.
https://doi.org/10.1021/ed077p1479

70. Foley, K.F. and Cozzi, N.V., *Drug Dev. Res.*, 2003, vol. 60, p. 252.
https://doi.org/10.1002/ddr.10297

71. Zhang, Z., Luo, Y.Z., Du, H.G., Xu, J.X., and Li, P.F., *Chem. Sci.*, 2019, vol. 10, p. 5156.
https://doi.org/10.1039/C9SC00568D

72. Cheon, C.H., Yamamoto, H., and Toste, F.D., *J. Am. Chem. Soc.*, 2011, vol. 133, p. 13248.
https://doi.org/10.1021/ja204331w

73. Das, A., Ayad, S., and Hanson, K., *Org. Lett.*, 2016, vol. 18, p. 5416.
https://doi.org/10.1021/acs.orglett.6b02820

74. Li, J., An, S.Y., Yuan, C., and Li, P.F., *Synlett*, 2019, vol. 30, p. 1317.
https://doi.org/10.1055/s-0037-1611849

75. Wenz, D.R. and Read de Alaniz, J., *Eur. J. Org. Chem.*, 2015, p. 23.
https://doi.org/10.1002/ejoc.201402825

76. Gomes, R.F.A., Coelho, J.A.S., and Afonso, C.A.M., *Chem. Eur. J.*, 2018, vol. 24, p. 9170.
https://doi.org/10.1002/chem.201705851

77. Cai, Y., Tang, Y., Atodiresei, I., and Rueping, M., *Angew. Chem. Int. Ed.*, 2016, vol. 55, p. 14126.
https://doi.org/10.1002/anie.201608023

78. Hammersley, G.R., Nichol, M.F., Steffens, H.C., Delgado, J.M., Veits, G.K., and de Alaniz, J.R., *Beilstein J. Org. Chem.*, 2019, vol. 15, p. 1569.
https://doi.org/10.3762/bjoc.15.160

79. Kim, K.-C., Reed, C.A., Elliott, D.W., Mueller, L.J., Tham, F., Lin, L., and Lambert, J.B., *Science*, 2002, vol. 297, p. 825.
https://doi.org/10.1126/science.1073540

80. Richardson, C. and Reed, C.A., *Chem. Commun.*, 2004, vol. 5, p. 706.
https://doi.org/10.1039/b316122f

81. Radtkea, M.A. and Lambert, T.H., *Chem. Sci.*, 2018, vol. 9, p. 6406.
https://doi.org/10.1039/c8sc02279h

82. Hoang, T., Huynh, T., Do, T., and Nguyen, T., *Chem. Pap.*, 2018, vol. 72, p. 1399.
https://doi.org/10.1007/s11696-018-0402-1

83. Mondal, S., Samanta, S., Singsardar, M., and Hajra, A., *Org. Lett.*, 2017, vol. 19, p. 3751.
https://doi.org/10.1021/acs.orglett.7b01594

84. Lian, X., Lin, L., Fu, K., Ma, B., Liu, X., and Feng, X., *Chem. Sci.*, 2017, vol. 8, p. 1238.
https://doi.org/10.1039/c6sc03902b

85. Kang, Z., Wang, Y., Zhang, D., Wu, R., Xu, X., and Hu, W., *J. Am. Chem. Soc.*, 2019, vol. 141, p. 1473.
https://doi.org/10.1021/jacs.8b12832

86. Noda, H. and Shibasaki, M., *Eur. J. Org. Chem.*, 2020, vol. 2020, p. 2350.
https://doi.org/10.1002/ejoc.201901596

87. Razzak, M., and De Brabander, J.K., *Nature Chem. Biol.*, 2011, vol. 7, 865. https://doi.org/10.1038/NCHEMBIO.709

88. Yuen, T.Y., Yang, S.H., and Brimble, M.A., *Angew. Chem. Int. Ed.*, 2011, vol. 50, p. 8350. https://doi.org/10.1002/anie.201103117

89. Flavin, M.T., Rizzo, J.D., Khilevich, A., Kucherenko, A., Sheinkman, A.K., Vilaychack, V., Lin, L., Chen, W., Greendwood, E.M., Pengsuparp, T., Pezzuto, J.M., Hughes, S.H., Flavin, T.M., Cibulski, M., Boulanger, W.A., Shone, R.L., and Xu, Z.Q., *J. Med. Chem.*, 1996, vol. 39, p. 1303. https://doi.org/10.1021/jm950797i

90. Grubbs, R.B., *Macromolecules*, 2017, vol. 50, p. 6979. https://doi.org/10.1021/acs.macromol.7b01440

91. Treator, A.J. and Leibfarth, F.A., *Science*, 2019, vol. 363, p. 1439. https://doi.org/10.1126/science.aaw1703

92. Song, J., Xu, J., and Tang, D., *J. Polym. Sci.*, *Part A: Polym. Chem.*, 2016, vol. 54, p. 1373. https://doi.org/10.1002/pola.27986

93. Kottisch, V., O'Leary, J., Michaudel, Q., Stache, E.E., Lambert, T.H., and Fors, B.P., *J. Am. Chem. Soc.*, 2019, vol. 141, p. 10605. https://doi.org/10.1021/jacs.9b04961

94. Kottisch, V., Jermaks, J., Mak, J.Y., Woltornist, R.A., Lambert, T.H., and Fors, B.P., *Angew. Chem. Int. Ed.*, 2021, vol. 60, p. 4535. https://doi.org/10.1002/anie.202013419

95. Wilkinson, G. and Piper, T.S., *J. Inorg. Nucl. Chem.*, 1956, vol. 2, p. 32. https://doi.org/10.1016/0022-1902(56)80101-2

96. Mann, B.E., *Comprehensive Organometallic Chemistry*, Wilkinson, G., Stone, F.G.A., and Abel, E.W., Eds., New York: Pergamon Press, 1982, vol. 3, p. 89.

97. Gridnev, I.D., *Coord. Chem. Rev.*, 2008, vol. 252, p. 1798. https://doi.org/10.1016/j.ccr.2007.10.021

98. Spangler, Ch.W., *Chem. Rev.*, 1976, vol. 76, p. 187. https://doi.org/10.1021/cr60300a002

99. Childs, R.F., *Tetrahedron*, 1982, vol. 38, p. 567. https://doi.org/10.1016/0040-4020(82)80199-3

100. Jutzi, P., *Chem. Rev.*, 1986, vol. 86, p. 983. https://doi.org/10.1021/cr00076a002

101. Mikhailov, I.E., Dushenko, G.A., Nikishina, I.S., Kisin, A.V., Mikhailova, O.I., and Minkin, V.I., *Russ. J. Org. Chem.*, 2002, vol. 38, p. 1449. https://doi.org/10.1023/A:1022592018924

102. Dushenko, G.A., Mikhailov, I.E., Mikhailova, O.I., Minyaev, R.M., and Minkin, V.I., *Russ. J. Gen. Chem.*, 2020, vol. 90, p. 161. https://doi.org/10.1134/S1070363220020012

103. Jefferson, E.A. and Warkentin, J., *J. Org. Chem.*, 1994, vol. 59, p. 463. https://doi.org/10.1021/jo00081a029

104. Hoffmann, R.W., and Backes, J., *Chem. Ber.*, 1976, vol. 109, p. 1928. https://doi.org/10.1002/cber.19761090534

105. Kompan, O.E., Antipin, M.Yu., Struchkov, Yu.T., Mikhailov, I.E., Dushenko, G.A., Minkin, V.I., and Olekhnovich, L.P., *Zh. Org. Khim.*, 1985, vol. 21, p. 2032.

106. Mikhailov, I.E., Dushenko, G.A., and Minkin, V.I., *Zh. Org. Khim.*, 1987, vol. 23, p. 2522.

107. Mikhailov, I.E., Kompan, O.E., Struchkov, Yu.T., Minkin, V.I., Dushenko, G.A., Klenkin, A.A., and Olekhnovich, L.P., *Zh. Org. Khim.*, 1987, vol. 23, p. 1029.

108. Dushenko, G.A., Mikhailov, I.E., Mikhailova, O.I., Minyaev, R.M., and Minkin, V.I., *Dokl. Chem.*, 2018, vol. 479, p. 53. https://doi.org/10.1134/S0012500818040067

109. Mikhailov, I.E., Minkin, V.I., Klenkin, A.A., Dushenko, G.A., Kompan, O.E., Yanovskii, A.I., and Struchkov, Yu.T., *Zh. Org. Khim.*, 1990, vol. 26, p. 28.

110. Mikhailov, I.E., Minkin, V.I., Klenkin, A.A., Dushenko, G.A., Kompan, O.E., Struchkov, Yu.T., Yanovskii, A.I., Olekhnovich, L.P., and Borisenko, N.I., *Zh. Org. Khim.*, 1988, vol. 24, p. 2301.

111. Minkin, V.I., Mikhailov, I.E., Dushenko, G.A., Sadekov, I.D., Maksimenko, A.A., and Chernysh, Yu.E., *Doklady Akad. Nauk SSSR*, 1992, vol. 322, p. 706.

112. Mikhailov, I.E., Dushenko, G.A., Sadekov, I.D., Zschunke, A., and Minkin, V.I., *Phosphorus*, *Sulfur*, *Silicon (PSSi)*, 1998, vol. 136, p. 541. https://doi.org/10.1080/10426509808545991

113. Erbland, G., Abid, S., Gisbert, Y., Saffon-Merceron, N., Hashimoto, Y., Andreoni, L., Gurin, T., Kammerer, C., and Rapenne, G., *Chem. Eur. J.*, 2019, vol. 25, p. 16328. https://doi.org/10.1002/chem.201903615

114. Kelch, A.S., Jones, P.G., Dix, I., and Hopf, H., *Beilstein J. Org. Chem.*, 2013, vol. 9, p. 1705. https://doi.org/10.3762/bjoc.9.195

115. Dushenko, G.A., Mikhailov, I.E., and Minkin, V.I., *Russ. J. Org. Chem.*, 2020, vol. 56, p. 1744. https://doi.org/10.1134/S1070428020100127

116. Gisbert, Y., Abid, S., Bertrand, G., Saffon-Merceron, N., Kammerer, C., and Rapenne, G., *Chem. Commun.*, 2019, vol. 55, p. 14689.
https://doi.org/10.1039/c9cc08384g

117. Dushenko, G.A., Mikhailov, I.E., Mikhailova, O.I., Minyaev, R.M., and Minkin, V.I., *Mendeleev Commun.*, 2015, vol. 25, p. 21.
https://doi.org/10.1016/j.mencom.2015.01.007

118. Mikhailov, I.E., Dushenko, G.A., Kisin, A.V., Mugge, C., Zschunke, A., and Minkin, V.I., *Mendeleev Commun.*, 1994, vol. 4, p. 85.
https://doi.org/10.1070/MC1994v004n03ABEH000358

119. Dushenko, G.A., Mikhailov, I.E., Mikhailova, O.I., Minyaev, R.M., and Minkin, V.I., *Russ. Chem. Bull.*, 2015, vol. 64, p. 2043.
https://doi.org/10.1007/s11172-015-1115-z

120. Minkin, V.I., Mikhailov, I.E., Dushenko, G.A., Yudilevich, I.A., Minyaev, R.M., Zschunke, A., and Mugge, K., *J. Phys. Org. Chem.*, 1991, vol. 4, p. 31.
https://doi.org/10.1002/poc.610040107

121. Mikhailov, I.E., Minkin, V.I., and Dushenko, G.A., *Zh. Org. Khim.*, 1987, vol. 23, p. 2028.

122. Dushenko, G.A., Mikhailov, I.E., Skachkov, R.V., Klenkin, A.A., Divaeva, L.N., and Minkin, V.I., *Zh. Org. Khim.*, 1994, vol. 30, p. 790.

123. Dushenko, G.A., Skachkov, R.V., Mikhailov, I.E., Divaeva, L.N., and Minkin, V.I., *Zh. Org. Khim.*, 1994, vol. 30, p. 1076.

124. Dushenko, G.A., Mikhailov, I.E., Skachkov, R.V., Zhunke, A., and Minkin, V.I., *Zh. Org. Khim.*, 1996, vol. 32, p. 1003.

125. Dushenko, G.A., Mikhailov, I.E., Zhunke, A., and Minkin, V.I., *Russ. J. Org. Chem.*, 1998, vol. 34, p. 1122.

126. Dushenko, G.A., Skachkov, R.V., Mikhailov, I.E., and Minkin, V.I., *Russ. J. Org. Chem.*, 1997, vol. 33, p. 414.

127. Mikhailov, I.E., Klenkin, A.A., Dushenko, G.A., Skachkov, R.V., Zhunke, A., and Minkin, V.I., *Zh. Org. Khim.*, 1994, vol. 30, p. 1074.

128. Mikhailov, I.E., Kompan, O.E., Dushenko, G.A., and Minkin, V.I., *Mendeleev Commun.*, 1991, vol. 1, p. 121.
https://doi.org/10.1070/MC1991v001n04ABEH000074

129. Dushenko, G.A., Mikhailov, I.E., Reck, G., Schulz, B., Zschunke, A., Kharabaev, N.N., and Minkin, V.I., *Russ. J. Org. Chem.*, 2002, vol. 38, p. 982.
https://doi.org/10.1023/A:1020897411534

130. Dushenko, G.A., Mikhailov, I.E., Kompan, O.E., Zschunke, A., Reck, G., Schulz, B., Mugge, C., and Minkin, V.I., *Mendeleev Commun.*, 1997, vol. 7, p. 127.
https://doi.org/10.1070/MC1997v007n04ABEH000761

131. Minkin, V.I., Mikhailov, I.E., and Dushenko, G.A., *Chem. Commun.*, 1988, p. 1181.
https://doi.org/10.1039/C39880001181

132. Bumber, A.A., Profatilova, I.A., Dushenko, G.A., and Mikhailov, I.E., *Russ. J. Electrochem.*, 2003, vol. 39, p. 699.
https://doi.org/10.1023/A:1024125916241

133. Platonov, D.N., Okonnishnikova, G.P., Novikov, R.A., Suponitsky, K.Yu., and Tomilov, Yu.V., *Tetrahedron Lett.*, 2014, vol. 55, p. 2381.
https://doi.org/10.1016/j.tetlet.2014.02.117

134. Tomilov, Yu.V., Platonov, D.N., Shulishov, E.V., Okonnishnikova, G.P., and Levina, A.A., *Tetrahedron*, 2015, vol. 71, p. 1403.
https://doi.org/10.1016/j.tet.2015.01.024

135. Platonov, D.N., Okonnishnikova, G.P., Salikov, R.F., and Tomilov, Yu.V., *Tetrahedron Lett.*, 2016, vol. 57, p. 4311.
https://doi.org/10.1016/j.tetlet.2016.08.043

136. Trainov, K.P., Litvinenko, V.V., Salikov, R.F., Platonov, D.N., and Tomilov, Yu.V., *Dyes Pigm.*, 2019, vol. 170, p. 107589.
https://doi.org/10.1016/j.dyepig.2019.107589

137. Trainov, K.P., Salikov, R.F., Luponosov, Y.N., Savchenko, P.S., Mannanov, A.L., Ponomarenko, S.A., Platonov, D.N., and Tomilov, Yu.V., *Mendeleev Commun.*, 2019, vol. 29, p. 304.
https://doi.org/10.1016/j.mencom.2019.05.021

138. Trainov, K.P., Salikov, R.F., Platonov, D.N., and Tomilov, Yu.V., *Mendeleev Commun.*, 2020, vol. 30, p. 647.
https://doi.org/10.1016/j.mencom.2020.09.032

139. Trainov, K.P., Chechekina, O.G., Salikov, R.F., Platonov, D.N., and Tomilov, Yu.V., *Dyes Pigm.*, 2021, vol. 187, p. 109132.
https://doi.org/10.1016/j.dyepig.2020.109132